POLYMER MEDIATED DELIVERY OF OLIGONUCLEOTIDE AND TRANS GENES TOWARD MORE EFFICIENT AND SPECIFIC THERAPIES FOR DYSTROPHINOPATHIES AND DYSTROGLYCANOPATHIES

by

Jason Driver Tucker

A dissertation submitted to the faculty of
The University of North Carolina at Charlotte
in partial fulfillment of the requirements
for the degree of Doctor of Philosophy in
Biology

Charlotte

2014

Approved by:

____
Dr. Qi-Long Lu

____
Dr. Ian Marriott

____
Dr. Jean-Luc Mougeot

____
Dr. Shan Yan

____
Dr. Donna Kazemi

©2014
Jason Driver Tucker
ALL RIGHTS RESERVED

ABSTRACT

JASON DRIVER TUCKER. Polymer mediated delivery of oligonucleotide and trans
genes toward more efficient and specific therapies for dystrophinopathies and
dystroglycanopathies
(Under the direction of DR. QI-LONG LU and DR. IAN MARRIOTT)

Muscular dystrophies are genetic disorders caused by mutations in more than 30 genes, with no cure or effective treatment. Duchenne muscular dystrophy (DMD) is caused by frame-shift mutations in the dystrophin gene with little or no functional dystrophin protein in muscles. One of the most effective experimental therapies for DMD is antisense oligonucleotide (AON) therapy, which corrects the disrupted reading-frame by skipping the mutated exon(s) during pre-messenger RNA splicing resulting in truncated but functional dystrophin protein. Proof of principle has been obtained with the most effective phosphorodiamidate morpoholino (PMO) chemistries in animal models and clinical trials. However, low efficiency and non-specific delivery remain critical barriers for AON therapy to achieve long-term efficacy.

My thesis has tested two hypothesis driven approaches to overcome these barriers: developing new polymers for effective delivery with low toxicity, and identifying ligands for tissue specific targeting. I have evaluated a new class of poly (ester-amine) (PEAs) primarily as vehicles for PMO delivery. The results demonstrate a significantly enhanced delivery and exon skipping efficiency in cell culture and *in vivo* with reduced toxicity compared with cationic polymer alone as delivery vehicles, providing a base to further optimize for clinical applications.

Applying a novel approach of phage array in combination with powerful next generation sequencing (NGS), my study revealed obstacles to identification of peptide ligands and allowed me to design novel procedure with potential to rejuvenate the technique for ligand identification with phage array both *in vitro* and *in vivo*. Collectively, these experiments address the most challenging issues currently in translational research.

DEDICATION

To my family and friends for their support, encouragement, and patience.

To all those personally affected or caring for those affected with muscular dystrophies.

To those who pursue their passions despite all obstacles they might face.

ACKNOWLEDGMENTS

I would like to thank my advisors Dr. Qi Long Lu and Dr. Ian Marriott for their support and encouragement. I would like to thank Dr. Jean-Luc Mougeot, Dr. Shan Yan, and Dr. Donna Kazemi for serving on my advisory committee, and providing valuable feedback and advice. I would also like to thank members of the Department of Biology at UNC Charlotte and the McColl-Lockwood laboratory at Carolinas Medical Center.

I would also like to thank the UNC Charlotte Graduate School for the Graduate Assistant Support Plan Award, Carolinas Healthcare Foundation Muscular Dystrophy Research Endowment and NCBC for providing much appreciated financial support during my research and graduate education.

TABLE OF CONTENTS

LIST OF TABLES x

LIST OF FIGURES xi

LIST OF ABBREVIATIONS xiv

CHAPTER 1: INTRODUCTION 1

- 1.1 Background on Inherited Myopathies and Muscular Dystrophies 4
- 1.2 Dystrophinopathies; Duchenne and Becker's Muscular Dystrophy 8
- 1.3 Antisense Oligonucleotide Induced Exon-Skipping 13
- 1.4 Gene and Oligonucleotide Delivery Systems 19
- 1.5 Synthetic Polymers as Non-Viral Delivery Vehicles 28
- 1.6 Challenges in Gene and Oligonucleotide Delivery 33
- 1.7 Dystroglycanopathies 34
- 1.8 Tissue-Targeted Delivery 36
- 1.9 Phage Array as a Method to Determine Tissue-Specific Epitopes 40
- 1.10 Specific Aims 47

CHAPTER 2: POLY(ESTER AMINE) TRIS [2-(ACRYLOYLOXY) ETHYL]ISOCYANURATE CROSS-LINKED POLYETHYLENIMINE POLYMERS AS GENE AND ANTISENSE OLIGOMER DELIVERY VEHICLES FOR THE TREATMENT OF DUCHENNE MUSCULAR DYSTROPHY. 61

2.1 Abstract 61

2.2 Introduction 62

2.3 Results 64

2.4 Discussion 79

2.5 Methods 80

CHAPTER 3: PHOSPHORODIAMIDATE MORPHOLINO CONJUGATED TRIS[2-(ACRYLOYLOXY)ETHYL]ISOCYANURATE LOW MW POLYETHYLENIMINE CROSSLINKED POLYMERS FOR ANTISENSE RESTORATION OF DYSTROPHIN EXPRESSION. 86

3.1 Abstract 86

3.2 Introduction 87

3.3 Results 90

3.4 Discussion 99

3.5 Methods 102

CHAPTER 4: IDENTIFICATION OF GLYCOSYLATED α–DYSTROGLYCAN EPITOPES THROUGH PHAGE ARRAY METHODS 107

4.1 Abstract 107

4.2 Introduction 111

4.3 Results 116

4.4 Discussion 137

4.5 Methods 142

CHAPTER 5: DISCUSSION AND FUTURE DIRECTIONS 154

5.1 Summary 154

5.2 Publications and Presentations 160

REFERENCES 162

LIST OF TABLES

TABLE 1: Mutations and associated muscular dystrophies 7

TABLE 2: Characteristics of synthesized Poly(Esteramine)s (PEAs) 66

TABLE 3: Characteristics of synthesized PEAs selected for PMO modification 88

TABLE 4: Comparison of NGS determined PCR amplified M13 *gIII* region 133

TABLE 5: Phage library amino acid expected and observed frequencies 136

TABLE 6: M13KE amino acid codon table 152

LIST OF FIGURES

FIGURE 1: Schematic representation of the sarcolemmal proteins 6

FIGURE 2: Dystrophin domains and mutations 12

FIGURE 3: Schematic illustration of antisense oligonucleotide induced exon skipping 16

FIGURE 4: Antisense oligonucleotide chemistries 21

FIGURE 5: Chemical structures of modified PMO 25

FIGURE 6: Graphical representation of optimal gene delivery vehicle characteristics 29

FIGURE 7: Schematic diagram of phage array procedure and selection 44

FIGURE 8: Determination of polymer/DNA binding 66

FIGURE 9: Particle size of PEA complexed with DNA 67

FIGURE 10: TEM of PEA/pDNA particles 68

FIGURE 11: Polyplex stability to serum and heparin degradation 69

FIGURE 12: Degradation of TAEI-PEI in simulated physiological conditions 70

FIGURE 13: Cell viability/toxicity and PEA polymers 71

FIGURE 14: PEA pDNA delivery to CHO cells and GFP expression 73

FIGURE 15: PEA pDNA delivery to C2C12 cells and GFP expression 73

FIGURE 16: Intramuscular PEA-delivery of pEGFP 74

FIGURE 17: PEA mediated dystrophin restoration western blot and RT-PCR 77

FIGURE 18: Confocal microscopy of PEA uptake and intracellular localization 78

FIGURE 19: Schematic of feed ratio controlled, PEA LPEI construction 89

FIGURE 20: PEA viability/toxicity *in vitro* (C2C12 e23) 91

FIGURE 21: PEA viability/toxicity *in vitro* (C2C12) 92

FIGURE 22: Transfection efficiency C2C12 e23 GFP expression 92

FIGURE 23: PEA+PMO and PEA-PMO conjugates *in vitro* 93

FIGURE 24a: H&E intramuscular pathology (experimental) 94

FIGURE 24b: H&E intramuscular pathology (control) 95

FIGURE 25: Intramuscular dystrophin restoration IHC 96

FIGURE 26: Dystrophin positive fiber count 97

FIGURE 27: Diffuse dystrophin positive fibers i.m. 98

FIGURE 28: Diffuse dystrophin positive fiber count 99

FIGURE 29: Schematic diagram of phage selection methods 115

FIGURE 30: Immunodetection of α-DG in CHO used for phage selections 118

FIGURE 31: IHC of α-DG of CHO Pro5 and CHO Pro5 +LARGE cells 119

FIGURE 32: HTS screening and validation of phage clones 120

FIGURE 33: Phage detection of α- DG epitopes on western blot 121

FIGURE 34: C57 WT and FKRP P448L α-DG muscle IHC 123

FIGURE 35: *Ex vivo* phage affinity to skeletal muscle 124

FIGURE 36: Representative histogram of phage *gIII* Sanger sequencing. 126

FIGURE 37: Initial PCR amplification of M13KE *gIII with* 100mer flankers 127

FIGURE 38: PCR optimization of 260 bp M13KE gIII amplifications 127

FIGURE 39: QC of 112 bp M13KE *gIII* PCR amplifications 128

FIGURE 40: Separation of target/fragment PCR products for NGS 132

FIGURE 41: Comparison of the most prevalent naïve and selected peptides from NGS sequencing 134

FIGURE 42: Heat-map of identified peptides compared with M13 proteome 135

FIGURE 43: General schematic of phage display methods employed 148

FIGURE 44: Extrapolation and analyses of phage expressed peptides 153

FIGURE 45: Proposed phage array NGS method diagram 158

FIGURE 46: Future vehicle design model 159

LIST OF ABBREVIATIONS

Ca2+:	calcium
CK:	creatine kinase
CMD:	congenital muscular dystrophy
DMD:	Duchenne muscular dystrophy
BMD:	Becker's muscular dystrophy
EBD:	Evans blue dye
EDL:	extensor digitorum longus
FGF:	fibroblast growth factor
ICAM-1:	intracellular adhesion molecule 1
LGMD:	Limb-Girdle muscular dystrophy
MDA:	Muscular Dystrophy Association
MRI:	magnetic resonance imaging
mRNA:	messenger ribonucleic acid
NF-κB:	nuclear factor-kappa B
PBS:	phosphate buffered saline
PFA:	paraformaldehyde
GFP:	green fluorescent protein
TA:	tibialis anterior
TALEN:	transcription activator-like effector nuclease
CRISPR:	clustered regularly interspaced short palindromic repeats
DMEM:	Dulbecco's Modified Eagle Medium

2’OmePs:	2’-O-Methyl Phosphorothioate
PMO:	phosphorodiamidate morpholino
PEI:	polyethyleneimine
PEA:	poly(ester)amine
PCM:	polycarbamate
N/P:	nucleic acid :polymer ratio
HLB:	hydrophilic-lipophilic balance
FKRP:	Fukitin-related protein
LARGE:	like-glycosyltransferase
PomGnT:	protein O-linked mannose N-acetylglucosaminyltransferase
MTS:	(3-(4,5-dimethylthiazol-2-yl)-5-(3-carboxymethoxyphenyl)-2-(4-sulfophenyl)-2H-tetrazolium)
AON:	antisense oligonucleotide
PNA:	peptide nucleic acid
DLS:	dynamic light scattering (photon correlation spectroscopy)
IHC:	immunohistochemistry
FACS:	fluorescence activated cell sorting
FCMD:	Fukuyama congenital muscular dystrophy
CMD/MDC:	congenital muscular dystrophy
WWS:	Walker-Warburg syndrome
MEB:	muscle-eye brain

CHAPTER 1: INTRODUCTION

Muscular dystrophies are genetic disorders caused by mutations in more than 30 genes with clinical manifestation ranging from mild disability to the premature lethality. There is no cure or effective treatment for all muscular dystrophies. Duchenne muscular dystrophy (DMD) is the most severe and common form of muscular dystrophy, affecting 1 in 3500 newborn males. DMD is an X-linked recessive disorder, caused by mutations in the dystrophin gene (*DMD Xp21.2*) disrupting the open reading frame of mRNA transcript, such that little or no functional dystrophin protein is produced.. Mutations of the same gene without alteration of the reading frame often cause a mild, non-life threatening allelic form of Becker's muscular dystrophy (BMD). One of the most effective experimental therapies for DMD is oligonucleotide therapy. Specific antisense oligonucleotides (AON) correct the disrupted reading-frame by skipping the mutated exon(s) during pre-messenger RNA splicing which results in truncated but functional dystrophin protein, converting the severe DMD phenotype to a milder like that of BMD. There have been many AON chemistries, but the high stability and low toxicity make phosphorodiamidate morpoholino (PMO) the most promising AON chemistry with studies in animal models and clinical trials demonstrating clear benefits to subjects, a rare success in pharmaco-genetic interventions. However, low efficiency and non-specific delivery remain critical barriers of PMO therapy to achieve long-term efficacy in DMD and other diseases.

Two approaches can be envisioned to overcome these barriers: developing new polymers for effective delivery with low toxicity and identifying ligands for tissue specific targeting. Increasing delivery of therapeutic oligos through incorporation of cationic peptides and other polymers has been the subject of much research. Cationic peptide modifications show increased transfection efficiency, but also increase toxicity as a result of strong positive charges of amino acids at such high density. Similarly, cationic polymers and peptides, such as poly-arginine peptides and cationic dendrimers in combination or in conjugation with PMO, have been examined. These modifications improve delivery efficiencies greatly, but significant toxicity *in vivo* prevents them from clinical trial. My attempt for this thesis is to test the hypothesis that tissue specific ligands can be identified through phage array methods. Such ligands could then be used for muscle targeted AON delivery approached through testing modified polymers.

My initial studies involved the examination of several novel classes of compounds for enhanced delivery of specific PMO AON for exon skipping in DMD models. These studies, together with knowledge accumulated through study of current literature for gene and oligo delivery have identified several critical characteristics of polymers for enhancing delivery of oligomers and transgenes. 1) Cationic polymer components, such as PEI appear to be essential for interaction between polymers/oligomers and especially cellular components. 2) While high molecular weight PEI with mw 25K cannot be used clinically because of high toxicity and short-circulation time, low molecular weight PEI remains effective to form nano-sized particles to deliver plasmid or oligomers with high efficiency and low toxicity. 3) Amphiphilic polymers such as Poloxamers (Pluronics) can provide essential hydrophobicity for the interaction of oligomers with hydrophobic membranes, thus enhancing delivery. 4). Balance between hydrophobicity and hydrophilicity is likely critical for delivery efficiency and acceptable toxicity. Systematically combining and balancing these components could maximize synergistic characteristics, uniquely increasing transfection efficiencies *in vitro* and *in vivo*, without additional toxicity. Based on the hypothesis that polymer modification of PMO would benefit transfection and delivery, a new class of poly(ester-amine) (PEAs) conjugated to PMO AON were tested in cell culture and *in vivo* through local and systemic administration, and their efficiencies in transfection, exon skipping and restoration of dystrophin were determined. I used PMOs targeting the mutated mouse dystrophin gene, and human dystrophin exons, thus likely relevant to clinical application of our target.

Another, more ideal approach to enhance delivery of PMO, or AON and transgene in general, without increasing toxicity would be to employ ligands as tissue specific, or muscle specific receptors as part/or whole of delivery vehicles. To date, no ligand with validated muscle specificity has been available for use. Identification of peptide ligands to accessible targets that are highly expressed in muscle tissue remains elusive. One such target in muscle tissue is the highly glycosylated receptor alpha-dystroglycan (α-DG), expressed at higher levels in muscle than other tissues. This glycosylated protein has been used by many viruses as the receptor for infection. With this in mind for my study, I attempted to use high throughput phage-array methods to select ligands specific to this protein with glycosylation mutant CHO cell lines. CHO cells overexpressing the like-glycosyltransferase (LARGE) which produces highly hyper-glycosylated α-DG, thus ideal for selective enrichment of phage peptides. Additionally, wild type (C57Bl6) and mice lacking functionally glycosylated α-DG (FKRP P448L mutation) were used to as positive and negative muscle tissue controls. Performing these studies address the sub-hypothesis that identification of small peptides can produce ligands specific to muscle tissue by affinity to glycosylated α-DG, demonstrating an effective method which can be applied for selection of peptide to any target tissue and cells.

Collectively, these experiments address one of the currently most challenging issues in translational research aiming to apply promising experimental therapies to treat human diseases, the low and non-specific delivery of therapeutic agents, oligonucleotide and transgene to preferred targeted cells *in vivo*. Thus, addressing the premise that synthetic polymers for gene delivery can be modified for targeted delivery, and that building upon advances in synthetic polymers as safe and efficient delivery vehicles, can be combined to benefit a potential therapy toward realistic *in vivo* and clinical applications. Essential information obtained through these studies will contribute to the collective understanding of oligonucleotide and gene delivery vehicles, especially for delivery of PMO AON for effective clinical treatment of Duchenne and other muscular dystrophies.

1.1 Background on Inherited Myopathies and Muscular Dystrophies

Myopathies are neurological or neuromuscular disorders, which can be acute or chronic in condition and primarily relate to dysfunction or dysregulation of muscle fiber integrity or muscle function. Myopathies are categorized as musculoskeletal, affecting the myofiber or neuromuscular which includes those directly involving the muscle but also including disorders of the nerve and neuromuscular junction. Inherited myopathies are a distinct set of muscle disorders with diverse and varied pathological presentation, which are the result of genetic mutations passed from one generation to the next. These genetic diseases are inherited in both dominant and recessive manners and can range from reduced enzymatic function in less severe forms to absence of functional proteins in more severe phenotypes resulting in an array of muscle membrane or contractile dysfunction leading to premature death of the afflicted individual. While all inherited myopathies share some common symptoms and follow progression with age, muscular dystrophies are a distinct set of inherited diseases affecting the muscles through defects in structural proteins, membrane supporting proteins, and enzymes, leading to muscle wasting through ongoing and progressive muscle degeneration and regeneration.

Muscular dystrophies are now known to be caused by mutations in more than 30 genes and can be categorized primarily into several groups, with Dystrophinopathies and Dystroglycanopathies being the most common groups, with specific biochemical as well as genetic features. Prior to the advent of molecular diagnostics which have greatly improved accuracy in identification of specific genetic mutations, differential diagnoses of the muscular dystrophies relied upon family history along with symptoms across muscle groups and pathological evidence.(Prior and Bridgeman 2005) As illustrated in table 1, mutations associated with muscular dystrophies can be found in at least 16 out of 23 chromosomes. Much work has been done to better understand the complex molecular pathology of the muscular dystrophies, yet our knowledge about disease progression remains limited and patients without genetic diagnosis account for about 20% of total muscular dystrophy cases.

Mutations in the genes coding for proteins of the extracellular matrix, myofiber membrane, transmembrane and cytoskeletal proteins, as well as glycosyltransferase enzymes, have been identified in at least 16 of 23 chromosomes. Mutations in a single gene with different severity can also be classified into different categories.

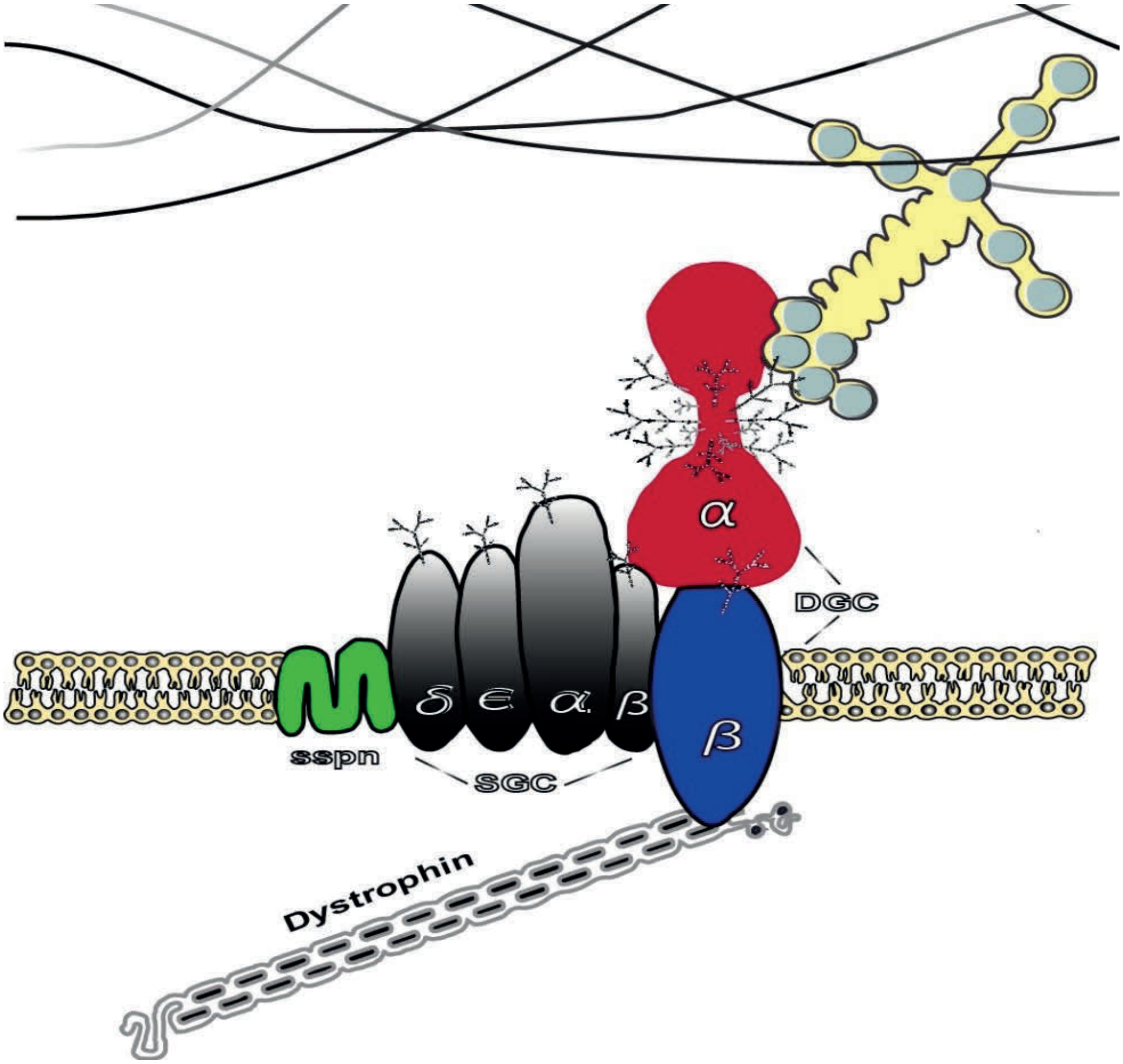

Figure 1: Schematic representation of the sarcolemmal proteins. Representation of some of the proteins involved in the muscular dystrophies, their location and interactions to link the extracellular matrix to the myofiber membrane and intracellular structural components. Collagen VI and Laminin-α2, as well as other proteins of the basal lamina bind integrins such as α7β1 and glycosylated α-dystroglycan through interaction of laminin globular (LG) domains. Defects in any of the gene products cause muscular dystrophy. Laminin-α2 or defects of glycosylation, specifically hypoglycosylation, of αDG lead to CMD or dystroglycanopathies (WWS, MEB, FCMD, MDC1C, MDC1D, LGMD2I) respectively. Mutations in the Sarcoglycan

complex (SGC) results in limb girdle muscular dystrophies LGMD2C, LGMD2D, LGMD2E and LGMD2F. Dystrophinopathies including DMD, BMD, and XLDCM result from absence or abnormalities in the structural protein dystrophin.

Table 1: Mutations and associated muscular dystrophies.

Disorder	Abbreviation	Gene	OMIM	Locus
Duchenne	DMD	DMD	300377	Xp21.2-p21.1
Dilated Cardiomyopathy	CMD3B XLCM	DMD	302045	Xp21.2-p21.1
Becker's	BMD	DMD	300376	Xp21.2-p21.1
Congenital	CMD	SCN5A	601154	3p22.2
Limb Girdle	LGMD2A	CAPN3	253600	15q15.1
	LGMD2B	DYSF	253601	2p13.2
	LGMD2C	SGCG	253700	13q12.12
	LGMD2D	SGCA	608099	17q21.33
	LGMD2E	SGCB	604286	4q12
	LGMD2F	SGCB	604286	5q33.3
	LGMD2I	SGCD	607155	19q13.32
Walker-Warburg	WWS	POMT1	236670	9q34.13
Muscle-Eye-Brain	MEB	POMT2	613150	14q24.3
Fukuyama CMD	FCMD	FKTN	253800	9q31.2
CMD 1C	MDC1C	FKRP	606612	19q13.32
CMD 1D	MDC1D	LARGE	603590	22q12.3

1.2 Dystrophinopathies; Duchenne and Becker's Muscular Dystrophy

Dystrophinopathies, as the name suggests are those forms of muscular dystrophy caused by mutations in the gene (commonly called the DMD gene) coding for the protein dystrophin. Defects in the relatively large proteins nebulin and titin were once reported as suspected causes of DMD, later contradicted by normal expression levels of these proteins.(Furst, Nave et al. 1987, Wood, Zeviani et al. 1987). Similar in size, the true product of the DMD gene was identified in 1987 by Hoffman et.al not as nebulin, but another structural protein given the name dystrophin. By sequence comparison, Hoffman found 90% homology between the mouse and human DMD transcript. DMD is the most severe and common form of muscular dystrophy, affecting an estimated 1 in 3500 newborn males or 420,000 individuals worldwide, yet due to its prevalence is categorized as an orphan disease.(Emery 1991, 107th Congress 2002, Wellman-Labadie and Zhou 2010) The disease is caused by mutations in the DMD (dystrophin) gene. Dystrophin is a 427 kDa protein encoded by the largest human gene 2.2 Mb in size at locus Xp21, with a mature mRNA transcript of 14 kb containing with 79 exons coding for 3500 amino acid residues.(Hoffman, Brown et al. 1987, Hoffman, Knudson et al. 1987, Wood, Zeviani et al. 1987)

Of the dystrophinopathies the best characterized are Duchenne and Becker's muscular dystrophies, as well as DMD-associated dilated cardiomyopathy (DCM/XLDCM). Usually diagnosed within the first 5 years of life, DMD is characterized by progressive muscle wasting first presenting as delayed motor development indicated by an abnormal gait or inability to rise from the floor, with varied often mild cognitive disability. The progressive muscle degeneration in DMD patients outweighs regeneration, causing a loss of ambulation near the tenth year of age. By the late teens patients exhibit scoliosis from assistive devices, with respiratory and cardiac complications leading to death before the mid twenties. While milder in comparison, inherited or spontaneous mutations within the dystrophin gene of BMD and DCM patients cause symptoms similar to DMD with a later and varied onset. BMD patients primarily present with symptoms of progressive skeletal muscle weakness, while XLDCM typically presents without skeletal muscle involvement. Roughly 70% of BMD patients develop dilated cardiomyopathies which like XLDCM results in heart failure as the primary cause of death (Nigro, Di Somma et al. 1995, Bushby, Muntoni et al. 2003, Kaspar, Allen et al. 2009). Some BMD (in-frame) mutations of the dystrophin gene and in female carriers may not cause obvious clinical manifestation. Muscle weakness and frequent contractures observed in the dystrophinopathies; result from a loss of muscle mass and fragmented muscle fibers which in turn are the result of constant degeneration and regeneration. Eventually, diseased muscles lose the capacity to regenerate and are replaced by non-functional collagen and adipocyte deposition, creating the hallmark muscle pseudohypertrophy. (Imbert, Vandebrouck et al. 1996, Goldstein and McNally 2010). Constant degeneration also leaves unstable myofiber membranes subject to osmotic dysregulation through Ca2+ influx, and inflammatory infiltration.

Currently, there is no effective treatment for the diseases. Clinically, administration of palliative therapies such as the use of calcium channel blockers, antioxidants, and especially immunosuppressant glucocorticoids have demonstrated some benefit for temporary stabilization of muscle degeneration and function.(Manzur, Kuntzer et al. 2008, Baudy, Reeves et al. 2012) During the last 3 decades, especially after the identification of the disease gene, great effort has been made to develop new therapies to treat the diseases. Most fundamental and promising of the experimental therapies have been gene therapy and stem cell therapy. However, gene therapy is effective only when viral vectors, such as retrovirus, adenovirus, or adeno-associated virus and lentivirus are used. The advantage of viral vectors is that, along with their capacity to deliver a gene of variable size, viral infection of cells both *in vitro* and *in vivo* can be very efficient. The disadvantages of viral vectors include several aspects: 1) Cell-type specificity limiting their use for certain types of tissue. For example, AAV virus is not very efficient to infect liver cells. 2) Proliferation dependence. For example, adenovirus infect most efficiently only to proliferating cells, not to mature non-proliferating cells such as muscle fibers. 3) The size limitation of exogenous transgene cargo. AAV virus for example, has a limitation of less than 5 KB DNA insertion. Therefore, transgenes larger than this size, such as the full length dystrophin gene coding sequence could not be packed within this vector for delivery. 4) Insertional mutagenesis. Certain viruses such as adenovirus and retrovirus pose a risk of random insertion of the transgene and their vector sequences to sites of critical genes, which could lead to activation or suppression of the gene functions with various detrimental consequences. 5) Immunostimulatory response. This could cause serious consequences from chronic and acute organ failure, rejection of infected cells and transgene, and prevention of further administration which may be necessary for treatment of genetic disorders to maintain a life-long production of therapeutic transgene such as dystrophin for Duchenne muscular dystrophies. Although the listed disadvantages may not apply to each viral vector listed, any of these side effects could be sufficient to significantly delay or disrupt an otherwise promising drug development program. Thus viral-mediated gene therapy is progressing very slowly towards clinical applications and in clinic trials. Stem cell therapy is effective for local replacement, but its application for systemic efficacy remains to be proven. This is especially important for treating muscular dystrophies as one would need to deliver a large amount of relevant cells to the vast amount of muscle tissue and control their fate towards muscle fibers, rather than undifferentiated stem cells or differentiation to some other cell type. No report has so far been able to show convincingly that systemically delivered muscle precursor cells can migrate efficiently into muscle tissue and differentiate effectively into myofibers with desirable functions.

Most recently, oligonucleotide therapy has emerged as a promising experimental treatment for many diseases either through its use as agents of gene expression knockdown or as gene expression modulator. One of the most advanced examples is the oligonucleotide mediated exon skipping for treating DMD.

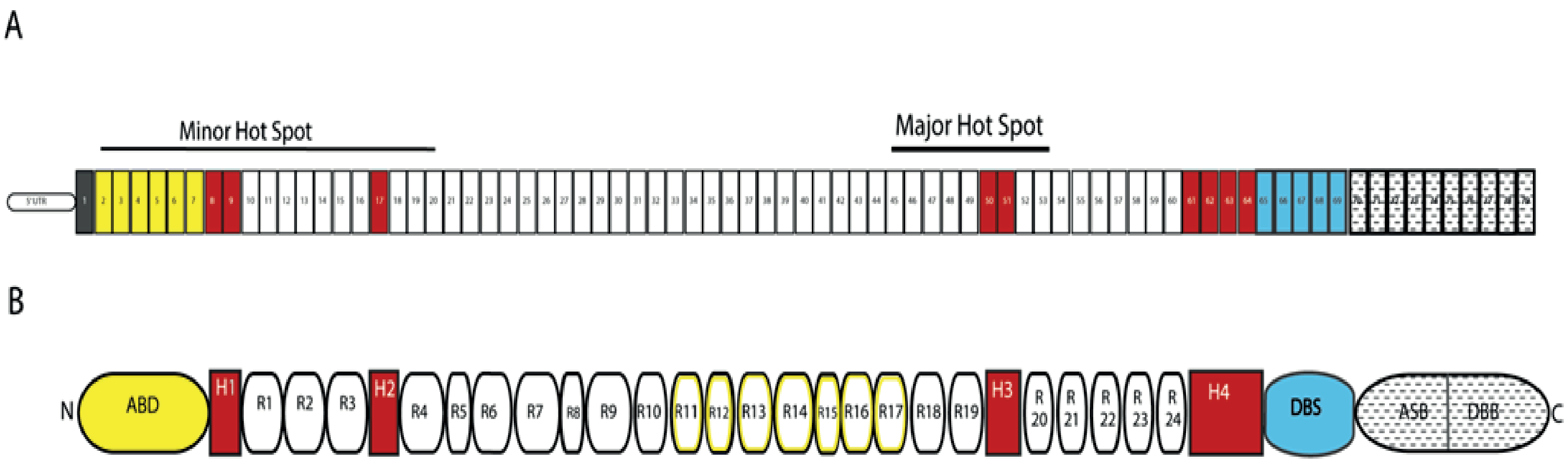
A
Minor Hot Spot
Major Hot Spot
5'UTR
B
N
ABD
H1
R1
R2
R3
H2
R4
R5
R6
R7
R8
R9
R10
R11
R12
R13
R14
R15
R16
R17
R18
R19
H3
R 20
R 21
R 22
R 23
R 24
H4
DBS
ASB
DBB
C

Figure 2: Dystrophin Domains and Mutations

Mutations of the DMD gene cause two allelic diseases DMD and BMD. DMD is caused by frame shift mutations disrupting the open reading frame, such that little or no functional dystrophin protein is produced. Frame shift mutations can be insertions, deletions, duplications and mutations affecting the splice motif. Lack of dystrophin expression can also be the result of nonsense mutations. The mild, non-life threatening allelic form, BMD, shows reduced levels of, but functional dystrophin expression

1.3 Antisense Oligonucleotide Induced Exon-Skipping

1.3.1 Antisense oligonucleotide therapy

Antisense oligonucleotides and their applications have been given much attention since molecular biologists Zamecnik and Stephenson first reported blocking Rous sarcoma virus replication by inhibiting 35s RNA with unique synthetic oligonucleotides in 1978.(Stephenson and Zamecnik 1978, Zamecnik and Stephenson 1978) The common principle among antisense applications is that an oligomer with complementary sequence binds to target mRNA interfering with translation such that gene silencing or pre-mRNA splicing is modified. In the case of gene silencing, binding of an oligo to a target mRNA creates either a steric block to translation, and/or leading to activation of ribonuclease H-dependent degradation of the transcript. A splice modulating or splice-switching oligonucleotide (SMO/SSO) similarly binds in a base dependent manner to a particular RNA target sequence, however unlike gene silencing mechanisms, the target RNAs are pre-mRNA rather than mature mRNA. The binding of pre-mRNA transcript interferes with splicing mechanisms resulting in a collection of possible alternatively spliced mature mRNA. The resulting spliced mRNA can produce unique proteins upon translation, not unlike more than 95% of genes which have been shown to undergo alternative splicing.(Keren, Lev-Maor et al. 2010, Nilsen and Graveley 2010) Therefore alteration of exon skipping can be used for many different purposes from creating new shortened transcripts, promotion of early termination, new transcripts with novel sequence inserted or extended coding for proteins with different functions, and to correct frame-shift mutations.

Antisense oligos as extension of natural RNAi have been developed for many applications with variable degrees of success. Clinical applications include the treatment of B cell Lymphoma, hepatitis C virus (HCV), and low-density lipoprotein (LDL) cholesterol management.(Cirak, Arechavala-Gomeza et al. 2011, Goemans, Tulinius et al. 2011) However, their advancement to mainstream products has been slower than anticipated, with the first FDA approval of Fomiversen (Vitravene) coming twenty years after Zamecnik's discovery.(Stein 2008, Chen, Zhang et al. 2011, Kole, Krainer et al. 2012). Most importantly, the limited progress in clinical applications of antisense oligo-mediated therapy is due to the limited target efficiency *in vivo*, lower than that required to achieve significant therapeutic values. (Watts and Corey 2012, Ming, Carver et al. 2013) Arguably, the most advanced clinical application of antisense oligo-mediated exon skipping is for the treatment of DMD.

The low efficiency and non-specificity in delivery is however not limited to antisense oligo therapy for exon-skipping, but also to many other applications of RNAi as drugs and gene therapy. The field of gene therapy primarily categorizes delivery systems into viral or non-viral delivery systems.

1.3.2 Dystrophin gene and exon skipping for DMD

The product of the DMD gene is dystrophin, a large rod-like protein with multiple domains. The muscle form of dystrophin protein can be divided into amino (N) terminal, rod, cysteine-rich and carboxy (C) terminal domains, with most essential functional domains being assigned to the amino- and carboxyl-terminal domains, and cysteine-rich domain. The dystrophib protein acts to stabilize the sarcolemma through binding the dystroglycan/sarcoglycan complexes at the myofiber membrane to actin filaments within the myofiber along its N-terminal actin-binding domain and to dystroglycan and sarcoglycans via its C terminal domain. However, the rod domain which spans more than half the length of the protein seems to have limited functional importance. This has been indicated by the report that patients with exon deletion from 17-49 only exhibit a mild dystrophic phenotype. Furthermore, truncated dystrophin with less than half of the length and deletion of most of the rod domain can provide effective protection of muscle from degeneration with viral mediated gene delivery. Although DMD mutations can occur along the entire length of the gene, most DMD mutations occur within the rod domain or regions which are not critical for its function. For example, intragenic deletions from exon 44 to exon 51 are "hotspots" containing roughly 10% of mutations (Oudet, Hanauer et al. 1992, Arechavala-Gomeza, Graham et al. 2007). This feature of the domain-function correlation provides the opportunity for manipulating the exon splicing for the restoration of dystrophin expression without severely compromising its functions. DMD mutations have been reported along the entire length of the gene with intragenic deletions accountable for ~70% of reported DMD mutations. However, based on domain-function correlation, any mutation outside the functionally critical domains can be manipulated to remove the "out of frame region" for the restoration of truncated, but functional dystrophin protein. Exon skipping uses specific antisense oligonucleotides (AON) targeting individual exon to correct the disrupted reading-frame by removing the mutated exon(s) or neighboring exon(s) during pre-messenger RNA splicing which results in truncated but functional dystrophin protein. It is estimated that more than 60% of DMD frame-shift mutations can be corrected with a severe DMD converted to BMD as depicted in figure 3 (Oudet, Hanauer et al. 1992, Aartsma-Rus, Kaman et al. 2006)

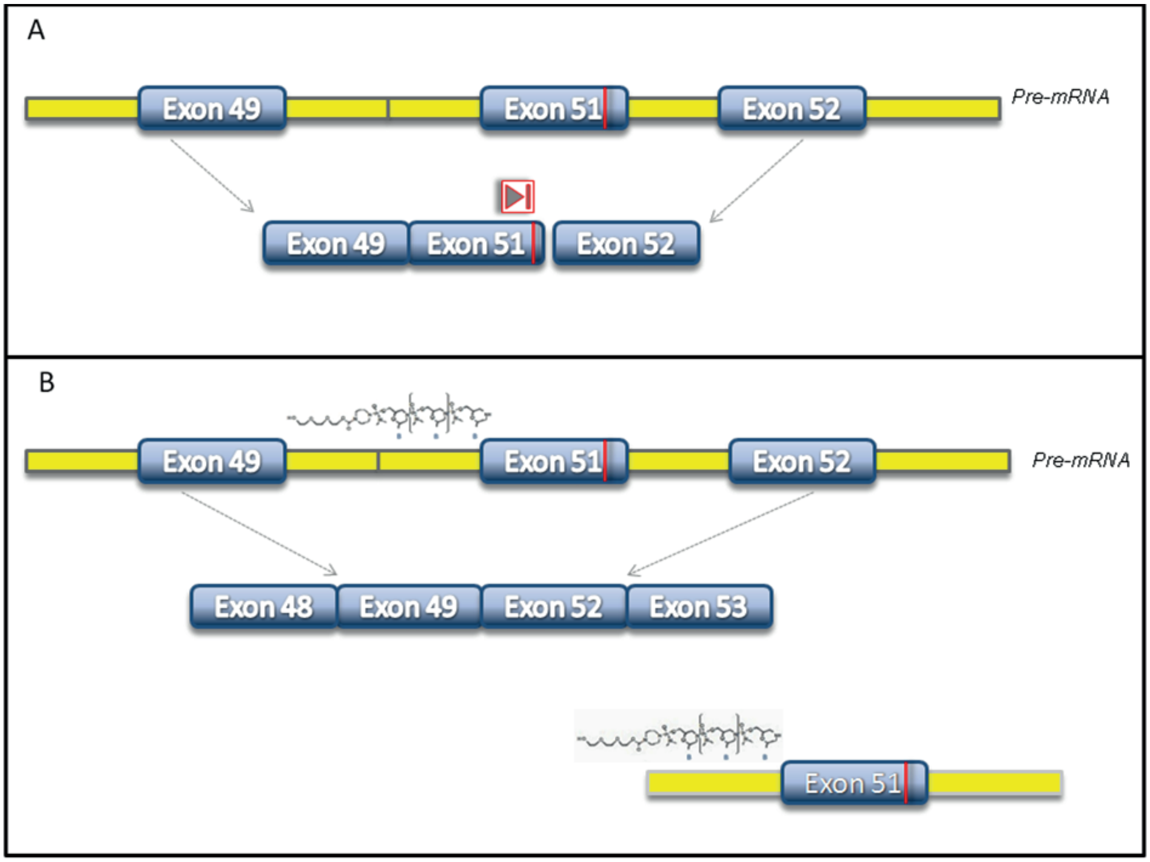
A
Exon 49
Exon 51
Exon 52
Pre-mRNA
Exon 49
Exon 51
Exon 52
B
Exon 49
Exon 51
Exon 52
Pre-mRNA
Exon 48
Exon 49
Exon 52
Exon 53
Exon 51

Figure 3: Schematic illustration of antisense oligonucleotide induced exon-skipping. Binding of sequence-specific antisense oligonucleotides (AON) targeted to intra-exon, intron-exon junctions, or splice-factor binding sequences, disrupts the normal Pre-mRNA splicing resulting in alternative splicing where one or more exons are removed along with flanking introns. In the case of DMD, this removal of mutation-bearing exon(s) restores the reading-frame during pre-messenger RNA splicing, resulting in a truncated but functional dystrophin protein. This alternatively spliced variant effectively converts the severe DMD phenotype to a milder phenotype more like the allelic variant, Becker's muscular dystrophy.

The first demonstration as a proof of principle that antisense oligonucleotides can be used to skip one exon to restore the out of frame dystrophin mRNA was published by

Dr. Matsuo in Japan in lymphocytes and later confirmed in myoblast culture by Dr. Muck Dunckley in UK(Matsuo, Masumura et al. 1991, Dunckley, Manoharan et al. 1998). The therapeutic potential of the therapy was then demonstrated in the mouse model of DMD, the mdx mouse, with specifically designed 2’0 methyl phosphorothioate (2OMePS) AONs delivered by i.m. injections. This mouse contains a nonsense mutation at exon 23 of the dystrophin gene, resulting in no expression of dystrophin proteins. The same 2OMePS AON was shown to induce dystrophin expression in body-wide muscles when delivered systemically.(Lu, Mann et al. 2003) Using a third generation oligo chemistry, phosphorodiamidate morpholino oligomers (PMO), regular systemic administration of the PMO targeting the same mouse dystrophin exon 23 induced effective exon skipping and produced functional levels of dystrophin in skeletal muscles.(Lu, Rabinowitz et al. 2005) Systemic effect of PMO for exon skipping was also demonstrated in dystrophic dog harboring a splice site mutation in intron 6, leading to exclusion of exon 7 from the mRNA transcript.(Yokota, Lu et al. 2009)

This principle has been substantiated for DMD by clinical trials over the last 7 years with two chemistries, the 2OMePS named PRO051/ Drisapersen initiated by Prosensa/GSK) and the PMO, named Eteplirsen initiated by AVI Biopharma .(van Deutekom, Janson et al. 2007, Kinali, Arechavala-Gomeza et al. 2009, Cirak, Arechavala-Gomeza et al. 2011) Both trials target dystrophin exon 51 and demonstrate the expected skipping of exon 51 and production of dystrophin protein following intramuscular injections. In a subsequent Phase IIb placebo-controlled trial, a significant benefit in 6MWT in the treatment over the placebo group was also reported. However, the phase III trial with 186 patients failed to show statistically significant improvements in the primary outcome measure of the 6MWT.(Lu, Cirak et al. 2014) During the same time period, PMO based trials using higher doses (30 and 50mg/kg/week) have reported increase in the number of dystrophin positive fibres in comparison to baseline biopsies and improvement in the 6-min walk test. The small cohort (10 patients) has now been treated for more than 2 years and yet the United States FDA refuse to consider the PMO drug Eteplirsen for accelerated approval (Mendell, Rodino-Klapac et al. 2013)The main reason is that the current antisense drug induced very limited amount of target dystrophin expression, generally considered insufficient to confer significant benefit.

1.3.3. Antisense oligo chemistry and delivery efficiency

The generally low antisense effect *in vivo* has led to great effort for improvement, as found in both the development of new chemistries for oligo synthesis, and new vehicles for improved delivery. A series of oligonucleotide chemistries have been developed over a number of years, many of which have been tested *in vitro* as well as *in vivo*. In the early stage of antisense oligo development, naked DNA and RNA oligonucleotides were used with very low efficacy especially *in vivo*, due to their vulnerability to nuclease degradation. To address this vulnerability, Eckstein et al introduced the phosphorothioate chemistry, replacing one of the two non-bridging oxygen atoms in the phosphate backbone resulting in an oligo chemistry far more resistant to nuclease degradation than unmodified oligonucleotides, later referred to as the first-generation. (De Clercq, Eckstein et al. 1969) The second generation of oligos include 2’-O-Methyl phosphorothioate(2OmePS), 2’-O-methoxyetyl(2”-MOE), phosphorodiamidate morpholino (PMO) and Locked nucleic acid (LNA)chemistries, demonstrating further increased resistance to enzymatic degradation and improved binding affinity to RNA targets.(Heemskerk, de Winter et al. 2009) Among these oligo chemistries, PMO possesses several unique properties. The ribose/deoxyribose of RNA/DNA is replaced by morpholine ring structures, and the phosphorothioate or phosphodiester groups are replaced by uncharged phosphorodiamidate groups. This substitution of neutral phosphorodiamidate groups makes PMO highly resistant to degradation and probably also reduces its potential toxicity due to reduced interaction with other charged cellular components.

1.4 Oligonucleotide Delivery Systems for Exon Skipping

1.4.1 Antisense chemistry

Development of new generation chemistries as antisense oligomers in general is not sufficient to enhance antisense effect to the degree required for therapeutic efficacy. This has been illustrated by numerous studies with different chemistries. The best examples of this are the use of the two most widely used chemistries, 2'OmePS and PMO. Repeated systemic delivery of approximately 60mg/kg 2OmePS targeting dystrophin exon 23 can produce detectable levels of dystrophin up to 5% of normal levels in skeletal muscles of mdx mice. However, no convincing expression of dystrophin is detected in the cardiac muscle. These levels of dystrophin protein however are less than optimal to achieve clinical significance (Lu, Rabinowitz et al. 2005) Similarly, repeated systemic delivery of PMO targeting the same exon 23 with the same dose and mouse model produced more than 10% dystrophin in some skeletal muscles, but as with the 2"OmePS, without detectable dystrophin in cardiac muscle.(Wu, Moulton et al. 2008) Again these levels of dystrophin induction are likely not sufficient to achieve significant clinical benefit.(Lu, Rabinowitz et al. 2005)

Furthermore, oligo chemistries also present concerns of toxicity. Phosphorothioate antisense oligonucleotides have been shown to have hybridization-independent toxicity varying with sequence and oligomer size, including pro-inflammatory responses, increased coagulation time, activation of the complement pathway, and some particular base sequences can interact with Toll-like receptors resulting in an immunostimulatory response.(Bhagat, Putta et al. 2011, Mo, Sun et al. 2013, Shoji-Kawata, Sumpter et al. 2013) At high concentrations, phosphorothioate oligonucleotides can cause renal tubule changes and increased risk of thrombocytopenia.(Bhagat, Putta et al. 2011)

These side effects have now been observed in GSK/Prosensa clinical trials, Limiting dosing, and thereby, the clinical value of the therapy. In contrast, the charge neutral PMO backbone appears to have less toxicity. Both pre-clinical and clinical trials reported no clearly observable toxicity although transient renal tubular particle accumulation was observed in experimental monkeys with high doses.

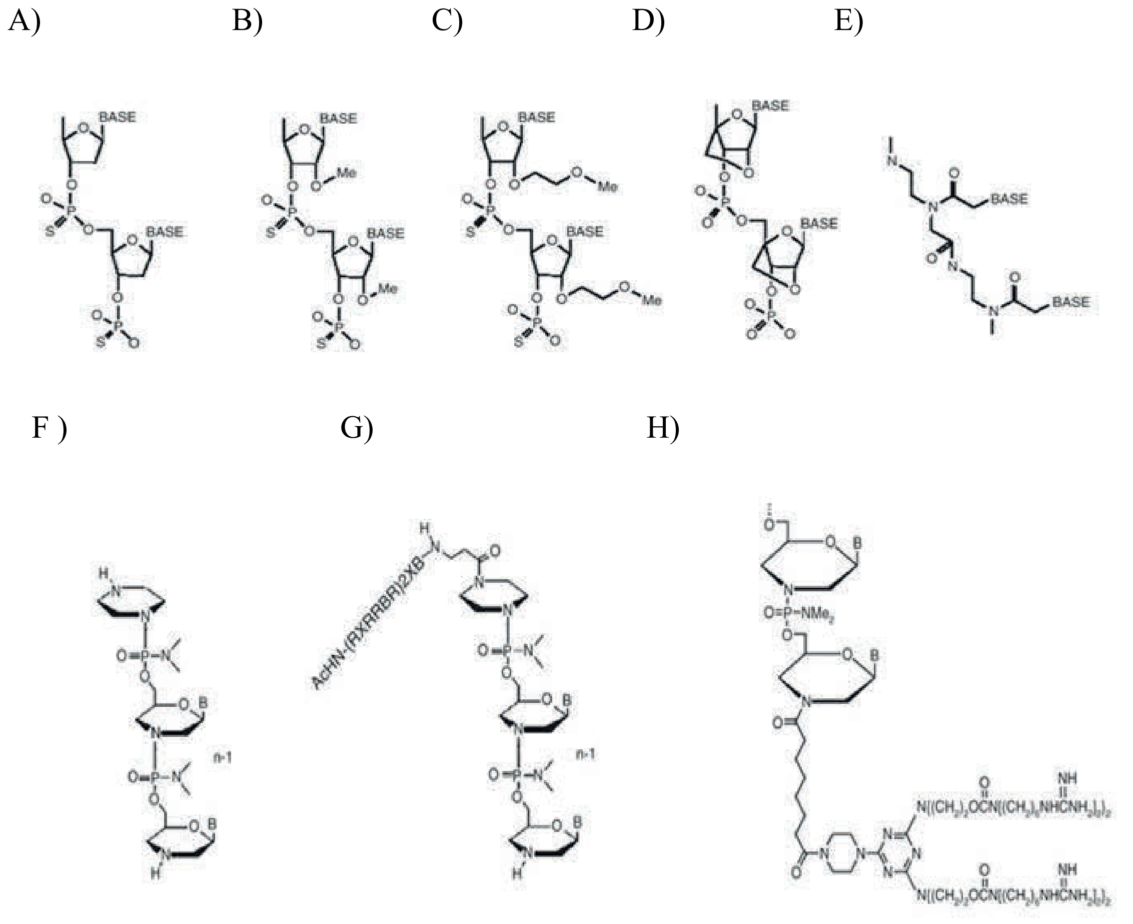

Figure 4: Antisense oligonucleotide chemistries. Chemical structures of typical AONs: phosphorothioate oligomer (b) 2'-O-Methylphosphorothioate (2'OMe) (c) 2'-O-Methoxyethyl phosphorothioate (2'MOE) (d) locked nucleic acid (e)peptide nucleic acid (PNA) (f) phosphorodiamidate morpholino oligomer (PMO) (g) AcHN-(RXRRBR)2XB peptide-tagged PMO (Vivo PMO) (h) octa-guanidine PMO (PPMO)

1.4.2 PMO delivery

The stability, low toxicity and relatively higher efficacy make PMO the most promising antisense oligonucleotide chemistry currently available. Again, the efficiency with PMO alone *in vivo* remains too low for achieving long term efficacy for DMD patients. This challenge has lead to extensive efforts to modify PMO with delivery moieties for enhanced delivery. The earliest effort to improve PMO delivery was based on the consideration that low delivery efficiency is the result of neutral charge of the molecule. Gebski et al, designed a complementary DNA sequence (termed a "leash") to complex PMO (Bruno et al. 2004 ; Gebski et al. 2003) . The leash provides negative charge to the DNA/PMO complex, such that commercially available gene/oligo delivery reagents, such as polyethyleneimine (PEI) and Lipofectamine could be used for enhanced delivery.

However, the improvement in exon skipping in cell culture was limited and the toxicity of the complex was much higher than simple PMO due to the use of positively charged delivery reagents. The leash/PMO/lipofection complex delivery was highly toxic, and was thus not continued for use *in vivo*.

A number of studies have approached the problem of morpholino delivery efficiency through combining administration with potentially complimentary compounds.(Wehrens, Lehnart et al. 2006, Kendall, Mokhonova et al. 2012) While highly stable, the relatively low level of charge of morpholino oligonucleotides reduces PMO delivery and intracellular uptake. The necessity of charge to overcome the hurdle of poor PMO uptake has led to development of directly modified morpholinos in an attempt to increase delivery efficiencies. Additionally, attempts have been made to modify morpholinos with peptides of specific sequence, such as TAT and others. (Zhang, Tung et al. 2006). Most prominent however is the modification of morpholinos with non-specific Octaguanidine, and poly-arginine additions to the 3' or 5' ends of constructed morpholinos. (Alonso, Stein et al. 2005, Yuan, Stein et al. 2006, Abes, Arzumanov et al.

2007, Moulton, Fletcher et al. 2007, Abes, Arzumanov et al. 2008, Lebleu, Moulton et al. 2008, Moulton and Jiang 2009, Yin, Moulton et al. 2010, Kang, Malerba et al. 2011, Neuman, Bederka et al. 2011, Popplewell, Abu-Dayya et al. 2012) Efficiency of PMO-induced exon skipping is improved with PMO conjugated with positively charged delivery-enabling polymers. Jearawiriyapaisarn reported that PMOs conjugated with a peptide of (RXRRBR)2XB (PPMO) enhance their potency in a GFP reporter transgenic mouse.(Jearawiriyapaisarn, Moulton et al. 2010). In the dystrophic *mdx* mice, Wu et al reported that systemic delivery of the PPMO produces dystrophin to near normal levels in most skeletal muscles by a single dose of 30mg/kg i.v. injection.(Wu, Lu et al. 2012) Regular systemic administrations are able to maintain the similar levels of dystrophin with significant improvement of muscle pathology and functions. Even cardiac muscle can be induced to express significant amount of dyustrophin after regular i.v. injections. These treatments have also demonstrated increased muscle strength and prevents cardiac pump failure induced by dobutamine stress *in vivo*. Similar to the PPMO, PMO tagged with a non-linear, non-peptidic octaguanidinium dendrimer (Vivo-PMO) is also able to produce near normal levels of dystrophin in the *mdx* mice.(Wu, Li et al. 2009) However, these strong cationic peptides and polymers are non-specific with high toxicity. The LD 50 of the less toxic PPMO is about 100mg/kg, and would therefore be high risk for clinical trial. (Summerton 2007, Moulton and Jiang 2009) (Lu, Yokota et al. 2011, Kole, Krainer et al. 2012) These chemistries and their unique structures are illustrated in figure 4 and figure 5.

1.4.3 Mechanisms of antisense oligo delivery to muscle *in vivo*

With the current chemistry and delivery methods of antisense oligo therapy for DMD, one significant limitation is the non-specific delivery of the therapeutic oligos. One feature observed with all oligonucleotide chemistries is that expression induced by systemically delivered AON is highly variable with very limited number of fibers expressing near normal levels of dystrophin. Variation can be observed between individual muscles and within muscles as groups of dystrophin positive fibers can be seen right adjacent to completely dystrophin negative fibers. Such variation is of great importance for achieving therapeutic effect in the body-wide affected muscles of DMD patients. The focal distribution of oligo delivery is not related to the fiber types, and neither to the levels of fiber maturation.(Lu, Rabinowitz et al. 2005) Studies of dystrophin induction by AON and muscle damage suggested that efficiency in oligo delivery is related to a more permeabilized vasculature system and fiber membrane. This leads to the hypothesis that delivery efficiency of the negatively charged 2OMePS and neutral charged PMO AON *in vivo* is closely related to the process of muscle degeneration and the delivery mechanism of these unmodified AONs is likely to be a process of passive diffusion. The likely repulsion of the negatively-charged 2OMePS AONs and the neutral charged PMO to the molecules at the surface of cell membranes would be expected to hinder efficient delivery of the AON into target cells with intact membrane, and thus the lower efficiency of antisense effect in normal fibers and those fibers with minimum membrane permeabilization. This is now supported by lower efficiency of AON delivery in normal muscle when compared to delivery efficiency in

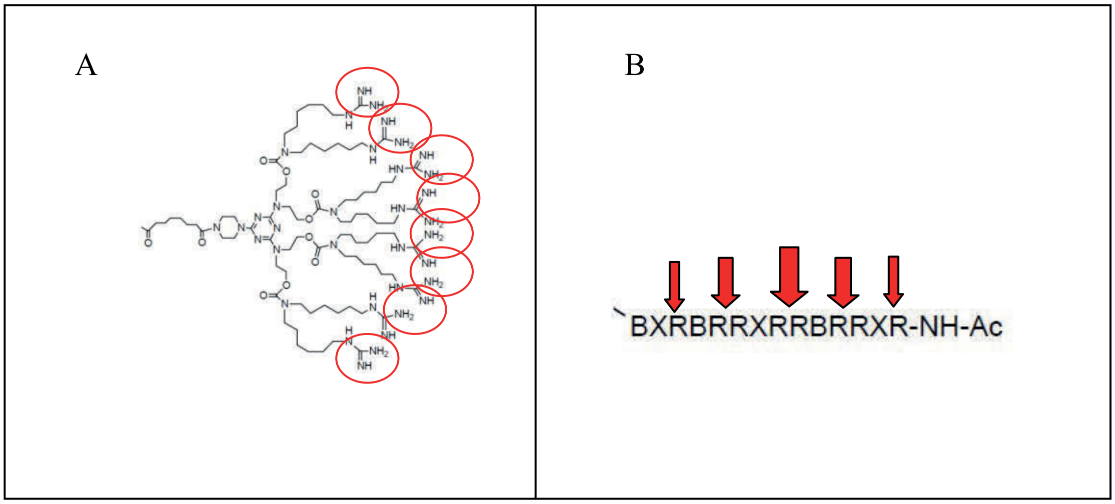

Figure 5: Chemical structures of modified PMO. Phosphorodiamidate morpholino oligonucleotide (PMO) commercially available. A) The poly-arginine Vivo-Morpholino (Gene Tools) and B) the (RxRRBR)$_2$XB motif-bearing Peptide-PMO (PPMO) Where B denotes β-alanine, R-Arginine,Ac-Acetyl and X-6-aminohexanoic acid (AVI) (Adapted from Moulton et al, 2009) To illustrate the densely charged groups within these PMO modifications, they have been highlighted in red.

dystrophic muscles. The dependence on muscle damage for effective delivery of AONs presents a potential barrier for effective treatment of DMD.(Alter, Lou et al. 2006) This model would predict that muscle fibers rescued earlier by AON-induced exon skipping, might have to reenter a myopathic state before they could again be protected by further entry of AON. Such a requirement for recurring cycles of rescue and degeneration in treated muscles would severely limit the value of antisense therapy for DMD patients. From all the reports of studies of oligo therapy, specifically from studies of antisense therapy to DMD, it becomes clear that successful application of antisense oligo for any disease treatment, especially for long term treatment, high efficiency tissue specific delivery of antisense oligos are the keys and two divergent approaches can be envisioned: developing new polymers for effective delivery with low toxicity, and identifying ligands for tissue specific targeting.

1.4.4 Polymer mediated AON delivery and toxicity

Increasing delivery of therapeutic oligos through the use of cationic peptides as well as synthetic polymers to impart cationic charge has been the subject of much research. Most AON molecules are net negative (2OMePS) or neutral charged (PMO) and do not easily cross cell membranes (Summerton 2007, Moulton and Jiang 2009). Use of cationic polymers and peptides, such as poly-arginine peptides and cationic dendrimers is intended to increase binding affinity of the AON/polymer complex to cell membrane and facilitate the entry to cells. The enhanced transfection efficiency is therefore apparently directly related to the intensity and the density of the charge. However, properties such as densely charged units are also similarly correlated to increases in toxicity when increased concentrations are applied to approach optimal transfection efficiency.(Wu, Li et al. 2009, Jearawiriyapaisarn, Moulton et al. 2010, Wu, Lu et al. 2012) While the exact mechanisms for the toxicity are not fully understood, it has been suggested that these charged moieties *in vivo* are likely binding to many negatively charges molecules, especially within the circulatory system, the endothelial wall, and extracellular matrix components. Such interaction will interfere with normal cell functions and interaction between those bound molecules to their normal companions. The internalized cationic polymers and peptides can also lead to cytotoxicity upon lysosomal degradation.

For these reasons, synthetic polymers composed of ethylene glycol (PEG), and Pluronics (amphiphilic) together with cationic polymers such as ethyleneimine (PEI), have been constructed to create a range of charge and resistance to provide a more balanced charge and hydrophobicity/hydrophilicity with the aim to promote interaction between the AON/polymer complex and cell membranes for uptake while only inducing tolerable toxicity when used *in vivo*. Examples include the copolymer of PEG-PEI-Pluronic and PCM construction for delivery of AONS. The combination of such copolymers with AONs results in a polyplex that is stable in physiological conditions and has sufficient charge to increase delivery efficiencies. Synthetic copolymers have been reported to bypass toxicities resulting from degradation, as innate enzymes for depolymerization or destruction are not present in natural systems and/or existing systems are unable to recognize or access points of possible cleavage. However, nearly all of the reported copolymers improving AON delivery efficiency *in vitro* lack efficacy and present toxicity when tested *in vivo*. Modifications shown to markedly improve delivery efficiencies *in vitro* have nearly always been associated with significant toxicity *in vivo,* which prevents progression of any such compound from further development (e.g. PEI 25k). Again while studies in polymer mediated delivery have demonstrated success in a number of applications *in vitro*, no copolymers have been reported with any muscle tissue specificity, especially in systemic administration.(Hubbell and Chilkoti 2012) Thus, effective polymers having low toxicity and/or muscle targeting property remain to be developed. The lower efficiency and non-specificity in delivery is not limited to antisense oligo therapy for exon-skipping, but also to many other applications of RNAi as drugs and gene therapy.

1.5 Synthetic Polymers as Non-Viral Delivery Vehicles

For achieving therapeutic effect for muscular dystrophies, AON, including PMO, must be delivered systemically. Therefore, AON drugs have to first survive in the blood circulation without significant degradation. The drug also needs to be maintained in the circulation long enough to allow effective penetration into specific tissue. This requires the drug to avoid rapid filtration by the kidneys to keep the agent in circulation. In order to reach intended targets the agent must then be able to escape the vasculature to tissue interstisium. This will be followed by the interaction of drug AON with the ECM components before they have the opportunity to encounter the target cell membrane. The efficiency of membrane penetration is also critical for overall efficiency of the AON delivery. Those AONs successfully entering the cells still require avoidance of cellular mechanisms, such as harsh pH of endolysosomes, and protease and/or nuclease that might degrade AONs, render them in useless compartment or impede the entry to specific cellular zones, such as nucleoli for their intended target and where they will have the opportunity to bind to their target sequences and serve their function such as splicing modulation. Clearly, the properties of compounds required to complete each step successfully will be different, and one compound with limited biochemical properties is unlikely to be sufficient to accomplish these multiple tasks. These numerous and complex barriers to delivery are the principle causes which make developing optimal delivery compounds or systems extremely challenging.

One possible solution for the challenges is to develop compounds with multiple biochemical properties. Previous studies have evaluated some of the approach largely for gene therapy. Only limited studies have been conducted for AON delivery in animal models. One of the most commonly used approaches is the combined use of polymers with different chemical properties. For example, co-polymers containing Polyethylene glycol (PEG), Polyethylenimine (PEI<10kd) and Poloxamers (Pluronics) have been examined for DNA based gene delivery. (Cho, Choi et al. 2006, Hao, Sha et al. 2009, Wang, Lu et al. 2013). This combined polyplex approach has also been used for oligonucleotide delivery with increased transfection efficiencies *in vitro* as well as *in vivo* and without additional toxicity as compared to the individual components of the polyplex.

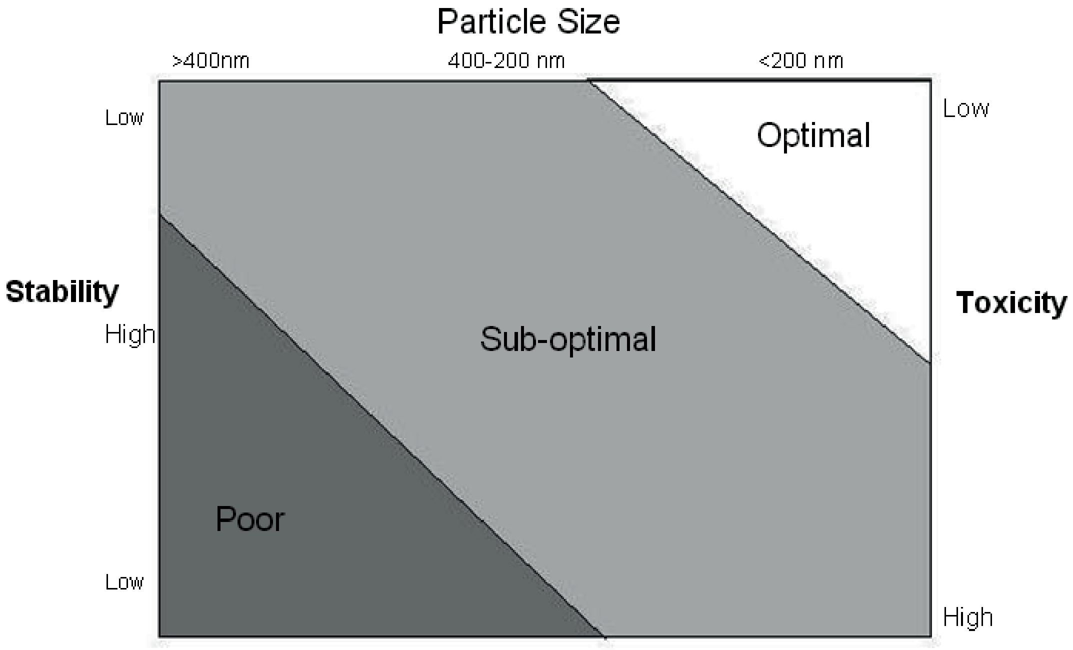

Figure 6: Graphical representation of optimal gene-delivery vehicle characteristics. This figure demonstrates the fine balance across particle size, transfection efficiency: cytotoxicity, and stability, necessary for most effective results.

Increasingly intricate polyplex construction examples include that of Zhang et al who tested a chelator-containing Tat peptide conjugated to a radiolabeled PMO AON to study cellular uptake and kinetics, or Alonso et al who used a peptide conjugated-PMO to block infectious hematopoietic necrosis virus *in vitro*.(Alonso, Stein et al. 2005, Zhang, Tung et al. 2006) While design and construction with core-shell component construction, inclusion of affinity ligands for targeting, and bioactive units continues, a careful review of the reported results indicate that increasingly complex delivery vehicles provide only marginal improvement.

However, all such copolymers either as a simple mixture or conjugated onto the target oligonucleotides have not been able to achieve significant enhancement for AON delivery *in vivo*. These results indicate that fine balance is needed for efficient oligo delivery with low toxicity and this will not be easily established. (Bates, Hillmyer et al. 2012, Jager, Schubert et al. 2012)

With a focus on AON delivery for DMD, the McColl Lockwood lab has been conducting series of studies developing and testing copolymers for both gene and AON delivery. Applying the principles known to be important for the delivery of negatively charged nucleic acids, the laboratory synthesizes copolymers, Poly ester amine (PEAS) with tris[2-(acryloyloxy)ethyl]isocyanurate (TAEI) as linker to low-molecular-weight polyethylenimine (LPEI, Mw 0.8k, 1.2k, and 2.0k) and evaluated their effect for gene delivery *in vitro* and *in vivo*.(Wang, Tucker et al. 2012) The results showed PEAs can effectively condense plasmid DNA with particle sizes below 200 nm and surface charges between 11.5 and 33.5 mV, considered to be optimal for delivery. The PEAs composed of PEI 2k showed higher transgene expression compared to PEAs of PEI 0.8k (A series) or 1.2k (B series) with significantly lower cytotoxicities when compared with PEI 25k in two different cell lines. Improved gene transfection efficiency was achieved in CHO, C2C12 myoblasts, and human skeletal muscle (HSK) cell lines. Increased transgene delivery and gene expression was also achieved as compared with PEI 25k *in vivo* through intramuscular administration with no obvious muscle damage. These results indicate the potential of the biodegradable PEA polymer series as safe and efficient transgene delivery vectors. The study is also unraveling one dilemma of using PEIs as gene/oligo delivery polymers. HPEI is highly effective for gene delivery, but also highly toxic; whereas LPEI alone is not effective for gene delivery, although it is effective in binding plasmid DNA with only limited toxicity. One possible explanation for the differential effect between HPEI and LPEI is that the LPEI/transgene complex does not form particles with optimal size(s) for effective internalization. However, when LPEIs were linked to a linker molecule, the lower toxicity maintains, but the delivery efficiency can be greatly enhanced. This is clearly related to the fact that the copolymer contains more than one LPEI unit, and becomes more effective to form conjugates with the plasmid DNA with optimal sizes for delivery (Wang, Bioconjugate Chem 2012)

Similarly, copolymers (PCMs) with low molecular weight polyethyleneimine (LPEI) conjugated to Pluronic and composed of relatively moderate size (Mw: 2000–5000 Da), intermediate HLB (12–23) of Pluronics, and LPEI produce much higher gene delivery efficacy and less cytotoxicity as compared with PEI 25k in C2C12 myoblasts and CHO cells *in vitro*. The PCM series, effective oligo delivery vehicles, were also able to enhance gene delivery in mdx mice *in vivo*. We then applied PCMs for the delivery of 2OMePS oligos which are also negatively charged. The PCMs retain strong binding capacity to 2OMePS oligos with the formation of condensed polymer/oligomer complexes at a wide-range of weight ratios. The condensed polymer/oligomer complexes form 100–300nm nanoparticles with tolerable polydispersity. Exon-skipping effect of 2OMePS was dramatically enhanced with the use of the most effective PCMs in comparison with 2OMePS alone in both cell culture and *in vivo*, respectively. More importantly, the effective PCMs, especially those composed of moderate size (2k–5kDa) and intermediate hydrophilic–lipophilic balance of pluronics, enhanced exon-skipping of 20-OMePS with low toxicity as compared with Lipofectamine-2000 *in vitro* or PEI 25k *in vivo*.

We have also applied PCMs for their potential to enhance delivery of Phosphorodiamidate morpholino oligomer (PMO) *in vitro* and in dystrophic *mdx* mice. Although the PMO molecules are nearly charge neutral, PCM polymers formulated with PMO can form some degree non-stable particles, most likely through their hydrophobic interaction with the hydrophobic component within the pluronics. The formulation of PMO with the PCM polymer containing pluronics of molecular weight (Mw) ranging 2–6 k, with hydrophilic-lipophilic balance (HLB) 7–23, significantly enhanced PMO-induced exon-skipping in a green fluorescent protein (GFP) reporter-based myoblast culture system with dystrophin exon 23 as the skipping target and demonstrated a significant increase in exon-skipping efficiency in dystrophic *mdx* mice.(Wang, Wu et al. 2013) Consistently, PCMs of moderate size (2–6 k) and intermediate HLB have been most effective whereas more hydrophilic polymers were found to be ineffective for PMO delivery. Furthermore, more hydrophobic polymer showed higher toxicity. Observed cytotoxicity of the PCMs was in general lower than Endo-porter and PEI 25 k. Tissue toxicity of PCMs in muscle was not clearly detected with the concentrations used, Thereby, optimization of molecular size and the HLB of pluronics were demonstrated as important factors for PCMs to achieve enhanced PMO delivery *in vivo*.

1.6 Challenges in Gene and Oligonucleotide Delivery

While restoration of dystrophin expression through exon-skipping has been clinically validated as a viable treatment for DMD, long term functional gains in patients will require dramatic increases in AON delivery efficiencies. To overcome the hurdle of systemic AON delivery efficiency, two approaches are necessary: First, increasing systemic distribution, prolonged half-lives, and stability of the AON/polymer complex through the use of copolymers; and secondly, increasing delivery to skeletal and cardiac muscle through incorporation of ligands with specificity to these target tissues. Several decades of efforts with numerous publications have demonstrated that achieving our goals of effective antisense oligo delivery (as well as to non-viral gene delivery) for therapy to human diseases has been stubbornly difficult, and remains a huge challenge for translational research to deliver these two highly promising therapeutic agents, transgenes and oligomers to the preferred target cells/tissue with sufficient amount and tolerable toxicity. Nevertheless further studies are warranted as achieving our goals will have far reaching effects on future clinical practice, not only to treatment of DMD, but many similar diseases. With more effective delivery vehicles, it can also greatly reduce the cost of the agent, such as PMO AON. One prominent example of the use of PMO is for DMD treatment. Currently, clinic trial results show that at least 50 mg/kg weekly injection is needed to achieve minimum clinically meaningful benefit to DMD boys. This will cost hundreds of thousands of dollar per boy per year. Such cost is therefore likely cost prohibitive for a great majority of patient families already burdened with the cost of concomitant therapies. Therefore, studies addressing AON delivery efficiency and tissue specificity would provide substantial information resulting in a greater number of patients having access to this therapy, at less cost, with fewer visits to the clinic. Additionally, if existing AON delivery barriers are overcome, the results could be quickly translated to delivery vehicles for treatment of many other conditions, providing a platform from which additional technologies can be developed. Further study in synthetic polymers as safe and effective therapeutic vehicles is needed.

1.7 Dystroglycanopathies

A number of congenital and limb girdle muscular dystrophies are the result of inherited mutations resulting in abnormal glycosylation of proteins of the muscle membrane that function to bind numerous extracellular proteins. There are currently 14 types of congenital muscular dystrophy and 18 types of limb girdle muscular dystrophy, ranging in severity from the early onset and severe cognitive and structural brain and/or eye abnormalities of Walker Warburg to the late onset and comparatively mild limb girdle muscular dystrophies. These forms of muscular dystrophy resulting from abnormal glycosylation are referred to as dystroglycanopathies. This nomenclature is due to the fact that some of the first and best characterized of these dystrophies are associated with abnormal glycosylation of the alpha-dystroglycan or beta-dystroglycan subunits of the dystroglycan complex (DGC).(Ervasti and Campbell 1991, Caruso, Hyeon et al. 2012) It is important to note however that this group of dystrophies also includes disorders previously referred to as syndromes, under the broad grouping of *amyotonia congenita*.(Magee and Shy 1956, Dubowitz and Crome 1969, Sparks, Quijano-Roy et al. 1993) These dystrophies result from defects in members of the glycosylation pathways for proteins of the sarcoglycan complex, defects in extracellular matrix proteins, as well as nuclear envelope and endoplasmic reticulum proteins.(Cardamone, Darras et al. 2008) Dystroglycan is a single gene (DAG1) product that is further processed into α and β subunits. The transmembrane β-dystroglycan subunit links the cytoplasmic protein dystrophin which interacts with the actin cytoskeleton, to the secreted glycoprotein α-dystroglycan. α-Dystroglycan is both N- and O-link glycosylated at its central mucin domain and is responsible for binding a number of extracellular proteins including laminin, agrin, neurexin, perlecan, pikachurin. While αDG is glycosylated with N-link and mucin-like O-GalNAc initiated glycans, research has shown that O-linked glycosylation, specifically the unique O-Mannosylation is critical for effective binding of laminin and other extracellular proteins. The appropriate glycosylation of αDG is essential for normal muscle function and degeneration/regeneration of muscle fibers. Aberrations in α-DG glycosylation result in a number of dystrophic phenotypes such as LGMD2I, WWS, MEB, CMD, MDC1C, MDC1D and others summarized in table 1. Primarily, defects in glycosyltransferase function or expression levels have been identified as the cause of phenotypes observed in a number of dystroglycanopathies. Mutations in Protein-O-mannosyltransferase 1 (POMT1) and POMT2 have been implicated in Limb-girdle muscular dystrophies LGMD2K and LGMD2N as well as the more severe Walker Warburg Syndrome. Fukitin (FKTN) is associated with WWS, MEB-like CMD, Fukuyama CMD and LGMD2M as is the highly homologous FKRP which is additionally associated with more commonly observed LGMD2I. Like-acetylglucosaminyltransferase or Like-Glycosyltransferase LARGE1 and its close homolog LARGE2 contain two different glycosyltransferase domains and catalyze the same reactions with slightly different biochemical properties. Defects in LARGE1/2 lead to hypoglycosylation of αDG, as observed in the severe WWS and the unique merosin-deficient CMD type 1D (MDC1D).(Hu, Li et al. 2011, Inamori, Yoshida-Moriguchi et al. 2012, Inamori, Hara et al. 2013) More recently, mutations causing diminished or loss of function in O-linked mannose β1, 2-N-acetylglucosaminyl-transferase (POMGnT1) and isoprenoid synthase domain-containing protein (ISPD) have been linked to MEB, WWS, and LGMD while the exact contribution to disease is still unknown.

Despite substantial advances and ongoing efforts to elucidate the genetic causes of the dystroglycanopathies, the etiologies of at least 20% of the phenotypic or pathologically observed dystroglycanopathies remain unclear, as they do not contain mutations in the currently described genes.(Oerlemans, Bult et al. 2010) This fact indicates that there are proteins and enzymes yet to be discovered and their role in disease identified and characterized.(Wells 2013)

1.8 Tissue-Targeted Delivery

1.8.1 Target consideration

Tissue –cell specific delivery has long been recognized of critical importance for gene and oligonucleotide therapy, as well as for delivery of drugs, imaging agents and proteins. Clearly, achieving such specificity will depend on the identification of ligands to specific receptors on target cells. Identifying specific molecules, the receptor, on target cells is therefore the first consideration. Such molecules ideally should be abundantly expressed at the target cell surface and have the property as receptor for ligand internalization. One of such molecules is alpha-dystroglycan, expressed abundantly in muscle tissues, but at much low levels in most of other tissues. Dystroglycan (DG) is a highly glycosylated basement membrane receptor with a role in many physiological processes, such as in the development of central neuron system. DG is critical for maintaining integrity of skeletal muscle membrane, central nervous system structure (Smalheiser and Schwartz 1987; Campbell and Kahl 1989; A. Varki et al. 2009; Oldstone and Campbell 2011) Dystroglycan is composed of two subunits, a α subunit (α-DG) and a transmembrane β subunit (□-DG). α-DG contains three domains with globular N-terminal and C-terminal domains flanking a central mucin domain and the protein undergoes extensive N-glycosylation, mucin-type O-glycosylation and O-mannosylation. α-DG binds extracellular matrix proteins such as laminin, agrin, and neurexin bearing the laminin-G-domain.(Ibraghimov-Beskrovnaya, Ervasti et al. 1992) Alterations in glycosylation, specifically hypoglycosyaltion of α-DG are a common feature observed in some muscular dystrophies collectively termed dystroglycanopathies. The diseases are the results of mutations in confirmed or putative glycosyltransferase genes as discussed in the above section (1.1). (Kobayashi, Nakahori et al. 1998; Brockington, Blake et al. 2001; Yoshida, Kobayashi et al. 2001; Beltran-Valero de Bernabe, Currier et al. 2002)

However, epitopes functionally important for the binding of ECM ligands and maintenance of membrane integrity have not been well defined. Currently, the only methods to define the functionality of the α-DG are the use of 2 monoclonal antibody, IIH6 and VI4 both recognizing sugar epitope(s) on α-DG, and laminin binding assay indicating the ability of the protein to bind to the ECM component as normal α-DG. The exact epitopes of α-DG recognized by these antibodies remain unclear, but recent report suggests that at least one repeat units of biglycan, [–3-xylose– α1,3-glucuronic acid-b1–] extended from the phosphoryl Mannose are one of such epitopes (Inamori et al., 2012).

It is likely that other functional epitopes exist and identifying them could greatly improve diagnosis, understanding of disease mechanisms and development of experimental therapy.

Relevant to muscle specific targeting, α-DG is most abundantly expressed in the peripheral of muscle fiber membrane and has been known to act as receptors for several Old World arenaviruses including LCMV, LFV, Oliveros, and Mobala viruses. Virus infection efficiency is closely related to the presence of α-DG. (Cao, Henry et al. 1998) These observations indicate that α-DG could be an effective receptor for ligand binding and internalization of muscle targeting drugs including AON.

1.8.2 Approaches and Selection of Target Ligand

The second consideration for targeted delivery of gene, AON or other drugs is the chemical nature of ligands. The importance of ligands has led to the exploitation of several classes of ligands, chiefly chemical compounds including polymers, peptides and more recently RNA/DNA Aptamers, all have the potential to be employed for delivery of oligonucleotides. The use of polymers has been discussed previously in introduction section 1.5.

1.8.3. Aptamer

Nucleotide Aptamers are single stranded DNA or RNA molecules with some binding specificity not only to complementary DNA and RNA, but also to proteins and other cellular epitopes. Therefore this technology has the potential as components of carriers for oligonucleotide delivery as well as specific drugs targeting proteins and nucleic acid sequences. Aptamers that spans 20–100 residues in length in general can be selected using *in vitro* techniques to bind target molecules with tissue and cell specificity.

Most applications of aptamers however have been for binding target proteins in blood circulation, and natural DNA/RNA aptamers are quickly degraded and cleared from circulation. A successful clinic application of aptamers is illustrated by the first aptamer-based drug, Macugen, approved by the U.S. Food and Drug Administration (FDA) in treatment for age-related macular degeneration (AMD) by OSI Pharmaceuticals. Macugen is anti-vascular endothelial growth factor (VEGF) aptamers, which bind specifically to the 165 isoform of VEGF. VEGF plays a critical role in angiogenesis. Macugen blocks VEGF to its receptor to achieve its therapeutic effect. Using aptamers of natural nucleic acids for drug delivery into cells is however difficult as they have short effective serum half-life and even more easily degraded within target cells. Despite significant efforts having been made to use chemically modified aptamers for serum/degradation resistance, the effectiveness of aptamers as vehicles for protein and oligonucleotide delivery remain to be established.

1.8.4 Peptide arrays

The cell/tissue specific peptide ligands can be selected by two main approaches, peptide library and phage-display. Small synthetic peptide libraries were initially used to study protein-protein interactions and for drug design. With the advances in peptide synthesis, it has become possible to synthesize a library of hundreds of thousands of short peptides with random or selective sequences. This in combination with the development of methods for peptides to be synthesized on solid phase, such as resin has made it possible to select peptides with specific binding affinity to cell/tissue specific proteins. Theoretically, it is possible to use either a purified protein or cells expressing specific proteins on cell surfaces to interact with an array of peptides on a chip. The bound cells or proteins can then be identified either through their markers such as GFP reporter expression or through detection of the cells by other means. Therefore, peptide array can identify peptide(s) directly with high potential of protein/cell specificity. However, currently, synthesis of large peptide library (for example with one million peptides) remains costly and un-affordable for most studies. The method has therefore mainly been used for further optimization of existing or predicted peptide(s) with a library extended from the known sequences. Another limitation is that the method is not well suited for *in vivo* peptide selection. For these reasons, phage displayed peptides are of choice as millions of peptide can be produced with limited cost and tested both *in vitro* and *in vivo*.

1. 9 Phage Array as a Method to Determine Tissue-Specific Epitopes

Bacteriophage is a collective term used to describe virus which have co-evolved with defined bacterial hosts that support the bacteriophage infection and replication. While the effect of these virus on bacteria was observed as early as 1890 and reported as an unidentified bactericidal in 1915 by Twort who hypothesized the agent was a virus, Felix d'Herelle is credited with initial characterization two years later and promotion.(Mady 2011) While bacteriophage present in a filtrate preparation from bacterial culture was reportedly used to treat dysentery years before, the nature of the bacteriophage was poorly defined until 1939 in some of the first electron micrographs by Helmut Ruska and microscope inventor and Nobel laureate physicist Ernst Ruska.(D'Herelle 1929, Chen, Zhu et al. 2013, David, Passirani et al. 2013) Bacteriophage was mostly abandoned as a therapeutic when Alexander Fleming characterized another poorly understood compound produced by the *Penicillium* mold, which he termed "penicillin" a discovery which bore life-saving antibiotics and the pharmaceutical industry. Bacteriophage research continued, resulting in identification of numerous bacteriophage and their host bacteria, and consequently produced many contributions to our current understanding of molecular biology.

The first application of bacteriophage expressing foreign DNA inserted into phage gIII gene and displaying the corresponding peptide as part of the phage coat protein was described in 1985 by George P. Smith.(Smith 1985) Since that time molecular modification and affinity screening of phage expressed peptides has enabled numerous investigators interested in determining or characterizing particular epitopes or interactions, to employ this technology. Selection of phage expressed peptides with an affinity to purified proteins, *in vitro* culture, and tissues of interest, along with basic research, provides for new understanding of disease mechanisms while also presenting potential therapeutic options. In this capacity, phage array has been used to define protein:protein and peptide:DNA interactions, enzyme catalytic sites, and to identify short peptides with affinity to specific cell or tissue types.

To date, despite numerous reports of *in vitro* specificities, minimal success has been achieved in applying phage-derived peptides to target specific tissues *in vivo*. One exception being the vascular $\alpha_v\beta_3$ targeting peptides selected *in vivo* by Arap et al. This particular success may be in part due to the high levels of ligand *in vivo*. Overall, success *in vivo* through the use of synthetic peptide or phage array has been lacking.

Recent attempts to identify muscle specific peptides have employed iterative *in vivo* selection methods, selecting for clones with greater affinity to muscle than liver, demonstrating some specificity of phage clones to C2C12 myoblasts by immunohistochemical methods and less convincingly using fluorescently labeled phage administered by systemic injection.(Seow, Yin et al. 2010)

Modification of attempts at similar or related studies with a more careful step-wise approach and controls, along with high-throughput methods could yield comparable if not more effective results.(Newton and Deutscher 2008) To date very few *in vivo* results of phage arrays have indicated much promise beyond *in vitro* and/or *ex vivo* published results.(Brown, Modzelewski et al. 2000, Brown 2000, Kelly, Clemons et al. 2006, Kelly, Waterman et al. 2006) The addition of high-throughput technologies not previously available as well as multiple disease model systems that are available in laboratories such as the McColl-Lockwood laboratory should yield a more specific and efficient methodology for selection of appropriate clones for further testing.(Brown, Modzelewski et al. 2000, Hruby 2002, Benedetti, Morelli et al. 2004, Kelly, Clemons et al. 2006, Kelly, Waterman et al. 2006, Krumpe and Mori 2006, Newton and Deutscher 2008, Yu, Yuan et al. 2009, Shi, Nguyen et al. 2010) Of particular note, is that although the panning experiments of others have been tested and reported within a tight selection of tissues and origins, present and future studies must address the ability through phage display to also study disease models of particular variation from, and including the wild-type. (Kelly, Waterman et al. 2006, Newton and Deutscher 2008)

The general procedure of a phage array in itself is neither novel nor necessarily technically challenging. Many reports have been made of success *in vitro* by others in identifying peptide ligand candidates for a variety of target molecules. Increasingly investigators are realizing that screening for specifically identified and unique receptors, such as muscle αDG must be applied in tandem with more generalized additional levels of selection such as whole cell or *in vivo* tissue selection in order to achieve significant and reproducible results. Previous studies have found the *in vitro* selection process to result in identification of multiple common peptide sequences relative to target molecules, but beyond selection methods and demonstrated affinities, provide little support for the relationship of identified ligands. The two greatest deficiencies in previous studies have been a lack of translation from *in vitro* results to *in vivo* application, and likely biased selection of peptides to targets in non-native states. One aim of the study reported in chapter 4 is focused on preliminary selection of phage clones which express peptides with a high affinity for both native and modified muscle targets.

The literature associated with muscle specific targeting through the use of phage array or synthetic peptide is limited to only a handful of reports. Although some common findings have been reported, all of these studies present *in vitro* results without reproducible application *in vivo*. The combination of purified components, followed by selection against specific positive and negative control cell types with careful iterations should result in a refined sub-library from which the majority of results are of value. This uniquely hypothesis driven potential is afforded by the stringent experimental design leveraging the best knowledge and models of disease available.

Whole and fractionated whole cell lysates, CHO derived purified α-Dystroglycan will be used as target molecules in multi-well format for screening of phage binding. Stable CHO cell lines with reduced LARGE and α-Dystroglycan expression will be used in selection as negative controls. As shown in the project schematic [Appendix 1] of this proposal. Although it may be only omitted from final publications, refinement of the sub-library is an important step before further experimentation. While the goal of the project overall is to achieve a small number of specific muscle-binding bacteriophage clones, it is important that any one phase of selection not eliminate a viable and unique clone. Given the sheer number of clones from the initial library, upwards of 1x10^{15} variations of phage-expressed dodecapeptide sequences, binding clones with less than maximum affinity in the array may be discarded as non-binding. Maximizing the number of binding clones with a variety of affinities will increase the overall chance of success in further testing or application.

Although the target selection affinity may be effective *in vitro* and *ex vivo*, certain conditions *in vivo* may limit the ligand availability, including conformational or other modification of ligands and/or receptors.

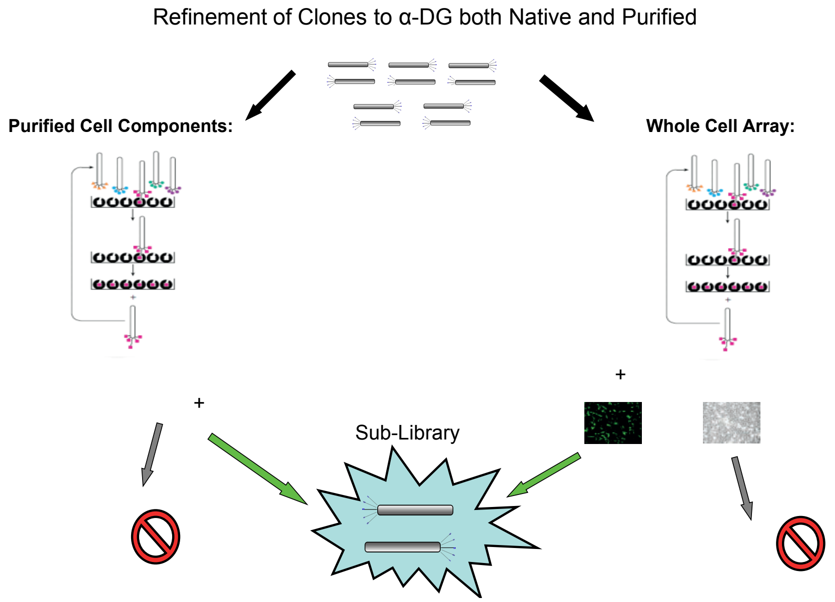
Refinement of Clones to α-DG both Native and Purified
Purified Cell Components:
Whole Cell Array:
+
+
Sub-Library

Figure 7: Schematic diagram of phage array procedure and selection.

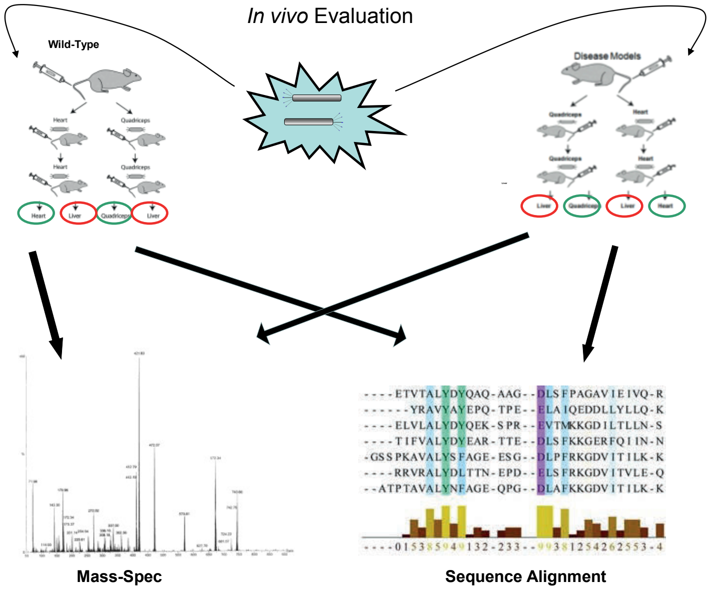
In vivo Evaluation
Wild-Type
Heart
Quadriceps
Heart
Quadriceps
Heart
Liver
Quadriceps
Liver
Disease Models
Quadriceps
Heart
Quadriceps
Heart
Liver
Quadriceps
Liver
Heart
----ETVTALYDYQAQ-AAG--DLSFPAGAVIEIVQ-R
------YRAVYAYEPQ-TPE--ELAIQEDDLLYLLQ-K
----ELVLALYDYQEK-SPR--EVTMKKGDILTLLN-S
----TIFVALYDYEAR-TTE--DLSFKKGERFQIIN-N
-GSSPKAVALYSFAGE-ESG--DLPFRKGDVITILK-K
----RRVRALYDLTTN-EPD--ELSFRKGDVITVLE-Q
--ATPTAVALYNFAGE-QPG--DLAFKKGDVITILK-K
----01538594913 2-233--99381254262553-4
Mass-Spec
Sequence Alignment

Figure 7 (Continued): Schematic diagram of phage array procedure and selection.

The selected clones from the previous arrays for particular ligands, cell types, or affinity should be applied systemically *in vivo* to both a WT control and for this study a muscular dystrophy disease model mouse. This delivery should have certain defined time points as the majority of delivered phage will become dispersed and eventually concentrated most likely in the liver/kidney for elimination. There are a number of reports claiming to have successfully identified novel muscle binding peptides. Primarily these have been selected *in vitro*. The reported *in vivo* results seem less than convincing.(Seow, Yin et al. 2010) One of the unique attributes are the animal models of disease. These animal models range in severity and phenotype, but are closely tied to the genetics that result in a number of dystrophies. These include the *mdx* mouse model along with FKRP mutant P448L and I276L mice. Along with comparison to wild-type mice, studies of bacteriophage arrays for muscle targeting in these models may yield some useful information. Along with a variety of observable phenotypes, the pathology and accordingly physiology of these mice is also varied. It is reasonable to expect that as a phage array is performed individual clones will perform better in binding this assortment of tissue epitopes while others maintain a minimal shared sequence for binding.

Unlike previous reported studies, which focused on the systemic delivery, dispersion and binding affinity for muscle tissues, this aim is to refine and characterize those high affinity clones from prior study within certain disease states. *Ex vivo* tissues in homogenate and plate-fixed sections will be used to further characterize the binding of phage clones, epitope loci and dispersion. Comparatively, when this array is performed using tissues from the dystrophic mice along with WT mice, that affinity or loci of binding may be altered. Quantitative results may be obtained by performing either ELISA or blot densitometry.

Although there have been suggested sequences yielding a muscle targeting peptide the evidence of an effect *in vivo* is not convincing. Complete specificity is not possible *in vivo* due to system complexity. However, sufficient targeting to be discernible as compared to non-targeted tissue types would be both informative and applicable. A selected set of sequences with the highest specific affinity throughout the experiments would present viable peptides for epitope detection, specific drug or biologic therapy delivery, and potentially a better understanding of expression or function of cell surface molecules in diseased states.

Once a “best set” of clones have been selected through the previous experiments, a select set of these clones will be sequenced to determine common conserved, as well as variant regions as compared to previous phage clones, murine and human genome by bioinformatic methodology, and by comparison functionally to currently reported antibodies and agonists/antagonists for ligands and targeted receptors.(Paul G. Higgs 2005) If a promising peptide sequence is found with reliable affinity to target muscle tissue, this sequence could be incorporated into a synthetically produced peptide to be studied on its own in multiple endeavors.

1.10 Specific Aims

As previously detailed in this chapter, without effective treatments to address the cause of disease, one of the most effective experimental therapies for DMD is oligonucleotide therapy. This therapeutic approach employs specific antisense oligonucleotides (AON) to correct the disrupted reading-frame created by inherited mutations through a process called exon skipping. AONs designed to target and bind a specific sequence of pre-messenger RNA interfere with normal splicing processes resulting in excision of mutation bearing exons, effectively converting the severe DMD phenotype to a milder BMD-like phenotype through truncated but functional dystrophin protein produced from the altered mRNA transcript. There have been many AON chemistries, but the high stability and low toxicity indicate phosphorodiamidate morpoholino (PMO) to be the most promising AON chemistry with studies in animal models and clinical trials demonstrating clear benefits to subjects, a rare success in pharmaco-genetic interventions. However, low efficiency and non-specific delivery remain critical barriers of PMO therapy to achieve long-term efficacy in DMD and other diseases.

To overcome these barriers two approaches are possible, developing new polymers for effective delivery with low toxicity, and identifying ligands for tissue specific targeting. Increasing delivery of therapeutic oligos through incorporation of cationic peptides and other polymers has been the subject of much research, however cationic peptide modifications which increase transfection efficiency, also increase toxicity as a result of strong positive charges of amino acids at such high density. Similarly, cationic poly-arginine peptides and cationic dendrimers in combination or in conjugation with PMO, are able to greatly improve delivery efficiencies, these modifications present significant toxicity *in vivo* preventing them from clinical trial. My attempt for this thesis is to test the hypothesis that tissue specific ligands can be identified and effective muscle targeted AON delivery can be approached by testing modified polymers.

My initial studies involved the examination of several novel classes of compounds for enhanced delivery of specific PMO AON for exon skipping in DMD models. These studies, together with knowledge accumulated through study of current literature for gene and oligo delivery have identified several critical characteristics of polymers for enhancing delivery of oligomers and transgenes. 1) Cationic polymer components, such as PEI appear to be essential for interaction between polymers/oligomers and especially cellular components. 2) While high molecular weight PEI with mw 25K cannot be used clinically because of high toxicity and short-circulation time, low molecular weight PEI remains effective to form nano-sized particles to deliver plasmid or oligomers with high efficiency and low toxicity. 3) Amphiphilic polymers such as Poloxamers (Pluronics) can provide essential hydrophobicity for the interaction of oligomers with hydrophobic membranes, thus enhancing delivery. 4). Balance between hydrophobicity and hydrophilicity is likely critical for delivery efficiency and acceptable toxicity. Systematically combining and balancing these components could maximize synergistic characteristics, uniquely increasing transfection efficiencies *in vitro* and *in vivo*, without additional toxicity.

Based on these hypotheses, a new class of poly(ester-amine) (PEAs) conjugated to PMO AON were tested in cell culture and *in vivo* through local and systemic administration, and their efficiencies in transfection, exon skipping and restoration of dystrophin were evaluated. I used PMOs targeting the mutated mouse dystrophin gene, and human dystrophin exons, thus likely relevant to clinical application of our target.

Another, more ideal approach to enhance delivery of PMO, or AON and transgene in general, without increasing toxicity would be to employ ligands as tissue specific, or muscle specific receptors as part/or whole of delivery vehicles. To date, no ligand with validated muscle specificity has been available for use. Identification of peptide ligands to accessible targets that are highly expressed in muscle tissue remains elusive. One such target in muscle tissue is the highly glycosylated receptor alpha-dystroglycan (α-DG), expressed at higher levels in muscle than other tissues. This glycosylated protein has been used by many viruses as the receptor for infection. With this in mind for my study, I attempted to use high throughput phage-array methods to select ligands specific to this protein with glycosylation mutant CHO cell lines. CHO cells overexpressing the like-glycosyltransferase (LARGE) which produces highly hyper-glycosylated α-DG, thus ideal for selective enrichment of phage peptides. Additionally, wild type (C57Bl6) and mice lacking functionally glycosylated α-DG (FKRP P448L mutation) were used to as positive and negative muscle tissue controls. Performing these studies address the sub-hypothesis that identification of small peptides can produce ligands specific to muscle tissue by affinity to glycosylated α-DG, demonstrating an effective method which can be applied for selection of peptide to any target tissue and cells.

Collectively, these experiments address one of the currently most challenging issues in translational research aiming to apply promising experimental therapies to treat human diseases, the low and non-specific delivery of therapeutic agents, oligonucleotide and transgene to preferred targeted cells *in vivo*. Thus, addressing the premise that synthetic polymers for gene delivery can be modified for targeted delivery, and that building upon advances in synthetic polymers as safe and efficient delivery vehicles, can be combined to benefit a potential therapy toward realistic *in vivo* and clinical applications. Essential information obtained through these studies will contribute to the collective understanding of oligonucleotide and gene delivery vehicles, especially for delivery of PMO AON for effective clinical treatment of Duchenne and other muscular dystrophies. To address this goal, I have identified the following specific aims:

- Specific Aim 1: To study synthetic polymers of PEG, PEI, Pluronic, and TAEI subunit construction as effective PMO delivery systems.

In previous studies of polymer development for gene and oligo delivery in the McColl-Lockwood Lab, we have identified several critical characteristics of polymers for enhancing delivery of oligomers and transgenes. First, cationic polymer components, such as PEI appear to be essential for interaction between polymers/oligomers and cellular components. While high molecular weight PEI cannot be used clinically because of high toxicity and short-circulation time, low molecular weight PEI remains effective to form nano-sized particles to deliver plasmid or oligomers with high efficiency and low toxicity. Second, incorporation of ethylene glycol (PEG) subunits has been shown to reduce toxicity, increase circulation time, and improve biocompatibility. Third, poloxamers (Pluronics) with an amphiphilic nature can be incorporated to provide essential hydrophobicity for the interaction of oligomers with hydrophobic membranes necessary for transfection, thus enhancing delivery. Systematically combining these components could maximize synergistic characteristics, uniquely increasing transfection efficiencies *in vitro* and *in vivo*, without additional toxicity. The proposed study will focus on one class of such polymers containing PEG, PEI, Pluronic, TAEI construction, to be tested with PMO in cell culture and *in vivo* through local and systemic administration.

- Specific Aim 2: To evaluate this new class of poly(ester-amine) (PEAs) as directly conjugated modifications to phosphorodiamidate (PMO) AON through experiments performed *in vitro* and *in vivo*, to determine their efficiencies in transfection, exon skipping and restoration of dystrophin.

I used PMOs targeting the mutated mouse dystrophin gene, and human dystrophin exons, thus likely relevant to clinical application of our target. To determine if this new class of synthetic poly(ester-amine) (PEAs) conjugated directly with therapeutic phosphorodiamidate morpholino (PMO) oligonucleotides can improve delivery *in vitro* and *in vivo*, optimal polymers were selected from those characterized in our previous studies, to be conjugated to PMO. The net-neutral charge of PMO is a feature that attributes to the stability of this AON chemistry, yet also results in a molecule that is non-specifically internalized through passive diffusion, requiring additional modification or delivery vehicle to increase transfection efficiency and intended therapeutic effect. While I and my study partners have demonstrated the benefit of PEA polymers for gene and AON delivery, another means to impart the beneficial characteristics of these polymers to PMO delivery is through direct conjugation of the polymer to PMO. Conjugation of PMO to selected polymers will result in a net cationic charge imparted by synthetic polymer additions. Polymer-PMO conjugates will be tested for potential to extend the effects in muscle tissues, and restore dystrophin expression. These experiments will address the sub-hypothesis that synthetic polymers employed as delivery vehicles, can also act as safe conjugates to increase PMO delivery without increasing toxicity. These experiments will build upon advances in synthetic polymers as safe and efficient delivery vehicles, combining established methods to benefit a validated therapy toward novel translational therapeutics. Essential information obtained through these studies will contribute to our understanding of gene delivery vehicles. Most importantly, these studies would address the specific problem of low AON delivery efficiencies, a critical barrier to efficient treatment of Duchenne and other muscular dystrophies.

- Specific Aim 3**:** To identify ligands through phage display with specificity to the glycosylated muscle membrane protein α-Dystroglycan.

The previous aims approach improving gene and oligonucleotide delivery efficiencies through the application of synthetic polymers, through incorporation of beneficial chemical component characteristics. Another possible approach to enhance delivery without increasing toxicity would be to employ ligands for a muscle specific receptor as part of delivery vehicles. To date, no ligands with validated muscle specificity are available for use. Identification of peptide ligands to accessible targets that are highly expressed in muscle tissue remains elusive. One such unique target in muscle tissue is the highly glycosylated receptor alpha-dystroglycan (α-DG), expressed at higher levels in muscle than other tissues. The proposed studies will use high throughput modifications to traditional phage-array methods with selection employing glycosylation mutant CHO cell lines, and characterized using myofibroblasts and ex-vivo muscle samples. In one selection method CHO cells hyper-glycosylated by like-glycosyltransferase LARGE, as well as wild type and mutant mice lacking functionally glycosylated α-DG (P448L) will be panned with phage libraries to identify small peptides with affinity for glycosylated α-DG. Performing these studies will address the sub-hypothesis that identification of small (7-mer, 12-mer) peptides can yield ligands specific to muscle tissue through affinity to glycosylated α-DG. Additionally, these studies will provide additional information about the cell and animal models used, the value of the unique approach employed, and applications of ligands or peptide motifs identified through selection.

Approach: Research Design

Specific Aim 1: To study Tris[2-(acryloyloxy)ethyl]isocyanurate Cross-linked Polyethylenimine (poly ester amine PEA) polymers for effective PMO delivery

Experimental design for specific aim #1

In this aim I will employ poly(ester-amine) polymers of Tris[2-(acryloyloxy)ethyl]isocyanurate Cross-linked Polyethylenimine construction in two experimental subaims to determine the relative importance of polyplex characteristics on efficacy and toxicity *in vitro*, and *in vivo* local and systemic administration. Polymer construction and characterization will be performed along with Dr. Mingxing Wang, Carolinas Medical Center, Charlotte NC. Polymers will be constructed of low molecular weight (M_w: 0.8k, 1.2k, and 2.0k) LPEI cross-linked with TAEI.(Cho, Choi et al. 2006, Hao, Sha et al. 2009, Wang, Lu et al. 2012) Polymer samples will be dialyzed using a spectrapore membrane with MWCO 2k against 10% ethanol, and lyophilized. Each of the polymer samples will be analyzed by MALDI-TOF-mass spectroscopy for molecular weight and apparent subunit composition. The polymers will then be characterized with and without addition of phosphorodiamidate morpholino antisense oligonucleotide, previously selected to target the mutated mouse dystrophin gene.

Subaim 1.1: In the first series of experiments I will employ a set of analyses for the purpose of characterizing each of the polymers constructed. The binding potential and stability of each polymer will be assessed after mixing with control oligomers (20bp) or PMO at ratios of [(1:1, 2:1, 5:1, 10:1) polymer:oligonucleotide] followed by agarose gel electrophoresis. Paired sets from the binding experiment will be used for analysis by digital light scattering to determine the effective particle size and degree of homogeneity. Stability of the polyplex in the presence of serum (FBS) from 0-50% as well as in the presence of heparin will be used to identify polyplex characteristics in simulated physiological conditions. Chinese hamster ovary (CHO) and C2C12 myofibroblast cultured cells will be used to assess polymer toxicities at concentrations relative to those anticipated to be tested for systemic delivery and *in vitro* assessment of transfection efficiency. These concentrations may be modified upon preliminary toxicity results but will generally be 2, 5, 10, and 20 μg /5×10^4 cells. To standardize characterization criteria, polymers will be ranked based upon particle size, ability to effectively bind PMO to form stable particles, and CHO toxicity assessed by MTS assay using concentrations up to 20 μg to determine effects on cell viability.

Subaim 1.2: In the second experimental series, myofibroblast GFP reporter lines (e23-C2C12) will be used to test polymers alone and polymers mixed with PMO at various concentration or mixture ratios for evaluation of *in vitro* transfection efficiencies. The reporter C2C12 line contains a GFP reporter gene consisting of two parts inserted into exon 22 and exon 24, such that skipping of exon 23 results in fusion of both exons necessary for translation of GFP. This reporter system allows for efficient evaluation of many compounds, lending itself to high throughput assay and quantitative assessment by flow cytometry, and exon skipping

The proposed experiments of specific aim #1 will achieve three goals. First, I will evaluate contemporary theoretical criteria in nanocarrier design by comprehensively characterizing polymers constructed to best fit the dynamic and poorly understood criteria. Hypothesis based testing of current dogmas in nanoparticle design will lead to more concrete standards for selection of candidate polymers for systemic administration. Second, I will determine the value of our applied polymer design criteria in selection of candidate polymers when tested in established *in vitro* assays. Third, I will attempt to add definition to the poorly understood relationships between nanoparticle design characteristics, and evaluation *in vitro*, and *in vivo*; towards optimal safety and efficacy for gene/drug delivery in systemic administration. Collectively, these studies are expected to provide compelling systematic criteria for development of synthetic polymers as PMO delivery.

Experimental design for specific aim #2:

Subaim 2.1: To determine if Tris[2-(acryloyloxy)ethyl]isocyanurate Cross-linked Polyethylenimine (poly ester amine PEA) polymers conjugated to PMO can improve transfection efficiency *in vitro* and *in vivo* two subaims have been defined. In this study PEA-PMO conjugates will be evaluated *in vitro* for their capacity to increase transfection efficiencies in GFP reporter (e23-C2C12) myofibroblasts. As these PEA polymers have been selected for their unique characteristics as evaluated in previous study, the PEA-PMO conjugates will also be assessed for stability, and *in vitro* toxicity to myoblasts and CHO cultures as compared to the individual components, PEA (A12 /B12/ C12) and PMO alone, as well as commercially available PPMO and Vivo-PMO. For the purposes of characterization of polymer attributes and contribution to efficacy, PEA-PMO conjugates and simple mixtures of PMO and A12, B12, and C12, will be evaluated.

Subaim 2.2: To evaluate these PEA-PMO conjugates *in vivo* for local and systemic delivery of PMO and restoration of dystrophin expression through exon skipping in the *mdx* mouse model of DMD. Intramuscular injections of PEA polymers mixed with PMO (5ug polymer:2ug PMO), and PEA-PMO conjugates, along with PMO and saline controls, will be administered to TA muscles of *mdx* mice in triplicate. After a period of 14 days, treated and control muscles will be excised from euthanized mice and snap frozen in 2-methylbutane. These tissues will be cryosectioned and evaluated for restoration of dystrophin expression by immunohistochemical (MAN DYS 1) detection of dystrophin in serial tissue sections and western blot, RT-PCR analysis of exon-skipping, and h&e staining to assess local toxicity. Following this experimental series, PEA polymers will be administered systemically to *mdx* mice by retroorbital injection to determine tolerable doses and toxicity profiles. Based upon this data, systemic delivery by retroorbital injection will be performed along with controls, and after 14 days systemic dissections of the euthanized mice will be conducted. Collected systemic tissue samples will then be assessed for dystrophin expression by immunohistochemical (MAN DYS 1) detection of dystrophin in serial tissue sections and western blot, and RT-PCR analysis of exon-skipping.The experiments detailed in this aim will contribute to our ongoing polymer attribute characterization, and provide an evaluation of this new series of biodegradable PEA polymers in applications as PMO conjugates for enhancing PMO delivery *in vitro* and *in vivo*.

Experimental design for specific aim #3

Subaim 3.1: In this study, M13 bacteriophage libraries (NEB E8100S, E8110S) with randomized linear dodecapeptide (12-mer) and heptapeptide (7-mer) sequences encoded by a diverse set of insertions into the phage *gIII* gene “displayed” at the termini of tail fibers (pIII protein) of the phage virion will be used in an array to select peptide sequences with highest affinity to bind α-dystroglycan. To achieve selection specificity, an *in vitro* system of Chinese hamster ovary (CHO) cell lines will be used. Positive selection, will utilize glycosylation mutant CHO cells transfected with Like-acetylglucosaminyltransferase (LARGE) such that high levels of hyperglycosylated α – dystroglycan are expressed on the cell membrane.(Hu, Li et al. 2011) While negative selection to target (and experimental control) will utilize mutant Pro-5 CHO cells lacking functional glycosylation will be used for negative selection. Leveraging high throughput screening methods and technological advances in sequencing technologies, the laborious process of iterative rounds of selection will be reduced, saving time but more importantly reducing the chance of introducing a clonal bias through multiple rounds of propagation and selection. Laminin overlay and the anti- αDG IIH6 antibody will be used for competitive inhibition of epitope binding will be used when applicable to further determine likely mechanisms of affinity as well as identification of off target peptides. All of the selected, isolated and partially characterized phage clones will be employed in subaim 3.2

Subaim 3.2: In the second experimental series, isolated phage clones selected through the selection methods in subaim 3.1 will be evaluated for functional detection of α-DG, resulting in a "best set" of phage candidates. Two methods will be used to determine the functional application of peptides expressed by this sub-library of selected phage. First, those selected clones grouped as the most appropriate candidates across selection methods and primarily validated by HTS will be pooled into a larger sub-library (<100) for additional characterization. For the purpose of further evaluation of these top candidates, prior to *in vivo* screening or submission for either Sanger or NGS sequencing, this subset will be tested in an *ex vivo* assay for appropriate histological location and signal to background using cryosectioned quadricep muscles from C57 wild type and the unique P448L Neo- mouse model of LGMD generated by the McColl-Lockwood laboratory. These tissue samples represent both the normal and disease state, and like the CHO cell lines used for initial selection vary remarkably in glycosylation, as shown in the tissue samples within chapter 4, detected by IIH6 immunohistochemistry. A small proportion of the top selected clones are expected to bind targets at the periphery of myofibers in both of the tissue types. However, the majority of these selected clones are expected to present markedly different patterns between the C57 and P448L Neo- tissue sections. This myofiber periphery particularly of a punctate pattern distinguishable on

C57 tissues as compared with the negative control of hypoglycosylated FKRP mutant P448L Neo- will indicate clones with appropriate and functional peptides recognizing glycosylated α–DG.

Secondly, to confirm appropriate binding of differentially glycosylated α-DG, purified protein from the LARGE transfected CHO mutants and isolated C57 muscle western blot membranes will be probed with the top phage candidates and detected by Rabbit anti-M13 phage antibody. Correct epitope recognition will be indicated, as compared with IIH6 immunodetection as a broad band ranging from 100 to 200 kD with a mean of 156 kD (4-20% Tris Glycine PAGE).

Subaim 3.3: In the third experimental series, those clones not removed as candidates through the *ex vivo* tissue array and immunoblot assay, will be prepared for and submitted for both Sanger chain-termination and NGS RNA Seq sequencing methods. Submission of isolated phage genomic ssDNA per manufacturer recommended process and primers should yield a conserved M13 genomic sequence flanking the clonal variable region of 36 or 21 bases in an NNK format, from which the peptide sequences can be determined. In an attempt to reduce background noise from the genomic DNA, primers may be designed to create smaller cDNA amplicons through PCR amplification with predicted product sizes of 300 bp or less. After initial rounds of sequencing, discernable peptide sequences will be determined using the M13 abbreviated codon table. Analysis of sequence results from these two technologies will consist of two parts. First, sequencing quality and diversity will be determined, as these technologies use vastly different approaches to determine positional sequence and reassembly. Secondly, the resulting peptides will be assessed for sequence similarity and divergence, motif similarity to characterized reference proteins, and the ability of each sequencing platform to determine phage variable regions across this "best set" of clones submitted.

Collectively, the HTS modifications and utilization of NGS sequencing technologies in this application of phage display to muscle target, along with careful and thorough selection design contributes a significant step forward and could provide truly applicable targeting peptides for-tissue/cell specific delivery of drugs as well as gene and oligonucleotides.

These experimental aims, if achieved, will address one of the most challenging issues in translational research aiming to apply promising experimental therapies to treat human diseases, the low and non-specific delivery of therapeutic agents, oligonucleotide and transgene to preferred targeted cells *in vivo*. Thus, addressing the premise that synthetic polymers for gene delivery can be modified for targeted delivery, and that building upon advances in synthetic polymers as safe and efficient delivery vehicles, can be combined to benefit a potential therapy toward realistic *in vivo* and clinical applications. Essential information obtained through these studies will contribute to the collective understanding of oligonucleotide and gene delivery vehicles, especially for delivery of PMO AON for effective clinical treatment of Duchenne and other muscular dystrophies.

CHAPTER 2: POLY(ESTER AMINE) TRIS[2-(ACRYLOYLOXY)ETHYL] ISOCYANURATE CROSS-LINKED POLYETHYLENIMINE POLYMERS AS GENE AND ANTISENSE OLIGOMER DELIVERY VEHICLES FOR THE TREATMENT OF DUCHENNE MUSCULAR DYSTROPHY.

2.1 Abstract

Hyperbranched poly (ester amine)s (PEAs) based on tris [2-(acryloyloxy)ethyl]isocyanurate (TAEI) cross-linked low molecular weight polyethylenimine (LPEI, Mw: 0.8k/1.2k/2.0k) have been evaluated for delivering pDNA and antisense phosphorodiamidate morpholino oligomer (PMO) *in vitro* and *in vivo* in the dystrophic *mdx* mouse. The results show that the PEAs constructed with PEI 2.0k (C series) improved PMO delivery more efficiently than those constructed with PEI 0.8k (A series) or 1.2k (B series) in a GFP reporter-based C2C12 mouse myoblast culture system. The highest efficiency of exon-skipping *in vitro* with the PMO oligonucleotide targeting human dystrophin exon 50 was obtained when the PEA C12 [TAEI-PEI 2.0k (1:2)] was used. Nearly all of the PEAs improved dystrophin expression in *mdx* mice by local injection with a 2-4 fold increase when compared to PMO alone. Improved transfection efficiency and lower toxicity indicate the potential of the biodegradable PEA polymers as safe and efficient PMO delivery vectors for *in vivo* applications.

2.2 Introduction

Achieving therapeutic effect in delivery of genes or antisense oligonucleotides must be delivered systemically, requiring stability and prolonged circulation upon introduction to the blood long enough to be delivered to the intended tissue. This requires avoiding rapid filtration by the kidneys, escape from the vasculature to tissue interstisium, followed by the interactions with ECM components, before they have the opportunity to encounter the target cell membrane. The efficiency of membrane interaction and penetration is critical for overall efficiency of the gene or AON delivery. Even those compounds successfully entering the cells still require avoidance of cellular mechanisms, such as harsh pH of endolysosomes, and protease and/or nuclease degradation, rendering them useless, preventing entry to specific cellular zones, such as nucleoli for intended targets, to serve their designed function such as AON splicing modulation. Clearly, the properties of compounds required to complete each step successfully will be different, and one compound with limited biochemical properties is unlikely to be sufficient to accomplish these multiple tasks. These numerous and complex barriers to delivery are the principle causes which make developing optimal delivery compounds or systems extremely challenging.

One possible solution for the challenges is to develop compounds with multiple biochemical properties, with limited studies conducted for AON delivery in animal models. One of the most commonly used approaches, combining the use of polymers with different chemical properties such as co-polymers containing Polyethylene glycol (PEG), Polyethylenimine (PEI<10kd) and Poloxamers (Pluronics) have been examined for DNA based gene delivery. (Cho, Choi et al. 2006, Hao, Sha et al. 2009, Wang, Lu et al. 2013). This combined polyplex approach has also been used for oligonucleotide delivery with increased transfection efficiencies *in vitro* as well as *in vivo* and without additional toxicity as compared to the individual components of the polyplex.

However, all such copolymers either as a simple mixture or conjugated onto the target oligonucleotides have not been able to achieve significant enhancement for AON delivery *in vivo*. These results indicate that fine balance is needed for efficient oligo delivery with low toxicity and this will not be easily established. (Bates, Hillmyer et al. 2012, Jager, Schubert et al. 2012)

With a focus on AON delivery for DMD, the McColl Lockwood lab has been conducting a series of studies developing and testing copolymers for both gene and AON delivery. Applying the principles known to be important for the delivery of negatively charged nucleic acids, the laboratory has synthesized copolymers, Poly ester amine (PEAS) with tris[2-(acryloyloxy)ethyl]isocyanurate (TAEI) as linker to low-molecular-weight polyethylenimine (LPEI, Mw 0.8k, 1.2k, and 2.0k) and evaluated their effect for gene delivery *in vitro* and *in vivo*.(Wang, Tucker et al. 2012) These studies are also unraveling one dilemma of using PEIs as gene/oligo delivery polymers. HPEI is highly effective for gene delivery, but also highly toxic; whereas LPEI alone is not effective for gene delivery, although it is effective in binding plasmid DNA with only limited toxicity.

Similarly, copolymers (PCMs) with low molecular weight polyethyleneimine (LPEI) conjugated to Pluronic and composed of relatively moderate size (Mw: 2000–5000 Da), intermediate HLB (12–23) of Pluronics, and LPEI produce much higher gene delivery efficacy and less cytotoxicity as compared with PEI 25k in C2C12 myoblasts and CHO cells *in vitro*. The PCM series, effective oligo delivery vehicles, were also able to enhance gene delivery in mdx mice *in vivo*. Importantly, the effective PCMs, especially those composed of moderate size (2k–5kDa) and intermediate hydrophilic–lipophilic balance of pluronics, enhanced exon-skipping of 20-OMePS with low toxicity as compared with Lipofectamine-2000 *in vitro* or PEI 25k *in vivo*.

The formulation of PMO with the PCM polymer containing pluronics of molecular weight (Mw) ranging 2–6 k, with hydrophilic-lipophilic balance (HLB) 7–23, significantly enhanced PMO-induced exon-skipping in a green fluorescent protein (GFP) reporter-based myoblast culture system with dystrophin exon 23 as the skipping target and demonstrated a significant increase in exon-skipping efficiency in dystrophic *mdx* mice.(Wang, Wu et al. 2013) Consistently, PCMs of moderate size (2–6 k) and intermediate HLB have been most effective whereas more hydrophilic polymers were found to be ineffective for PMO delivery.

2.3 Results

PEAs successfully prepared by Dr. Mingxing Wang, by Michael addition reaction between TAEI and LPEI as shown in table 2, were characterized for biophysical properties to determine their capacity as and oligonucleotide delivery vehicles. These PEA polymers were mixed and allowed to complex with pDNA (polyplex) which was then characterized for stability, resulting particle size, and delivery of gene (and oligonucleotides) *in vitro* and *in vivo*. The ability of polymers to complex with plasmid DNA was assessed using agarose gel electrophoresis, where effective binding of the PEAs to DNA retarded the migration of DNA in the gel due to increase in molecular size and/or changes in charge of the DNA when bound by PEAs. A shown in figure 8, all PEAs bound pDNA effectively with DNA completely retained within the loading wells when the weight ratio of the polymer/pDNA was at or above 2.0.Within the B series constructed with LPEI 1.2k, B12 and B14 showed stronger binding affinity to DNA than B11 when applied at the same concentration, likely due to B12 and B14 having relatively higher PEI content than B11. This was further supported by the strong DNA binding capacity of A12 and C14, which also have higher PEI content.

Table 2: PEA Series Polymer Characteristics

Polymer	PEI:TAEI	LPEI Mw	Mv*	% PEI**
A11	1 : 1	0.8	4980	63.2
A12	2 : 1	0.8	4570	72.5
A14	4 : 1	0.8	4390	53.4
B11	1 : 1	1.2	7160	51.7
B12	2 : 1	1.2	5940	70.3
B14	4 : 1	1.2	5580	63.5
C11	1 : 1	2	9870	54.8
C12	2 : 1	2	8430	65.6
C14	4 : 1	2	7650	71.4

*Determined by viscosity measurements in 0.9% NaCl, 25^0C

** Determined by ^{1}H NMR in $CDCl_3$

Almost all pDNA was retained in the loading well even when the ratio of polymer/ pDNA was only 0.5 for these two polymers. In contrast, B11 had relatively lower PEI composition and retained all DNA in the loading well only when the ratio of polymer/pDNA reached 2.0. These results are consistent with our earlier observation that the density of cationic groups within a polymer contributes significantly to the binding affinity for negatively charged DNA cargo.

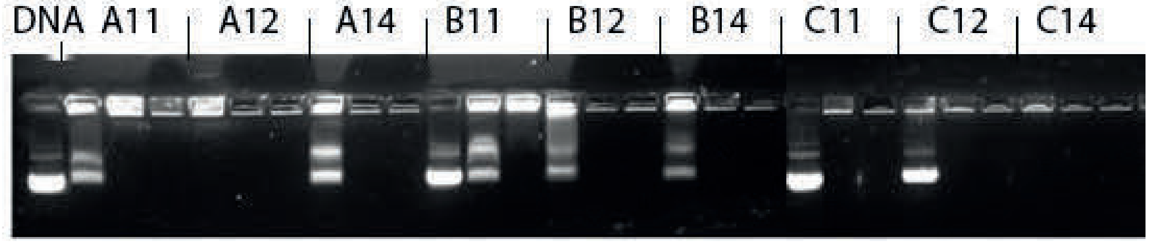

Figure 8: Determination of polymer/DNA binding. Agarose gel electrophoresis of PEA:DNA complexes at mixed ratios of 0.5:1, 1:1, 2:1 (Polymer:DNA) to determine effective bonding concentrations of each unique PEA polymer to pDNA cargo..

The size and surface charge of PEA/DNA complexes was measured using dynamic light scattering (DLS) as shown in Figure 9. All three series of the PEAs effectively condensed DNA into nanosized, positively charged complexes at the ratio of 2:1. Lower amounts of polymer tended to give larger nanoparticles owing to aggregation. An increase in PEA/DNA weight ratio (up to 5) produced smaller-sized nanoparticles (below 150 nm). Most PEAs formed DNA polyplexes with sizes below 200 nm except for A11 (2 μg) and A14 (5 and 10 μg), which are considered optimal for intracellular delivery. All polyplexes had positive surface charges in the range of 11.5− 33.5 mV, with an increase in the weight ratio from 2 to 10 of polymer/pDNA (an example was given in Figure 3b). The results of zeta potential with the PEA/DNA polyplexes are therefore consistent with previous findings that DNA binding neutralizes cationic groups including those within the PEAs. The charge neutralization was also consistent with the retardation of DNA in gel analysis described above. The particle sizes and zeta potentials indicated that polymer/DNA complexes were cationic with effective diameters around 200 nm and surface charges strong enough for attachment to anionic cell surfaces, possibly promoting endocytosis.

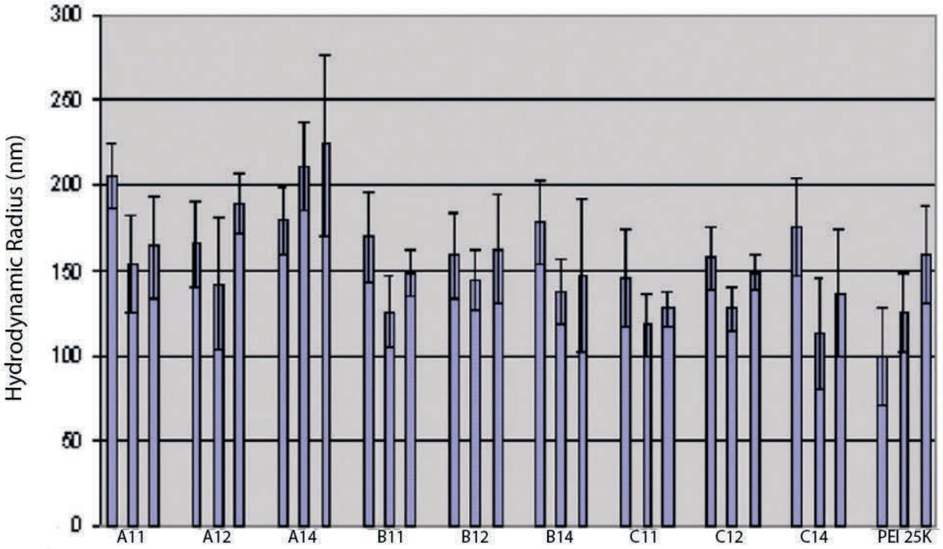

Figure 9: Particles size of PEA complexed with DNA. Using 2,5,and 10:1 weight ratios as determined by DLS

To further define polyplex particle morphologies of PEA/pDNA at weight ratio 5 were analyzed by TE microscopy. These polyplexes formed spherical nanoparticles with an average diameter below 100 nm observed under TEM. The sizes of the polyplexes were therefore smaller than that obtained by DLS measurement, which is largely attributed to the dry process in the sample preparation of TEM. PEI 25k/DNA formulation yielded aggregated particles. These results taken together indicate that the PEAs bind and condense DNA effectively.

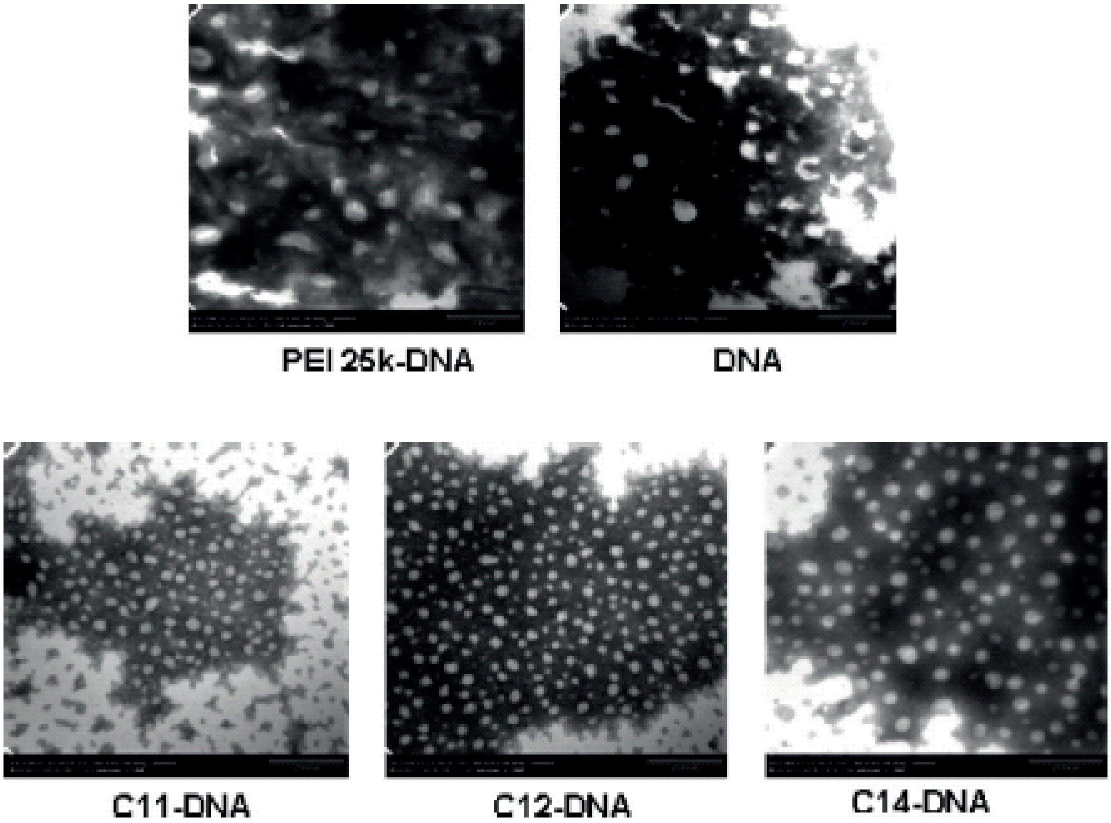
PEI 25k-DNA

DNA

C11-DNA

C12-DNA

C14-DNA

Figure 10: TEM of PEA:pDNA particles. Complexed pDNA and PEA polymer/control Transmission electron microscopy at 5:1 weight ratios. (Scale bar = 200nm)

To further characterize the PEA polymer series, a set of experiments to mimic challenges to polyplex stability were conducted to determine the necessary weight ratios of PEA to DNA. Polymer:DNA complex at 5:1 weight ratio (polymer:pDNA) were exposed to relevant levels of serum (0, 10%, 25%, 50%) and heparin (0, 10, 25, 50 ug/ml) exposure assessing polyplex stability and resistance to these conditions. The result of destabilized polyplex is release of the cargo, as demonstrated by gel electrophoresis, shown in figure 11 below.

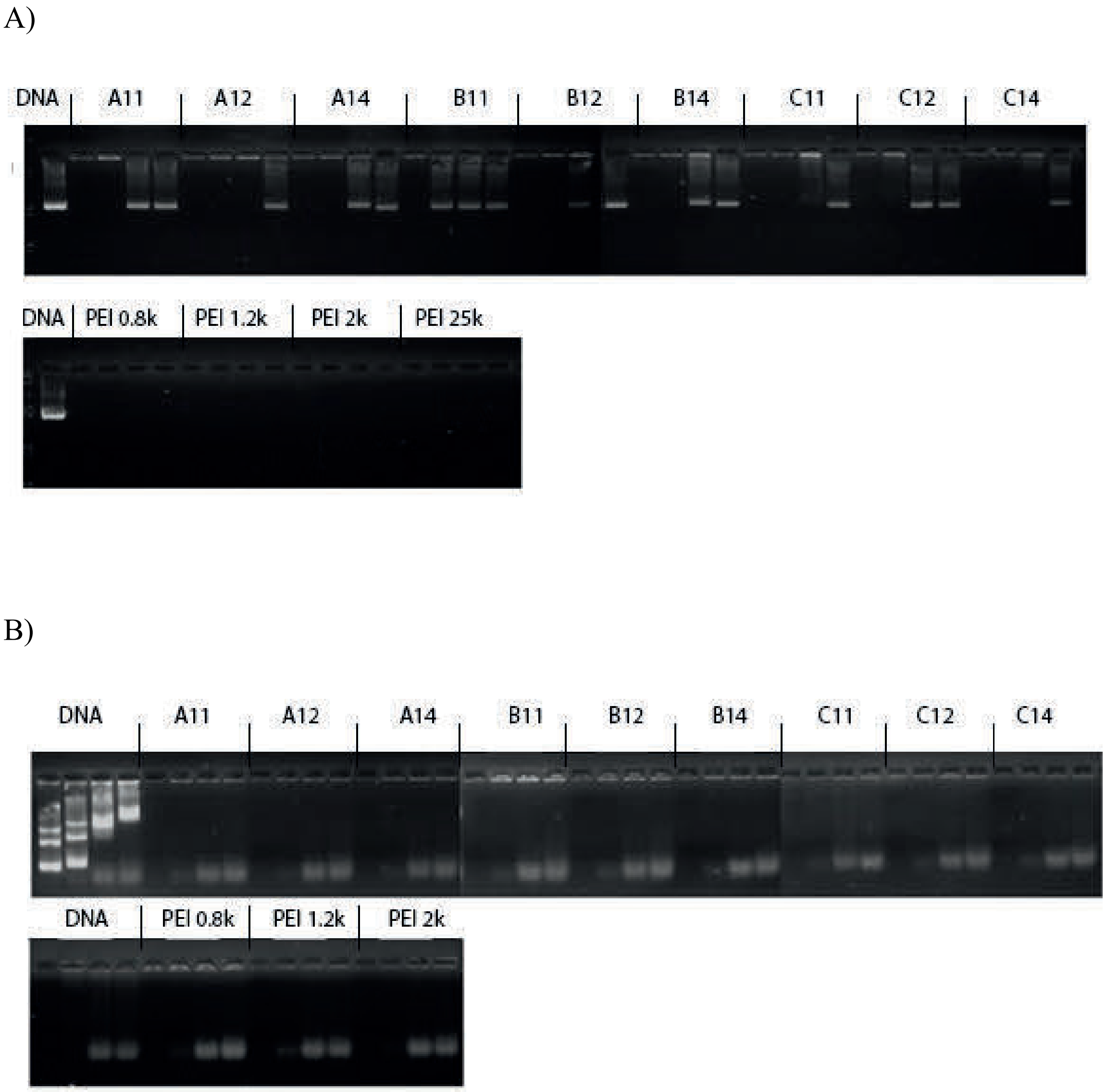
A)
DNA
A11
A12
A14
B11
B12
B14
C11
C12
C14
DNA
PEI 0.8k
PEI 1.2k
PEI 2k
PEI 25k
B)
DNA
A11
A12
A14
B11
B12
B14
C11
C12
C14
DNA
PEI 0.8k
PEI 1.2k
PEI 2k

Figure 11: Polyplex stability to serum and heparin degradation. Polymer:DNA complex stability and resistance to serum (a) (at 0, 10%, 25%, 50%) and heparin (b) (0, 10, 25, 50 ug/ml) exposures (5:1 weight ratio Polymer:pDNA).

Polymer Toxicity *in vitro*

Among the many attempts to reduce cytotoxicity of gene carriers so far, the most popular strategy is the use of biodegradable polymers through ester linkages. () The PEA polymers with LPEI and biodegradable linkage may possibly reduce cytotoxicity through the low toxicity of individual components upon biodegradation products from the ester backbone in physiological conditions. This process was assessed using conditions to mimic physiological conditions, as demonstrated in figure 12.

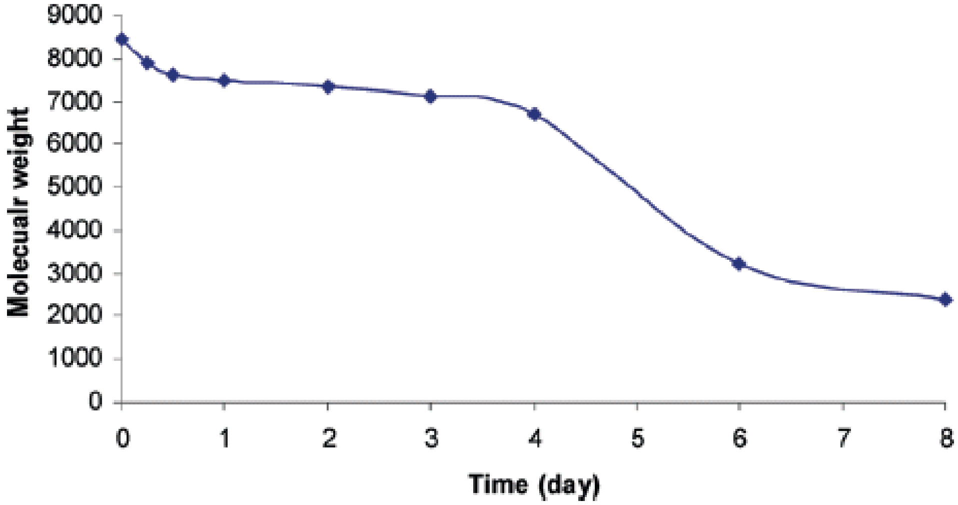

Figure 12: Degradation of TAEI-PEI in simulated physiological conditions. (2.0K-C12) as determined by Mw shift from starting materials.

Using both C2C12 myoblasts and CHO cells with MTS -based cell viability assay 24 h after the treatment, PEI 25K showed much higher cytotoxicity reflected by the fact that over 50% of the cells were killed at the concentration of 25 μg/mL. In contrast, the PEAs have remarkably low cytotoxicity in both cell lines, with most PEAs showing above 80% cell viability even at a high dose of 50 μg/mL as depicted in figure 13. Only

C11 showed slightly higher toxicity than the LPEIs, likely by reason of the higher molecular weight compared with other PEAs. The low cytotoxicity of the PEAs is undoubtedly due to the reduced toxicity of LPEI components as compared with high molecular weight PEI 25k. The increase in the total unites of LPEI within the PEAs without substantial increase in toxicity may be attributed to a more dispersed PEI components within the TAEI crosslinked structures.

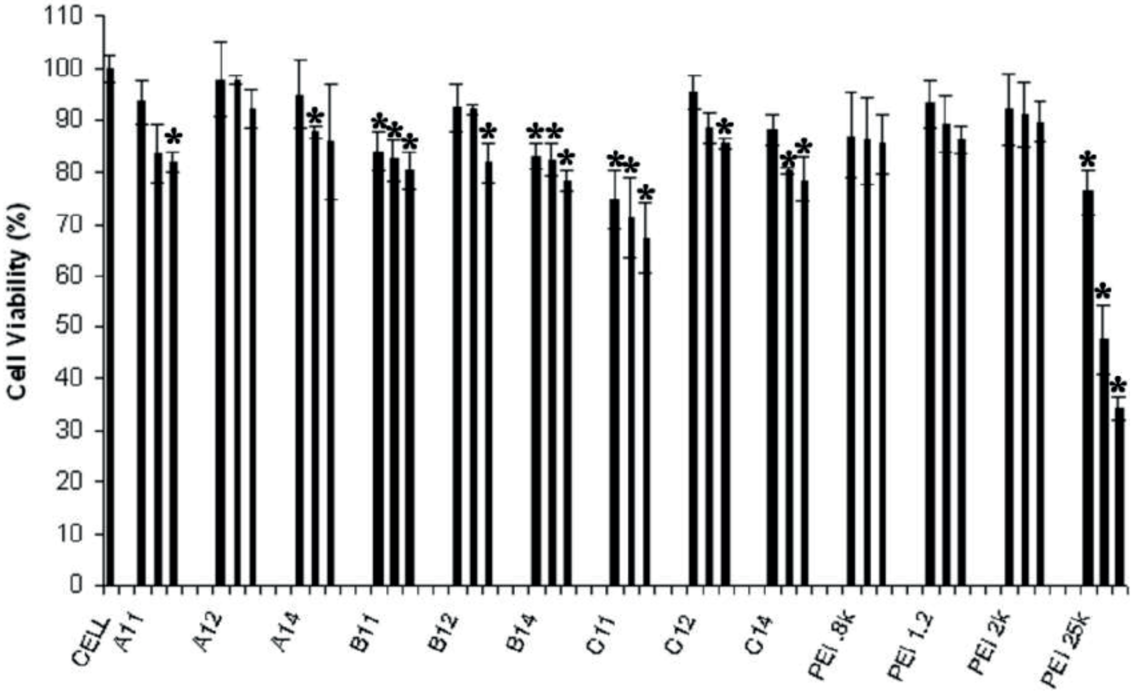

Figure 13: Cell Viability/toxicity and PEA polymers. Various concentrations, compared with commercially available transfection reagents as tested in C2C12 myoblast culture.

High-molecular-weight PEI 25k aggregates with DNA and impairs important membrane function, therefore reducing cell viability.33 Lipofectamine-2000 also reduced the cell viability down below 60% in both cell lines at the dose of 50 μg/mL. The viability, results demonstrating the potential of these new PEAs as safe gene delivery carriers.

Transfection Efficiency of PEAs *in vitro*.

The efficiency of PEAs to deliver pDNA in cell culture was determined using GFP as the transgene with its expression levels measured by flow cytometry quantitatively and also recorded with microscopy semi quantitatively in CHO, C2C12, and HSK cell lines. pDNA was complexed with each PEA at various weight ratios of 2, 5, and 10. All PEAs showed an increase in reporter gene expression when compared to the cells treated with GFP only. As depicted in Figure 7, increasing transfection efficiency (TE) in CHO cells was detected in the order of C12 > C11,C14 ≫ Bs > As. The highest transgene expression was observed in the cells treated with C12 (5 μg) with 87% TE. Similar efficiencies in transgene expression were detected in the C2C12 cells, with C12 (10 μg) producing up to 82% GFP expression. However, levels of transgene expression were much lower in the HSK cells, indicating a cell type- dependent nature for TE with PEAs. Nevertheless, relative transgene expression remained accordant with that observed in the other two cell lines. The efficiency of transgene expression with the C serial polymers was clearly higher than that of commercially available Lipofectamine-2000 and PEI 25k. The fact that TE of C series is higher than the TEs of A or B series as well as PEI 25k indicates the importance of a balanced positive charge for effective gene delivery. Specifically, the size of cross-linked PEIs, the structural arrangement of the positive charge, as well as toxicity of polymers could all contribute to TE. Transfection efficiency with PEAs was affected by the presence of serum, with GFP expression decreasing from 80% to 64% without serum to 55−30% in the presence of serum.

Furthermore, TE with PEI 25K was even more significantly affected, decreasing from 22% without serum to only 5% in the presence of serum.

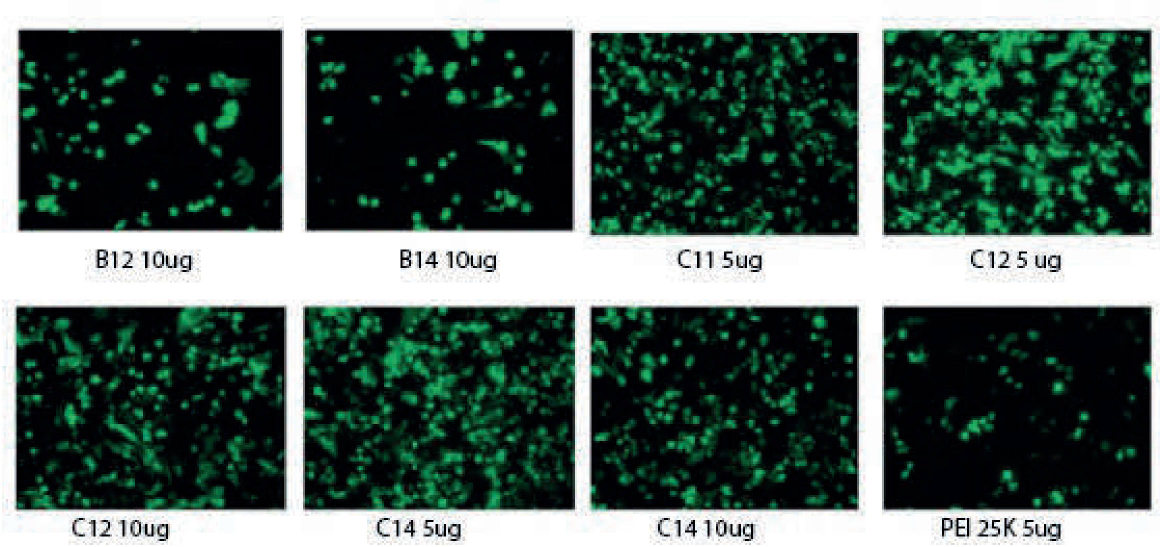
B12 10ug
B14 10ug
C11 5ug
C12 5 ug
C12 10ug
C14 5ug
C14 10ug
PEI 25K 5ug

Figure 14: PEA pDNA delivery to CHO cells and GFP expression. Polymer mediated pGFP delivery and resulting expression in transfected CHO cells.

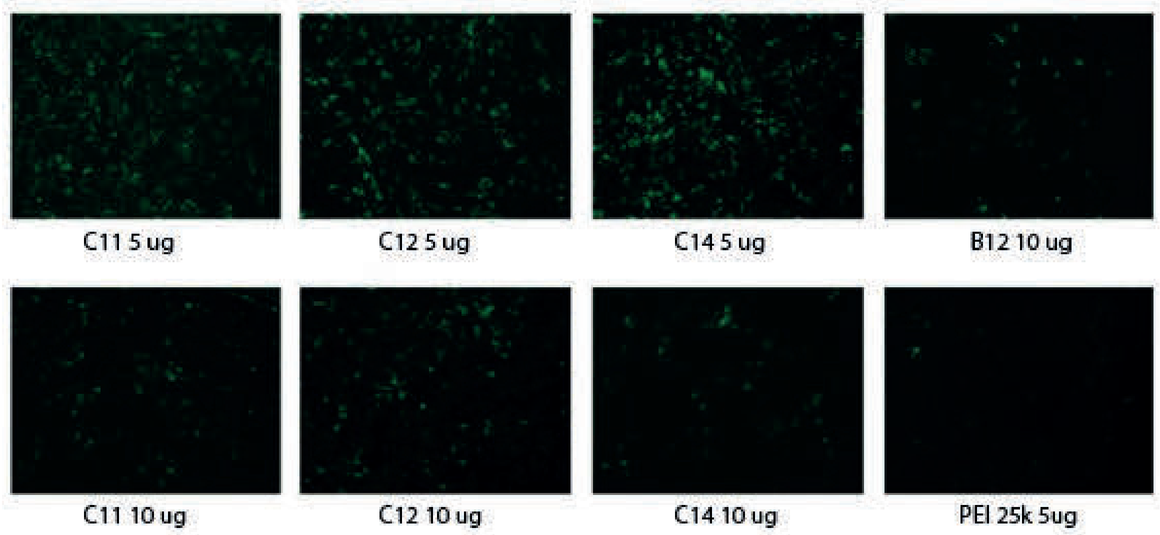
C11 5 ug
C12 5 ug
C14 5 ug
B12 10 ug
C11 10 ug
C12 10 ug
C14 10 ug
PEI 25k 5ug

Figure 15: PEA pDNA delivery to C2C12 cells and GFP expression. Polymer mediated pGFP delivery and resulting expression in transfected C2C12 cells.

Transfection Efficiency of PEA:pDNA *in vivo*.

Based on the TE and cytotoxicity data obtained from *in vitro* systems, I selected

C12 and C14 as candidates to further examine their potential for gene delivery in muscle by intramuscular (i.m.) injection. Plasmid GFP expression vector at the dose of 10 μg combined with 10 μg corresponding polymer was injected into the TA muscles of the mdx mice, a model of Duchenne muscular dystrophy, with GFP expression examined 5 days after the injection. The numbers of GFP expressing muscle fibers were 125 ± 15 and 72 ± 13 for C12 and C14, respectively. As a control, PEI 25k at the dose of 5 μg induced only 15−20 positive muscle fibers (Figure 16).

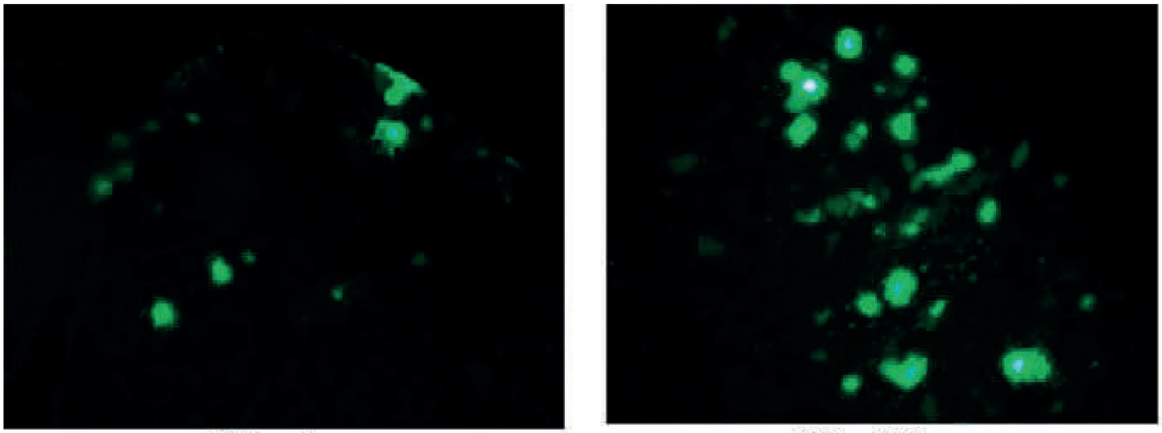

pDNA only

C12:pDNA

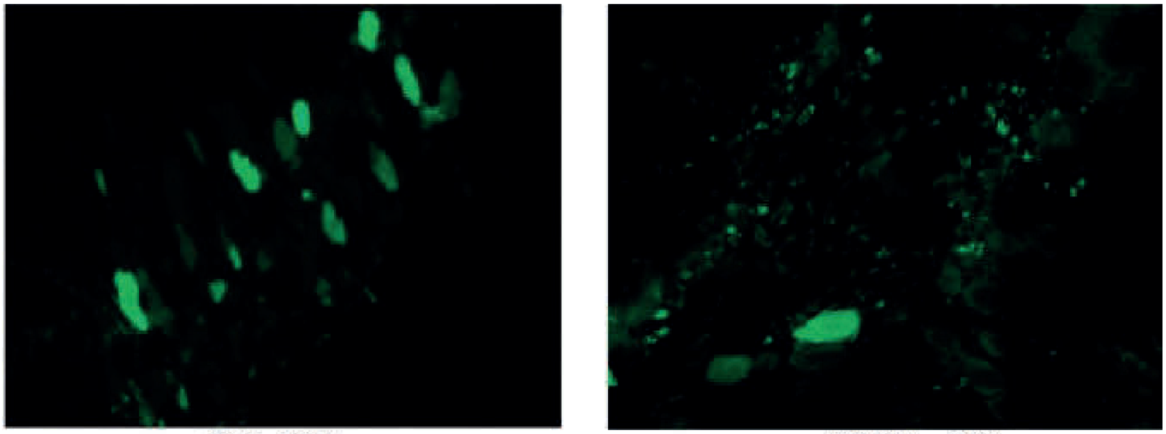

C14:pDNA

PEI 25k:pDNA

Figure 16: Intramuscular PEA-delivery of PeGFP. PEA polymer mediated intramuscular delivery and expression of PeGFP

Histologically, there was limited muscle damage after the treatment with the two polymers at the dose tested. However, similar damage was also observed in the muscles injected with saline only. In contrast, 5 μg PEI 25k induced significantly larger areas of muscle damage indicated by the presence of necrotic fibers and focal infiltrations. These results therefore indicate that the PEA polymers, especially the TAEI cross-linked PEI 2k polymers, have the potential for *in vivo* applications as gene delivery carriers.

Delivery of PMO with PEAs *in vivo*

We next evaluated the effect of the PEA polymers for PMO delivery *in vivo* by i.m. injection. PMOE23 targeting mouse dystrophin exon 23 was injected to each TA muscle of *mdx* mice aged 4-5 weeks. The mouse contains a nonsense mutation in the exon 23, preventing the production of functional dystrophin protein. Targeted removal of the mutated exon 23 is able to restore the reading frame of dystrophin transcripts, and thus the expression of the dystrophin protein.

All PEA polymers were examined at the dose of 5 μg pre-mixed with 2 μg of PMOE23 in 40 μl saline. The treated TA muscles were harvested 2 weeks later. Immunohistochemistry showed that the PMOE23 alone induced up to 12% maximum dystrophin positive fibers in one cross-section of the TA muscle. Dystrophin positive fibers dramatically increased in the muscles treated with PEAs formulated PMOE23, reaching over 30% with all PEAs except for B11. In particular, the use of A12, A14, B12, B14, C11, and C12 increased the dystrophin positive fibers up to 41, 37, 36, 35, 37, and 48%, respectively. As controls, PEI 0.8k, PEI 1.2k, and PEI 2.0k achieved about 22, 19 and 25% dystrophin positive fibers, respectively.

Dystrophin expression and levels of exon-skipping were also examined by Western-blot and RT-PCR. The levels of exon-skipping were 25, 23, 29, 22, 24, and 19% for A14, B12, C11, C12, C14 and PEI 25k, respectively. Dystrophin protein expression levels were found to be 45, 57, 39, 27, 37, and 28% of normal levels for A12, A14, B11, B12, C11 and PEI 25k respectively. Figure 17 illustrates the difference in dystrophin expression between A12, C12 and controls. These results suggest that PEAs with higher molecular size and/or higher PEI content are more effective for PMO delivery. It should be noted that although this enhancement in exon-skipping with the PEAs by local injection is only 2-4 fold higher when compared with PMO only, this improvement indicates the potential for evaluation of systemic delivery, since the highly effective peptide-PMO conjugate (PPMO) was only able to improve local delivery efficiency by 5 fold compared to PMO alone (Wu et al., 2008).

Histologically, the muscles treated with PEA copolymers were similar to the controls of saline-treated samples, indicating no obvious local toxicity at the test dose. Similarly, no toxicity was seen with the LPEIs. However, 5 μg PEI 25k induced large areas of muscle damage indicated by the presence of necrotic fibers and focal infiltrations. Collectively these data further confirms the importance of charge-balance and molecular size in vector microstructure for effective gene/AO delivery with reduced toxicity (Wang et al., 2012b; Wang et al 2013).

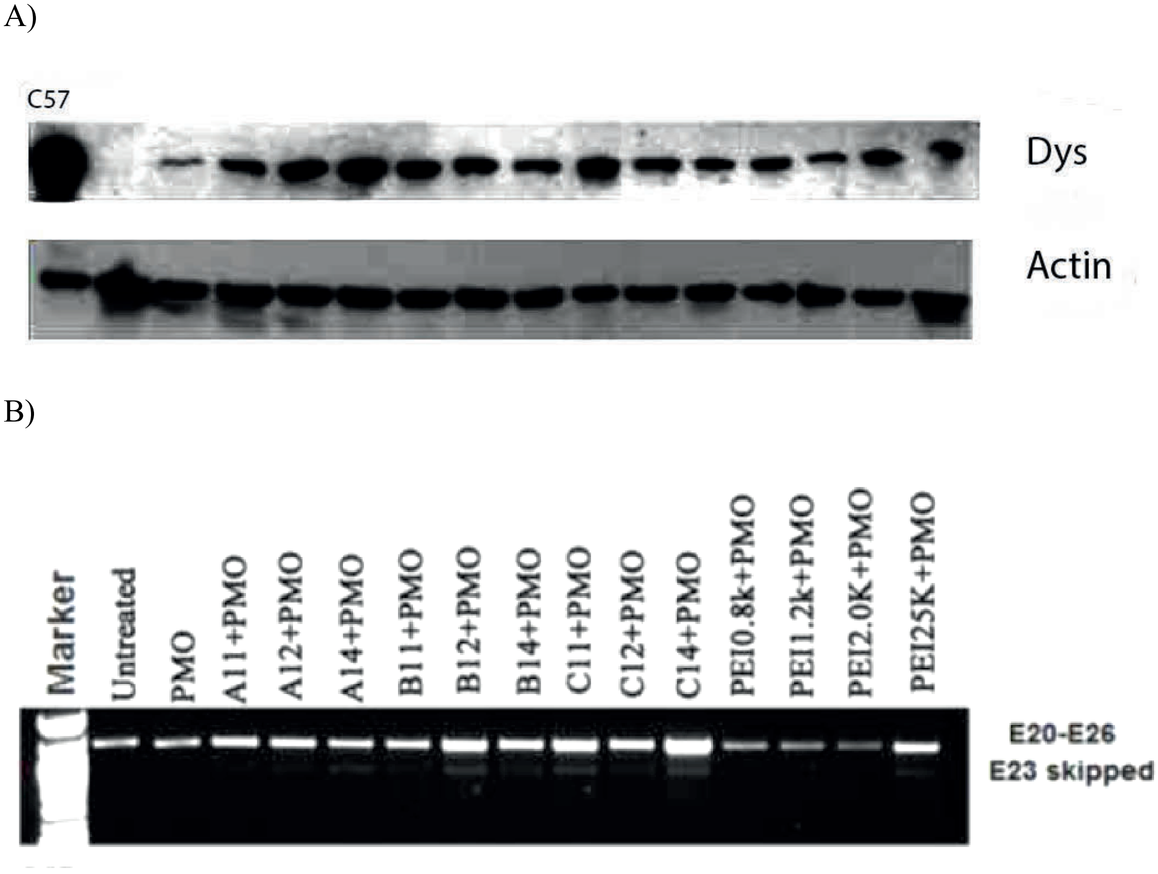
A)
C57
Dys
Actin
B)
Marker
Untreated
PMO
A11+PMO
A12+PMO
A14+PMO
B11+PMO
B12+PMO
B14+PMO
C11+PMO
C12+PMO
C14+PMO
PEI0.8k+PMO
PEI1.2k+PMO
PEI2.0K+PMO
PEI25K+PMO
E20-E26
E23 skipped

Figure 17: PEA mediated dystrophin restoration western blot and RT-PCR.

(A) Western blots demonstrating expression of dystrophin protein from treated *mdx* mice compared with C57BL/6 and untreated *mdx* mice. Dystrophin (Dys) detected with monoclonal antibody Dys 1. α-Actin was used as the loading control. Total 20 μg protein was loaded per sample. (B) Detection of exon 23 skipping by RT-PCR. Total RNA of 100 ng from each sample was used for amplification of dystrophin mRNA from exon 20 to exon 26. The upper bands (indicated by E20-E26) correspond to the normal mRNA, and the lower bands (indicated by E23 skipped) correspond to mRNA with exon E23 skipped confirmed by sequencing

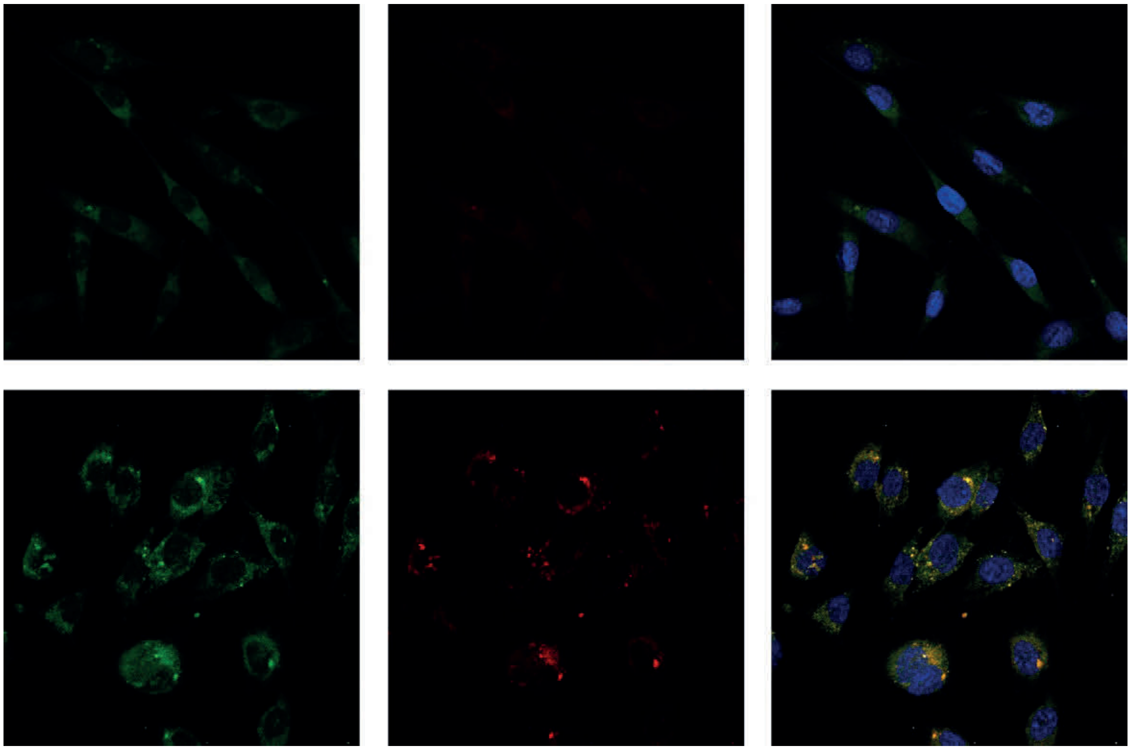

Figure 18: Confocal microscopy of PEA uptake and intracellular localization.

One of the most important hurdles in the delivery of therapeutic oligonucleotide for an intended effect in the nucleus, such as AON induced exon-skipping for DMD, is effective intracellular transport and functional endosomal escape. In the figure above, C2C12 myoblasts were treated with 3’-carboxyfluorescein-labeled PMO alone (top panel) and complexed with PEA A12 (bottom panel). Lysosomal labeling (red) and Hoechst nuclear counterstaining enable visualization of PMO distribution within the cytoplasm, and more importantly punctate perinuclear co-localization of PMO within labeled endolysosomes.

2.4 Discussion

PEA polymers synthesized by Michael addition reaction between TAEI and LPEI exhibit biophysical properties amenable to gene and oligonucleotide delivery. For the delivery of DNA such as pGFP reported here, these properties include a desirable polyplex size below 200 nm, a surface charge in the range 11.5−33.5 mV in applied concentrations, maintained stability in the presence of physiologically relevant serum and sodium heparin. The LPEI-based PEAs, although larger than their corresponding PEI subunits retain relatively low molecular weight as compared to PEI 25k. It appears that this characteristic along with a greater dispersion of positive charge likely offers explanation for their relatively low toxicity observed in cell culture and *in vivo*. Importantly, the TAEI linkage within these PEA polymers allows hydrolytic degradation of PEAs, which could also contribute significantly to reduced toxicity as degradation and clearance or exocytosis of the charged PEI subunits is possible. The elevated levels of transgene expression observed in these applications of PEAs over their PEI subunit suggest that optimization of polymer size and dispersion of cationic PEI group in combination with consideration of polymer biodegradability could achieve further enhanced gene delivery of PEI component polymers without increasing toxicity. Collectively, the PEA polymers tested are able to condense large DNA cargo such as pDNA to nanoscale particles, while also retaining the ability to be used in other applications as reported for the delivery of the near-neutral charged PMO. While further studies will likely elucidate additional applications for these PEA polymers, it is expected that to be employed for systemic delivery, particularly for PMO AON delivery for the treatment of DMD, will require refinement or further characterization of these polymers.

2.5 Methods

Polyethylenimines (Mw: 0.8, 1.2, 2.0, and 25kDa), tris[2- acryloyloxy)ethyl] isocyanurate (TAEI) and anhydrous methanol were purchased from Sigma (St. Louis, MO, USA). Cell Titer 96 Aqueous One Solution Reagent for cell viability, pEGFP (4.7 kb), was obtained from BD Biosciences. Cell culture media RPMI 1640, Dulbecco's Modified Eagle's Medium (DMEM), penicillin−streptomycin, fetal bovine serum, L-glutamine, and HEPES buffer solution (1 M) were purchased from GIBCO, Invitrogen Corp (USA). All other chemicals were reagent-grade without further treatments. Fluorescence was visualized using both the Olympus IX71 and BX51fluorescent microscopy. Digital images were captured using Olympus DP70 camera and DP manager software.

Synthesis and Characterization of PEAs.

PEAs were successfully synthesized by Michael addition reaction as reported. by Dr. Mingxing Wang (16,19) Briefly, TAEI and LPEI were separately dissolved in methanol, and TAEI solution was slowly added to PEI solution at three different TAEI/PEI feed ratios (Table 2). The reaction was kept at room temperature with constant stirring for 48 h. Subsequently, the reaction mixtures were dialyzed at 4 °C for 24 h using Spectra/Por membrane (molecular mass cutoff of 2 kDa) against 20% methanol and followed by distilled water. The final products were lyophilized and stored at 4 °C.1H NMR spectra of samples were recorded in CDCl3 using JEOL500 spectrometer. Capillary viscosity measurements were carried out to estimate molecular weights. The polymers were dissolved in 0.9% NaCl at concentration from 20 mg/mL to 5 mg/mL, and the molecular weights of polymers were calculated using the Mark−Houwink equation

$[\eta] = KM\alpha$, where M is the molecular weight and K and α are Mark−Houwink parameters determined from PEI standards of known molecular weights (PEI 0.8, 2.0, and 25 kDa) at 25 °C.23,24

The degradability of the new PEAs was estimated by measuring the reduction in molecular weight. Polymers dissolved in phophate buffered saline (PBS, 0.1 g/ mL) were incubated in a shaking incubator (37 °C) and sampled at various time intervals. Subsequently, the lyophilized samples were subjected to capillary viscosity analysis to estimate molecular weights.

Preparation and Purification of pDNA.

One ShotTOP10 chemically competent Escherichia coli (Invitrogen) were transformed with pEGFP vector as reporter gene (Clontech Laboratories, Inc.) per manufacturer's instructions. The transformed bacteria were grown on LB agar overnight at 37 °C with selection antibiotic, ampicillin. Single clones were selected and grown for 8 h in broth media. The plasmid was extracted from the bacterial cultures using the Concert Miniprep protocol, digested with Eco R1 restriction enzyme, and electrophoresed on 1% agarose gel to confirm the correct size. The pDNA was purified using the Qiafilter plasmid purification kit from Qiagen, dissolved in purified water, and stored at −80 °C until further use. Plasmid DNA concentration was determined by UV spectrophotometry at 260/280 nm and further confirmed by 1% agarose gel electrophoresis. All polymer/DNA complexes were prepared immediately before use by gently vortexing a mixture of DNA and polymer solution at various polymer/DNA weight ratios. The complexes were incubated at room temperature for 30 min in 24 μL volume and loading dye was added. Samples were then loaded onto 1% agarose gel with ethidium bromide

(EB, 0.1 μg/mL) in Tris-acetate (TAE) buffer (100 V, 40 min). The gel was analyzed on UVilluminator.

Particle Size, Zeta Potential, and Morphology Analysis.

The hydrodynamic diameters of polymer/pDNA complexes were determined by light scattering. Two milliliters of polyplex solution containing 5 μg of pDNA was prepared at various weight ratios (polymer/pDNA = 2, 5, 10). After 30 min incubation, polyplex sizes were measured by photon correlation spectroscopy using Zetaplu Zeta Potential Analyzer (Brookhaven Instrument Co.) equipped with a 15 mV solid-state laser operated at a wavelength of 635 nm. Scattered light was detected at a 90° measurement angle. The refractive index (1.33) and the viscosity (0.89) of 0.9% sodium chloride were used at 25 °C. The zeta potentials were also measured using the same instrument with different software. The sampling time was set to automatic. Values were presented as the average of six runs.

The polymer/DNA complex morphologies were analyzed using transmission electron microscopy (TEM, PhllipsCM-10). The samples were prepared using negative staining with 1% phosphotungstic acid. Briefly, one drop of polymer/ DNA complex solution was placed on a Formvar- and carboncoatedcarbon grid (Electron Microscopy Sciences, Hatfield, PA) for 1 h, and the grid was blotted dry. Samples were then stained for 3 min. The grids were blotted dry again. Samples were analyzed at 60 kV. Digital images were captured with a digital camera system from 4 pi Analysis (Durham, NC).

Resistance to Serum and Heparin: For each sample 10 μL of 5:1 ratio of polymer/DNA complexes were added to 0.5 mL Eppendorf tubes. Fetal bovine serum (FBS) was then added by volume to achieve final concentrations relative to physiological conditions, mixed, and incubated for 30 min at 37 °C. These samples were then electrophoresed in 1% agarose gel to determine the stability of the complexes. For the analysis of their resistance to heparin, varying amounts of 1 µg /µL heparin sodium was added to polymer/DNA complexes of 5:1 ratio to achieve final concentrations of 0, 10, 25, 50 µg/mL. Samples were then incubated at 37 °C for 20 min and electrophoresed in a 1% agarose gel to determine stability.25 Cell Viability Assay. Cytotoxicity was evaluated using the MTS assay by Cell Titer 96Aqueous One Solution Proliferation Kit 24 h after the treatment with different doses of polymers. Cells were seeded in a 96-well tissue culture plate at 104 cell per well in 100 µL medium containing 10% FBS. Cells achieving 70−80% confluence were exposed to different doses of polymers for 24 h in the presence of 10% FBS. Cells not exposed to samples were taken as controls with 100% viability and wells without cells as blanks. The relative cell viability was calculated by (Atreated − Abackground) × 100/(Acontrol −Abackground). All cell viability assays were carried out in triplicate.

Transfection *in vitro*.

GFP reporter C2C12 myoblasts (ATCC), Chinese hamster ovary (CHO), and human skeletal muscle cell (HSkMC, Cell Applications, Inc.) were grown in DMEM or RPMI-1640, respectively, and maintained at 37 °C and 10% CO2 in a humidified incubator. 5 ×104 cells per well were seeded in a 24 well plate in 500 µL medium containing 10% FBS and grown to reach 70−80% confluence prior to transfection. Cell culture medium was replaced with either serum-free or serum-containing media prior to addition of polymer/DNA polyplexes formulated with varying ratio of polymer/DNA. Formulation of 1 µg GFP vector and appropriate amount of polymers was added into the wells 20 min after combination. PEI 25k was used as control for delivery. Transfection efficiencies were determined quantitatively with flow cytometry (BD FACS calibur, BD) and relative efficiency was also recorded using Olympus IX71 inverted microscopy. Transfection *in vivo*.

Ten mdx mice aged 4 to 6 weeks were used for each experimental group. For each tibialis anterior (TA) muscle, 10 μg of plasmid DNA with or without 10 μg polymer in 40 μL saline was used. The muscles were examined 5 days after injection by Olympus BX51 upright fluorescent microscopy for the expression of GFP. The numbers of GFP expressing muscle fibers were counted from a minimum of 6 sections spanning at least half the length of the muscles. A maximum number of GFP positive fibers in one section for each TA muscle was used for comparison of transfection efficiency. Experimental protocols were approved by the Institutional Animal Care and Use Committee (IACUC), Carolinas Medical Center.

The PEAs were prepared from nucleophilic addition of amines to acrylates under mild reaction conditions with low molecular weight PEI(Mw: 0.8, 1.2, and 2.0 kDa) as amine nucleophile and TAEI as a cross-linker at different feed ratios. Triacrylate linker reacts with PEI by Michael addition reaction to either primary or secondary amines, generating ester-based polymers. The compositions of synthesized PEAs were confirmed through1H NMR spectroscopy. The signals at δ 4.6 ppm were related protons. The signals at δ 2.2−3.0 ppm belong to PEI (−CH2−) and TAEI (−CH2−) protons. The molecular weights of PEAs ranged from around 4 to 10 kDa determined by viscosity at 25 °C. No significant difference in the Mw of PEAs was observed at variation in feed ratio of TAEI to LPEI for each series, although slightly higher-molecular weight PEAs were obtained using equal feed ratio of TAEI/PEI (1:1) than the ratio 1:2 or 1:4. This is likely the result of reactions of some of the secondary amines in PEIs with TAEI. The characteristics of synthesized PEAs at different TAEI/PEI feed ratios are summarized in Table 2. Biodegradability of a gene delivery polymer could circumvent long-term toxicity. The kinetics of ester bond degradation of PEAs were investigated by measuring the molecular weight. Figure 12 indicates the typical degradation pattern of PEAs under mimic physiological condition. The PEA underwent hydrolysis forming respective acid and alcohol, thereby generating LMW by-product. A biphasic degradation pattern was observed in that only a small proportion of the PEAs underwent cleavage within 4 days. However, a more rapid degradation was observed 4 days later.

Cell Cytotoxicity

The PEA toxicity assays were performed using both C2C12 myoblasts and CHO cells with MTS -based cell viability assay 24 h after the treatment, usually 1, 2, 5, 10, and 20 ug/ml of media.

CHAPTER 3: PHOSPHORODIAMIDATE MORPHOLINO CONJUGATED TRIS[2-(ACRYLOYLOXY)ETHYL]ISOCYANURATE LOW MW POLYETHYLENIMINE CROSSLINKED POLYMERS FOR ANTISENSE RESTORATION OF DYSTROPHIN EXPRESSION.

3.1 Abstract

A series of Hyperbranched poly (ester amine)s (PEAs) based on tris[2-(acryloyloxy)ethyl]isocyanurate (TAEI) cross-linked low molecular weight polyethylenimine (LPEI, Mw: 0.8k/1.2k/2.0k) have been evaluated for delivering pDNA and antisense phosphorodiamidate morpholino oligomer (PMO) *in vitro* and *in vivo* in the dystrophic *mdx* mouse. The results show that the PEAs constructed with PEI 2.0k (C series) improved PMO delivery more efficiently than those constructed with PEI 0.8k (A series) or 1.2k (B series) in a GFP reporter-based C2C12 mouse myoblast culture system. The highest efficiency of exon-skipping *in vitro* with the PMO oligonucleotide targeting human dystrophin exon 50 was obtained when the PEA C12 [TAEI-PEI 2.0k (1:2)] was used. Many of the PEAs improved dystrophin expression in *mdx* mice by local injection compared to PMO alone. In an attempt to further improve transfection efficiency and lower toxicity the potential of the biodegradable PEA polymers have been evaluated as PEA-PMO conjugates for delivery, particularly systemic applications.

3.2 Introduction

Based upon the promising results of the PEA polymer mediated delivery of genes and oligonucleotides as reported in the previous chapter, I investigated the potential application of PEA-conjugated PMO as a means to increase oligonucleotide delivery while attempting to further characterize the role of the polymer LPEI subunits. As detailed previously, two critical factors that the field of drug delivery have determined necessary for optimal delivery vehicles are increased membrane interactions imparted by charge and/or amphiphilic nature, along with a resulting particle size of the vehicle below 200 nm. To best address these criteria, three PEA polymers (A12, B12, and C12) were chosen based upon previous data for *in vitro* transfection efficiency, toxicity profiles, and gene and oligonucleotide delivery efficacy on intramuscular and systemic injection.

Results from our lab and others have determined that cationic oligonucleotide conjugates, in the form of commercially available octaguanidine and poly-arginine subunits improve delivery in cell culture, as well as local and systemic injection leading to encouraging levels of dystrophin restoration by antisense exon skipping. While effective at low doses, these cationic and non-specific AON-conjugates cannot be applied for maximal effect by increased dose concentration, due to toxicity. To approach a balance between efficacy in AON delivery and the inherent toxicities associated with the introduction of concentrated charged particles, biodegradable PEA polymers as AON conjugates are promising candidates. While the selection of PEA candidates to evaluate as AON conjugates was supported by our previous studies, the LPEI (mw 0.8,1.2 and 2 kD)components and the ratio to a common TAEI core, this study also aims to better elucidate the role of LPEI in mediating necessary interactions in the process of AON delivery. While LPEI is able to bind and condense negatively charged DNA or oligos, it is not effective alone for increasing transfection efficiencies. However, where HPEI (eg. PEI 25k) is quite effective to increase transfection efficiencies it has a toxicity profile making it unsuitable for *in vivo* applications. The beneficial characteristics of PMO, such as its low toxicity and stability are closely tied to the oligo chemistry's neutral charge, with transfection in systemic applications relying on passive diffusion or entry via permeabilized "leaky membranes". The premise of this study is that by direct conjugation with PEA polymers, the net-neutral charge of PMO can be modified to increase transfection efficiencies.

Table 3: Characteristics of PEA Polymers selected for PMO modification

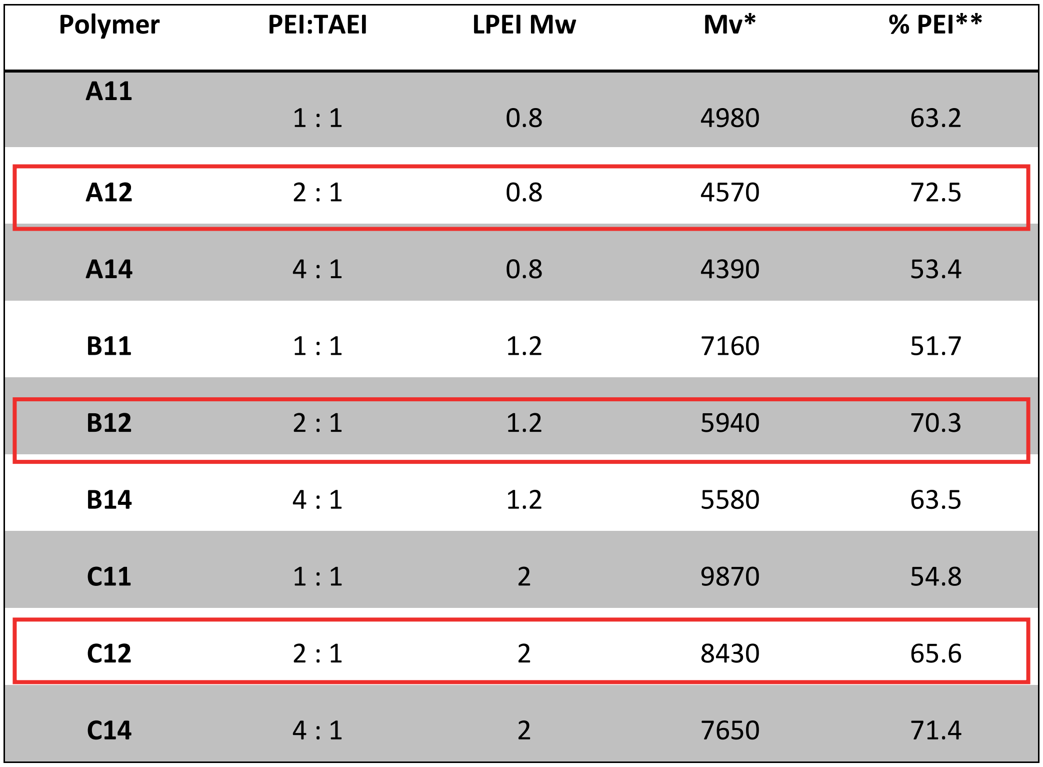

Polymer	PEI:TAEI	LPEI Mw	Mv*	% PEI**
A11	1 : 1	0.8	4980	63.2
A12	2 : 1	0.8	4570	72.5
A14	4 : 1	0.8	4390	53.4
B11	1 : 1	1.2	7160	51.7
B12	2 : 1	1.2	5940	70.3
B14	4 : 1	1.2	5580	63.5
C11	1 : 1	2	9870	54.8
C12	2 : 1	2	8430	65.6
C14	4 : 1	2	7650	71.4

*Determined by viscosity measurements in 0.9% NaCl, 25^{0}C
** Determined by ^{1}H NMR in $CDCl_3$

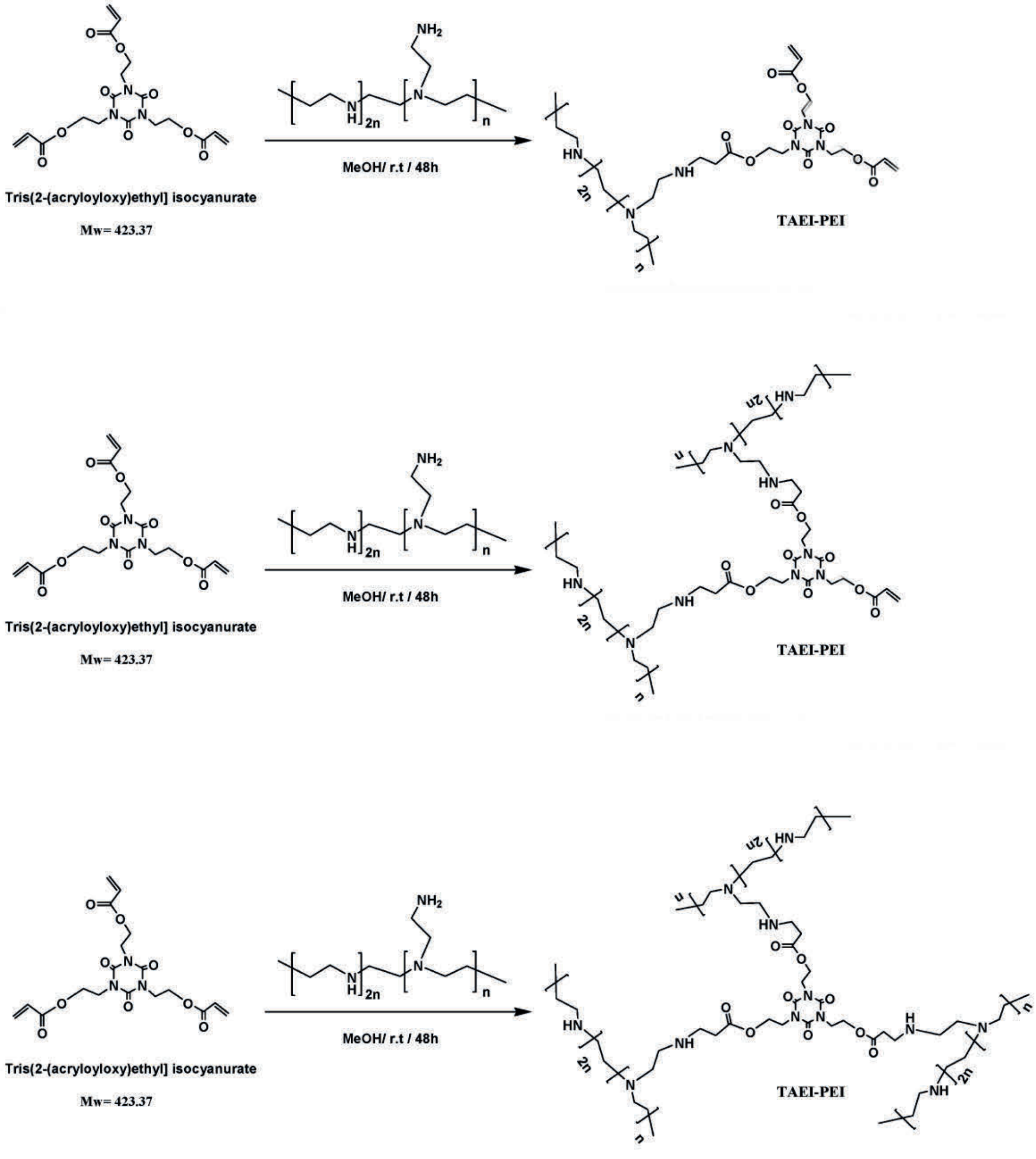
Tris(2-(acryloyloxy)ethyl] isocyanurate
Mw= 423.37
MeOH/ r.t / 48h
TAEI-PEI
Tris(2-(acryloyloxy)ethyl] isocyanurate
Mw= 423.37
MeOH/ r.t / 48h
TAEI-PEI
Tris(2-(acryloyloxy)ethyl] isocyanurate
Mw= 423.37
MeOH/ r.t / 48h
TAEI-PEI

Figure 19: Schematic of feed ratio controlled, PEA LPEI construction. PEAs constructed by Dr. Mingxing Wang, representing the LPEI content of the selected polymers A12, B12, and C12 with component PEI 0.8kD, PEI 1.2 kD, and PEI 2.0 kD respectively, where the TAEI-PEI feed ratio has generated the remaining members of this polymer series.

3.3 Results

To determine the relative toxicity of the PEA-PMO conjugates, a series of *in vitro* experiments were conducted using both C2C12 myoblasts and CHO cells with MTS - based cell viability assay 12 and 24 h after treatment at relevant concentrations. For comparison, LPEI 0.8k, 1.2k and 2k subunits of the PEA polymer construction, were used, along with commercially available poly-arginine and octaguanidine (PPMO and Vivo-PMO). Additionally, the PEA polymers chosen for conjugation were compared, without PMO for variance in toxicity. The LPEI components showed only slight toxicity as was expected, with doses as high as 20 ug/ml having no significant impact on cell viability in the cell lines tested. Consistent with previous experiments and *in vivo* experiments, elevated concentrations of PPMO, Vivo-PMO and the PEA C12 with and without PMO conjugated demonstrated the highest levels of *in vitro* toxicity.

In contrast to HPEI 25k the PEAs and PEA-PMO conjugates have consistently lower cytotoxicity in the cell lines tested. Interestingly, the PEA-PMO conjugates demonstrate additional toxicity than the same levels of PEA alone. To remove one possibility, *in vitro* toxicity with the linker used in synthesis DTBP to conjugate the PEA and PMO, but this difference in toxicity cannot be attributed to the linker DTBP. This toxicity was only observed at concentrations far higher than would likely be used for *in vitro* transfection or *in vivo* delivery, depicted in figure 20 and 21. Importantly, the PEA-PMO conjugates demonstrated a pattern consistent with numerous previous experiments correlating the PEI component and the overall molecular weight being the most likely factors contributing to toxicity. The low cytotoxicity of the PEAs and PEA-PMO conjugates is likely the result of lower toxicity of LPEI components and the biodegradable nature of the PEA construction. Of the approaches to reduce cytotoxicity of gene carriers, the most popular strategy is the use of biodegradable polymers through ester linkages. The PEA polymers with LPEI and biodegradable linkage likely reduce cytotoxicity as the low toxicity of individual components upon biodegradation from the ester backbone in physiological conditions. Unlike previous studies, the increase in the total units of LPEI within the PEA-PMO conjugates without substantial effect on toxicity cannot be attributed to more dispersed PEI components within the TAEI crosslinked structures, as the feed ratio and limitation of conjugation to only functional terminus of the PMO are shared across the PEAs used for conjugation. One possible explanation in addition to toxicity as a function of molecular weight of the materials tested, is that the process of conjugation may reduce the otherwise biodegradable nature of the PEA polymers. This theory however, was not explored in the current study.

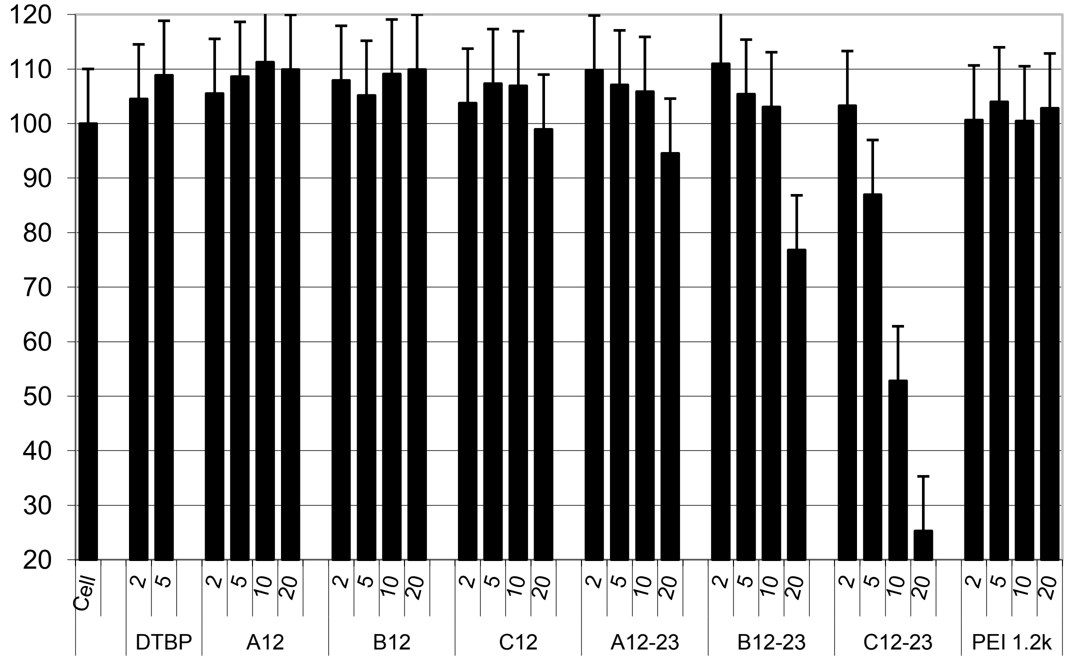

Figure 20: PEA viability/toxicity *in vitro* (C2C12 e23)

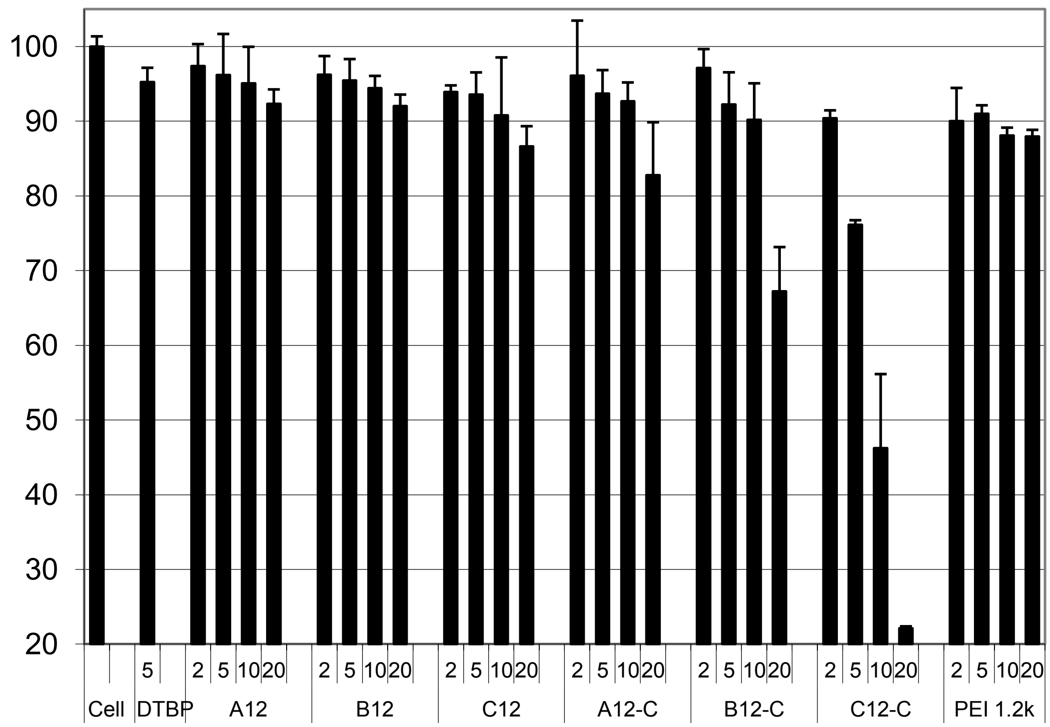

Figure 21: PEAviability/toxicity *in vitro* (C2C12)

To evaluate the effect on *in vitro* transfection efficiency generated by these PEA-PMO conjugates a GFP reporter cell line (C2C12 e23) was used. Effective exon skipping induced by PMO, joined the two GFP encoding exons otherwise separated by the mouse exon 23 sequence, was observed as production of GFP for qualitative and quantitative purposes as compared to untreated, PMO alone, or PEI 2k controls.

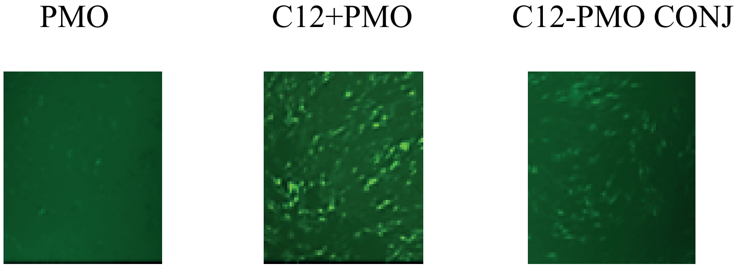

Figure 22: Transfection efficiency (C2C12 e23) GFP expression

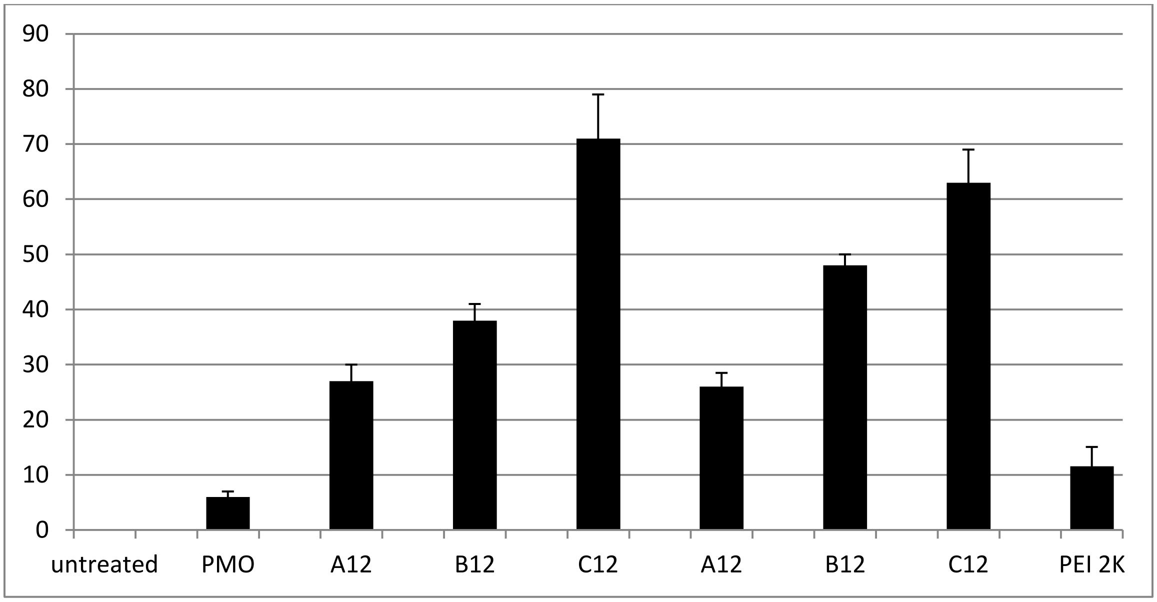

Figure 23: PEA+PMO and PEA-PMO conjugates *in vitro.* Transfection efficiency *in vitro* (C2C12 e23) GFP reporter line (% GFP positive /total cell count by DAPI)

Transfection efficiencies in C2C12 e23 cells showed an increased expression level of GFP from exon-skipping in all of the PEA polymer applications tested. The greatest improvement in transfection, the C12 when mixed with PMO at 5:2 ratio polymer/PMO, however the same level of GFP expression was not observed in the C12-PMO conjugate. While still comparably improved as compared to the PMO alone and PEI 2k delivered PMO, the less efficient transfection of the PEA-PMO conjugate of the C12 PEA was an interesting finding. As well, PMO conjugation of the B-series B12, did show improvement between the complexed and the latter PMO conjugated series, while the A12 PEA in both applications was relatively unchanged in transfection efficiency.

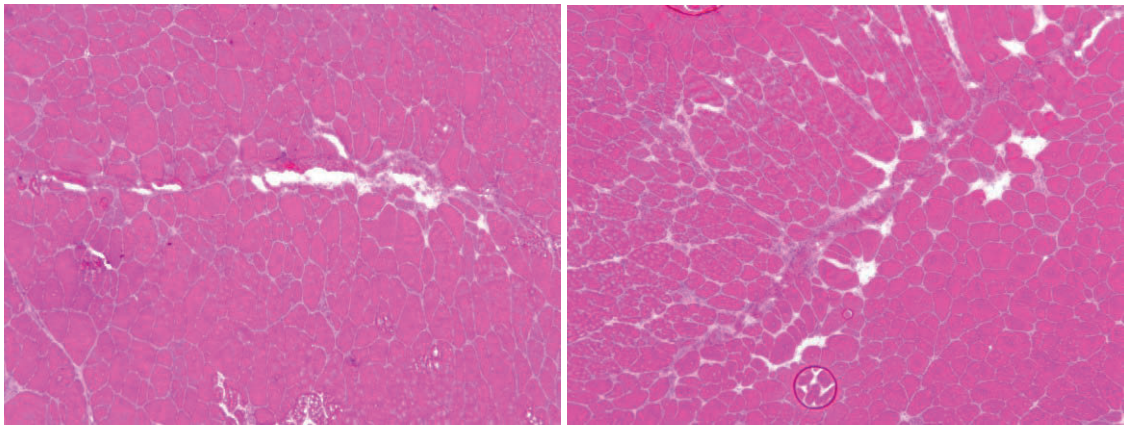

A12 + PMO MIXED

A12-PMO CONJ.

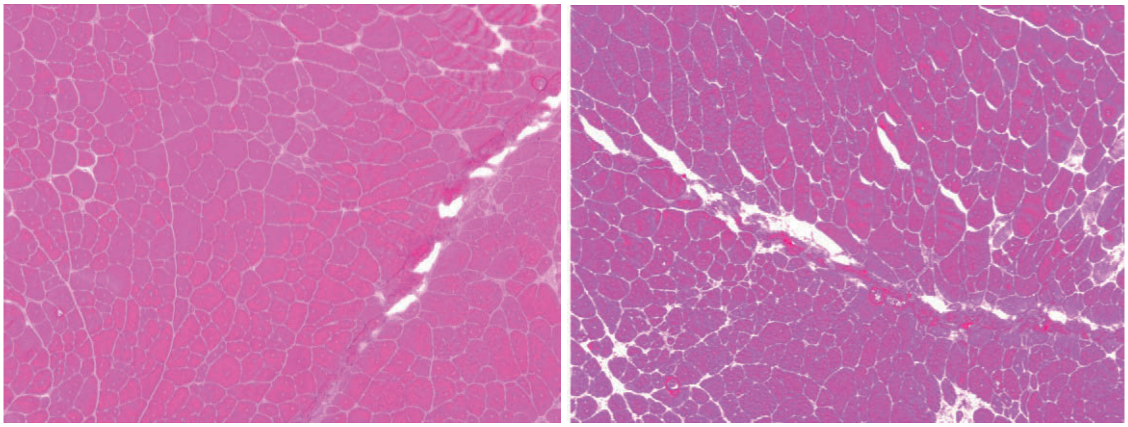

B12+PMO MIXED

B12-PMO CONJ.

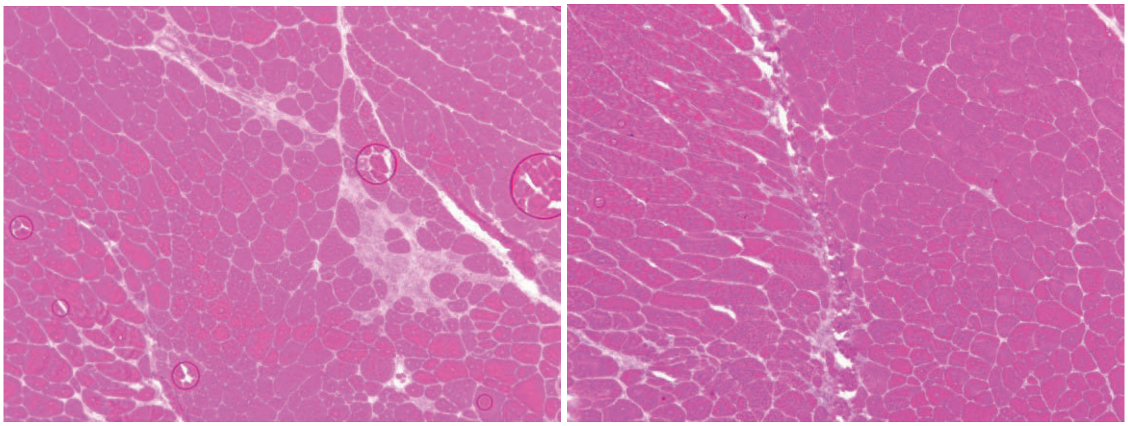

C12+PMO MIXED

C12-PMO CONJ.

Figure 24a: H&E intramuscular pathology.(experimental) treated *mdx* TA muscles

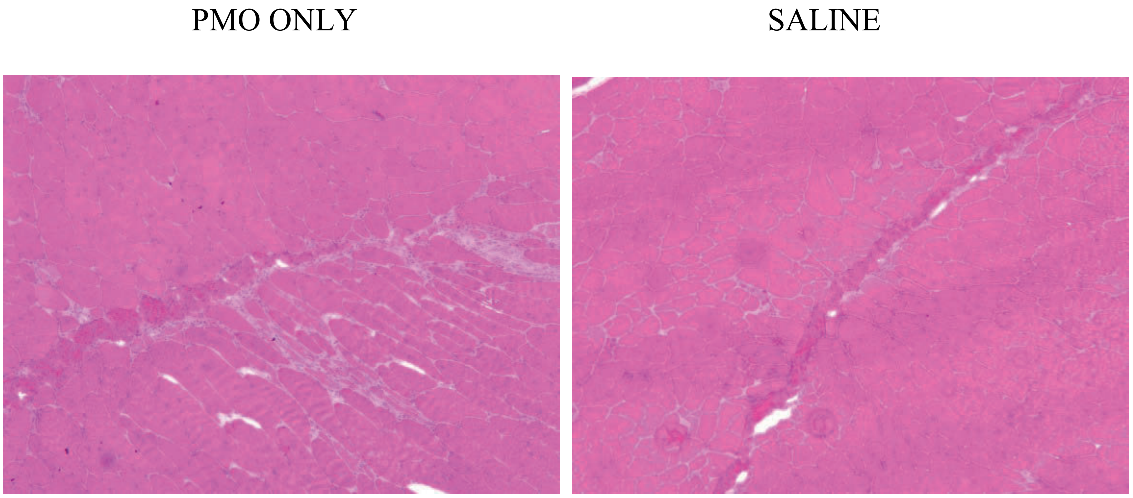

PMO ONLY

SALINE

Figure 24b: H&E intramuscular pathology(control). Treated *mdx* TA muscles

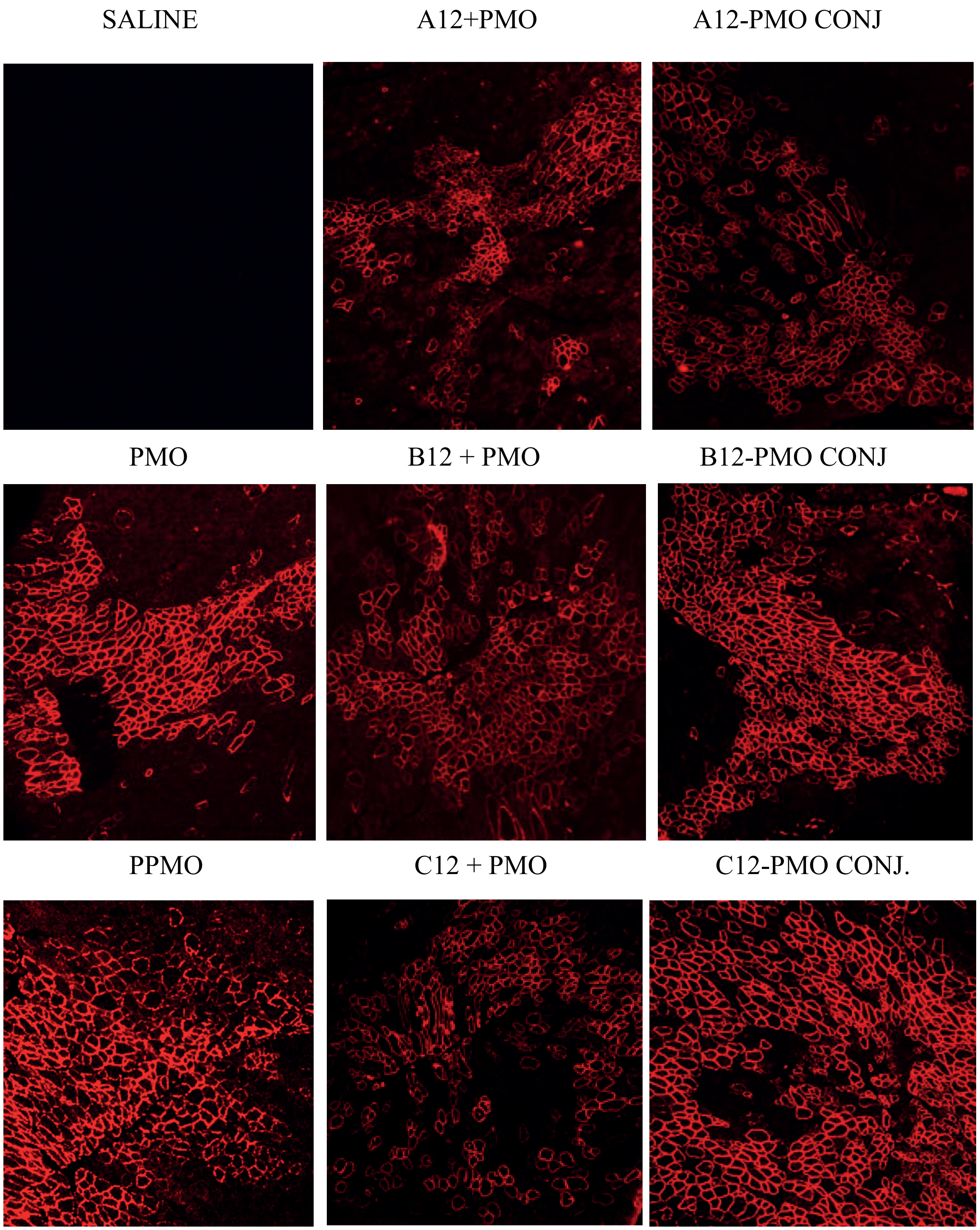
SALINE
A12+PMO
A12-PMO CONJ
PMO
B12 + PMO
B12-PMO CONJ
PPMO
C12 + PMO
C12-PMO CONJ.

Figure 25: Intramuscular dystrophin restoration IHC.

PEA+PMO PEA-PMO conjugates for restoration of dystrophin in mdx mice treated through i.m. administration.

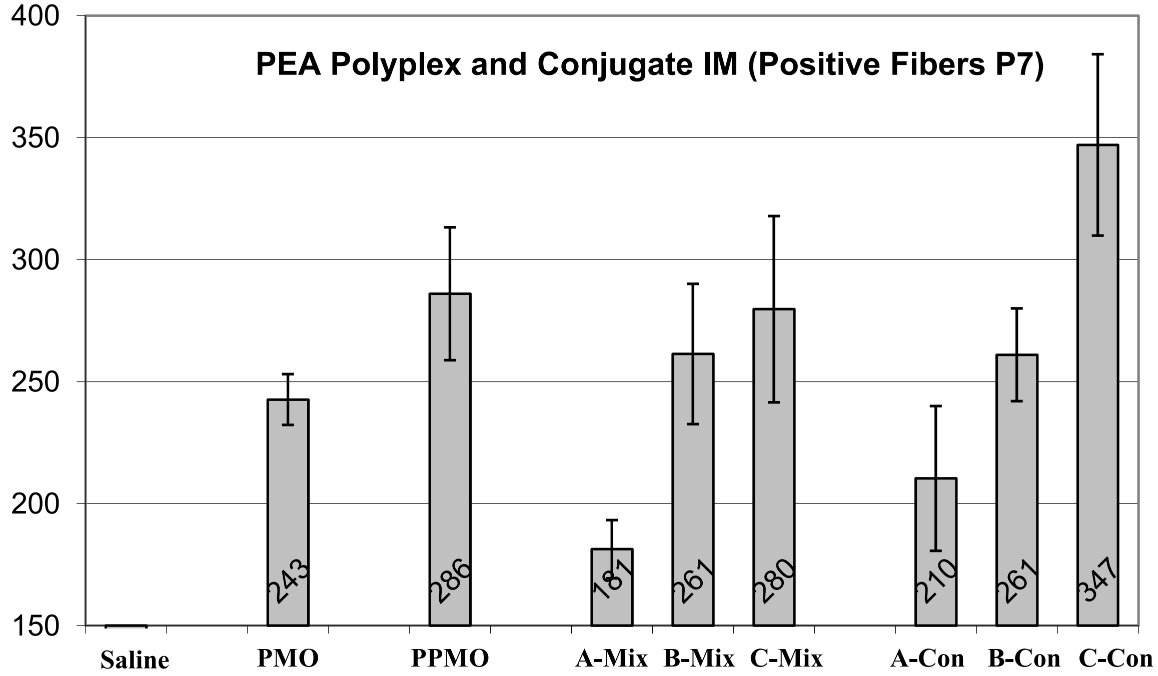

Figure 26: Dystrophin positive fiber count.Counts as detected by P7 anti-dystrophin immunohistochemistry of i.m. treated TA for each treatment.

With data from *in vitro* toxicity and transfection experiments, as well as past studies with the PEA polymers, intramuscular injections in triplicate were performed using the PEA series mixed with PMO to form a polyplex particle, and tested with dose matched PEA-modified-PMO of A12, B12 and C12. The results after P7 anti-dystrophin staining as shown in figure 25, presented a number of interesting results. Dystrophin positive fiber counts were performed to assess the restoration of dystrophin through PMO therapy as compared to PMO only and the modified PMO, PPMO. The most dystrophin restoration through intramuscular administration in the *mdx* mouse was observed from the C12-PMO conjugate and the PPMO tested. While i.m. PPMO has been previously tested, the similarity of function from two quite different PMO modifications, to increase effect was substantial. Moreover, across a number of samples, a pattern of diffuse fibers with dystrophin restoration was common to the C12-PMO and PPMO, while PMO only treated muscles showed the dystrophin restoration closest to and along the area of injection. These characteristic patterns described can be observed below in figure 27.

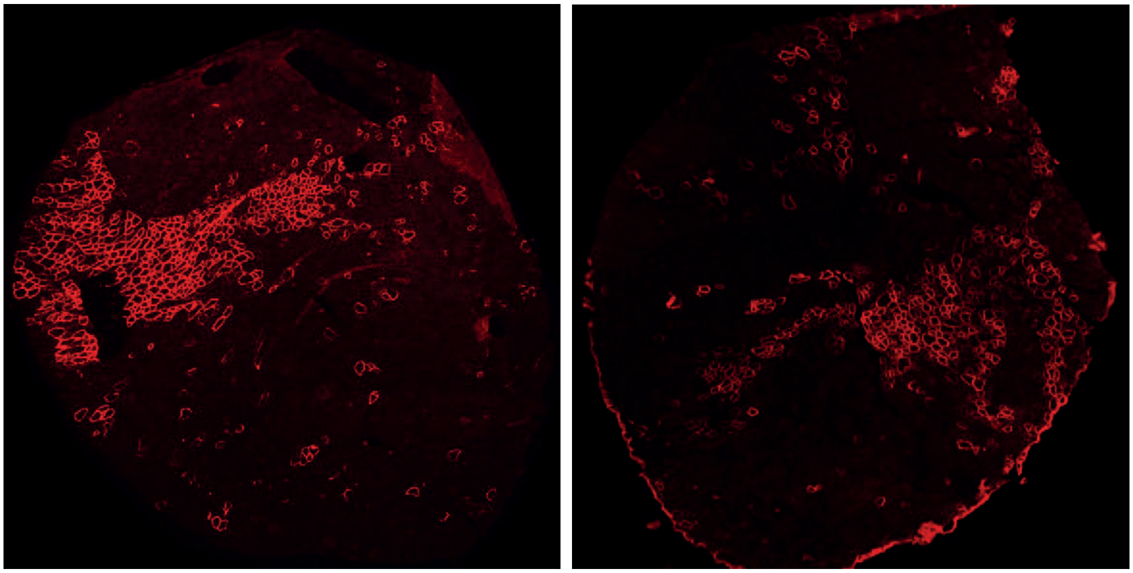

PMO

PPMO

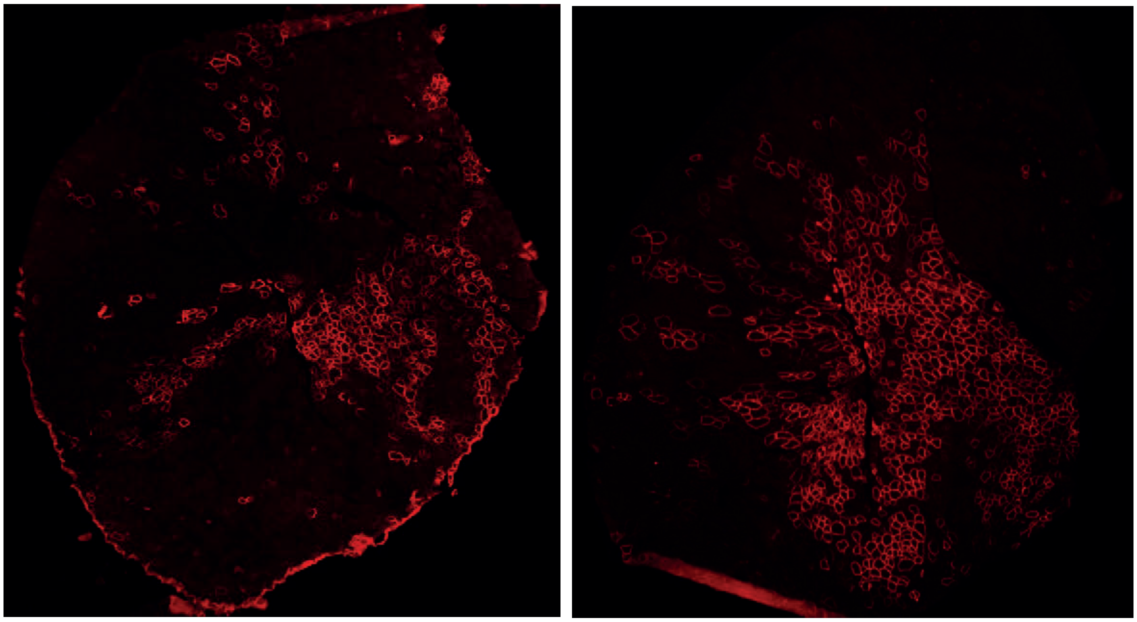

C12+PMO

C12-PMO CONJ.

Figure 27: Diffuse dystrophin positive fibers i.m. Restoration with PMO alone, PPMO, and PEA C12+PMO as vehicle mixed or conjugated.

vehicle (mixed) or C12 PEA-PMO conjugate, administered by i.m injection to TA of *mdx* mice.

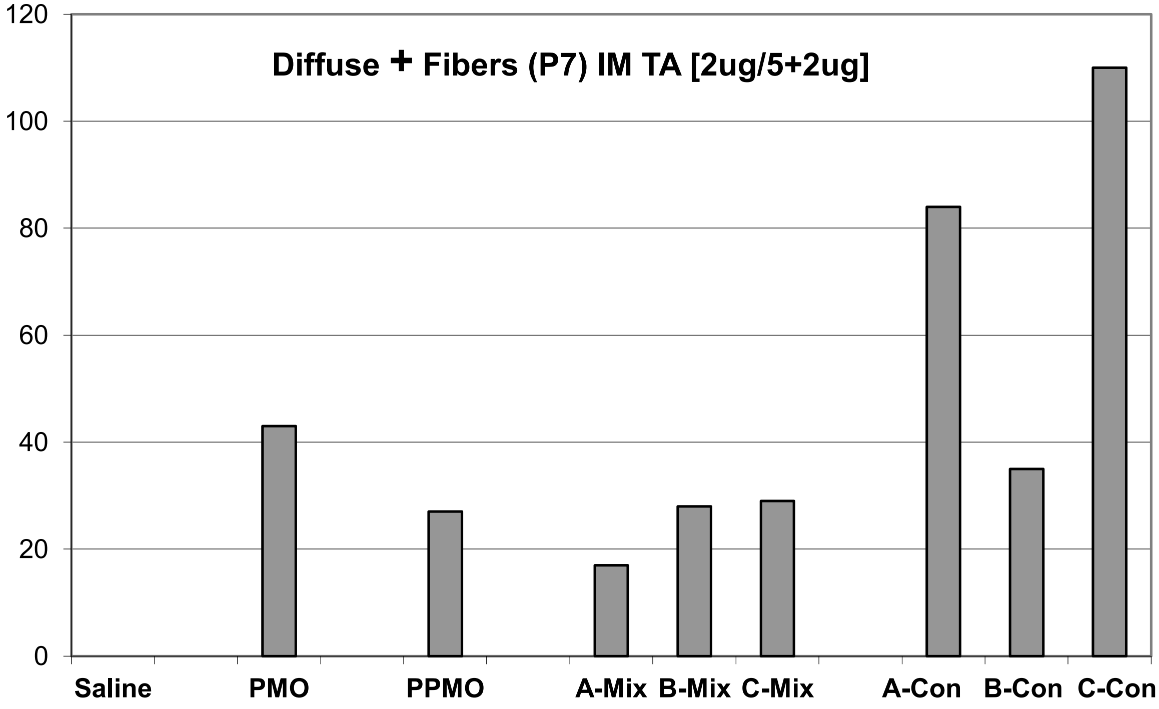

Figure 28: Diffuse dystrophin positive fiber count. Diffuse from point of i.m. injection.

This pattern on i.m. injection of the PEA-PMO conjugates, especially the C12-PMO and PPMO was pronounced and regular enough to be counted as shown in figure 28 above. Perhaps complicating the figure however, is the high count for diffuse fibers on applications of PMO alone. This observation seemed more closely tied to membrane damage in the mouse model, and was observed to be varied across a number of tissues sectioned and P7-anti-dystrophin staining performed.

3.4 Discussion

Biodegradable PEAs were successfully prepared through the Michael addition reaction between TAEI and LPEI and exhibited biophysical properties suitable as gene delivery carriers. These properties include a desirable polyplex size below 200 nm, and stability in the presence of serum and sodium heparin. The LPEI-based PEAs, although larger than their corresponding PEI subunits, still have relatively low molecular weights when compared to PEI 25k. This together with a more dispersed positive charge likely explains their low toxicity in cell culture and *in vivo*. The use of TAEI linkage provides hydrolytic degradation of PEAs, possibly contributing to their low toxicity. The higher levels of transgene expression with PEAs over parent PEIs as previously demonstrated suggest that optimization of polymer size and density of the positively charged PEI groups in combination with consideration of biodegradability could achieve enhanced gene delivery of PEI based polymers without increasing toxicity. Transfection efficiencies in myoblast cultures as demonstrated in the previous chapter are enhanced with PEA both in complex and as conjugates of PMO.

In local intramuscular delivery, PEA complexed PMO as well as PEA conjugated PMO toxicity is histologically comparable to PMO or saline, with similar muscle damage and signs of regeneration. On local delivery toxicity is generally well matched to previous observations and reports. While study is ongoing to determine the efficacy of PEA-PMO conjugates in systemic delivery, PEA-PMO conjugates and PEA complexed with PMO is effective to restore dystrophin restoration in *mdx* mice, a model of DMD.

In performing these experiments to evaluate PEA polymers as conjugates of PMO I have identified a number of beneficial characteristics, primarily for local delivery. However, I have also identified in the course of my study a number of findings or observations for which I can only offer some hypotheses and propose further study aims.

1. The peculiar difference in toxicity between PEA-PMO polyplexes and PEA-PMO-conjugates cannot be easily explained without further study. In principle, the addition of a biodegradable polymer directly to PMO should impart sufficient charge to promote efficient transfection while decreasing toxicity as compared with the multiple PEA units that may be bound to cargo in the polyplex.

Perhaps, through modification to conjugate them to PMO the biodegradability of the PEA polymers are affected, causing additional stress on transfected cells, instead of simple dissociation of the PEA/PMO polyplex which can be accommodated by lysosomal processing.

2. PEA polymers complexed with PMO by mixing have been shown in this study and others to increase transfection efficiencies and dystrophin restoration on local injection. It is my observation that on intramuscular injection the PEA-PMO conjugates tested exhibit higher numbers of dystrophin positive fibers in a diffuse manner farther from the site of injection, a similar pattern as observed in PPMO treated tissues. Cationic destabilization of membranes, not unlike the destabilization caused by muscle degeneration and regeneration observed in DMD, could possibly be employed to increase delivery and uptake of PMO, through modification of the tissue micro-environment to increase transfection efficiencies. Particles effectively delivered to tissues such as muscle by local administration may then be passed by a process of exocytosis to neighboring or non-adjacent fibers, in a similar manner as demonstrated by Sahay et al where delivery of siRNA with LNPs are limited by endocytic recycling. These authors suggest that efficacy may be improved by designing delivery vehicles able to avoid endocytic recycling, however for the purposes of AON therapy for DMD, the design of vehicles promoting

exocytosis by endocytic recycling may present new avenues for more effective dystrophin restoration.

3. PEA-PMO conjugates, while effective for transfection and dystrophin restoration on intramuscular injection, present significant toxicity upon systemic administration. This is not a characteristic exclusive to this model of PMO modification, and while daunting, is an issue which should be addressed. It is my belief that by addressing this characteristic, observed in many of the otherwise promising delivery methods two outcomes are likely to result.

First, further basic study to examine the fundamental mechanisms of this toxicity are necessary. A number of common features have been observed, but have not yet been fully elucidated. While there are a growing number of reports approaching this quandary, it would seem that this is an opportunity for growth amongst the field of drug and gene delivery. As an example, HPEI toxicity remains poorly characterized, and this rather effective yet toxic delivery reagent, has otherwise been abandoned. Further examination of the specific mechanisms of toxicity demonstrated by the most effective transfection methods would likely present new opportunities for improvement in future delivery vehicle designs, through identification of the underlying problems with previous designs.

3.5 Methods

Polyethylenimines (Mw: 0.8, 1.2, 2.0, and 25kDa), tris[2-acryloyloxy)ethyl]isocyanurate (TAEI) and anhydrous methanol were purchased from Sigma (St. Louis, MO, USA). Cell Titer 96 Aqueous One Solution Reagent for cell viability, was obtained from BD Biosciences. Cell culture media Dulbecco's Modified Eagle's Medium (DMEM), penicillin−streptomycin, fetal bovine serum, L-glutamine, and HEPES buffer solution (1 M) were purchased from GIBCO, Invitrogen Corp (USA). All other chemicals were reagent-grade without further treatments. Fluorescence was visualized using both Olympus IX71 and BX51fluorescent microscope. Digital images were captured using Olympus DP70 camera and DP manager software.

Synthesis and characterization of PEAs.

PEAs were successfully synthesized by Michael addition reaction as reported.(Wang, 2012) Briefly, TAEI and LPEI were separately dissolved in methanol, and TAEI solution was slowly added to PEI solution at three different TAEI/PEI feed ratios (Table 2). The reaction was kept at room temperature with constant stirring for 48 h. Subsequently, the reaction mixtures were dialyzed at 4 °C for 24 h using Spectra/Por membrane (molecular mass cutoff of 2 kDa) against 20% methanol and followed by distilled water. The final products were lyophilized and stored at 4 °C.1H NMR spectra of samples were recorded in CDCl3 using JEOL500 spectrometer. Capillary viscosity measurements were carried out to estimate molecular weights. The polymers were dissolved in 0.9% NaCl at concentration from 20 mg/mL to 5 mg/mL, and the molecular weights of polymers were calculated using the Mark−Houwink equation $[\eta] = KM\alpha$, where M is the molecular weight and K and α are Mark−Houwink parameters determined from PEI standards of known molecular weights (PEI 0.8, 2.0, and 25 kDa) at 25 °C.23,24

Polymer/DNA Complexation.

All polymer/PMO complexes were prepared immediately before use by gently vortexing a mixture of PMO and polymer solution at various polymer/DNA weight ratios. The complexes were incubated at room temperature for 30 min before being used.

Samples for injection were suspended in sterile saline, while those for *in vitro* experiments were resuspended in serum-free medium.

Particle Size, Zeta Potential, and Morphology Analysis.

The hydrodynamic diameters of polymer/pDNA complexes were determined by light scattering. Two milliliters of polyplex solution containing 5 μg of pDNA was prepared at various weight ratios (polymer/pDNA = 2, 5, 10). After 30 min incubation, polyplex sizes were measured by photon correlation spectroscopy using Zetaplu Zeta Potential Analyzer (Brookhaven Instrument Co.) equipped with a 15 mV solid-state laser operated at a wavelength of 635 nm. Scattered light was detected at a 90° measurement angle. The refractive index (1.33) and the viscosity (0.89) of 0.9% sodium chloride were used at 25 °C. The zeta potentials were also measured using the same instrument with different software. The sampling time was set to automatic. Values were presented as the average of six runs.

Cell Viability Assay.

Cytotoxicity was evaluated using the MTS assay using Cell Titer 96Aqueous One Solution Proliferation Kit 24 h after the treatment with different doses of polymers or modified PMO. Cells were seeded in a 96-well tissue culture plate at 104 cell per well in 100 μL medium containing 10% FBS. Cells achieving 70−80% confluence were exposed to different doses of polymers for 24 h in the presence of 10% FBS. Cells not exposed to samples were taken as controls with 100% viability and wells without cells as blanks. The relative cell viability was calculated by (Atreated − Abackground) × 100/(Acontrol −Abackground).All cell viability assays were carried out in triplicate.

Transfection *in vitro*. GFP reporter C2C12 myoblasts (ATCC), chinese hamster ovary (CHO) were grown in DMEM or RPMI-1640, respectively, and maintained at 37 °C and 10% CO2 in a humidified incubator. 5 ×104 cells per well were seeded in a 24 well plate in 500 μL medium containing 10% FBS and grown to reach 70−80% confluence prior to transfection experiments. Cell culture medium was replaced with either serum-free or serum-containing media prior to addition of polymer/PMO polyplexes or polymer-PMO conjugate. All formulations of polymer/PMO polyplex were performed with a fixed ratio of polymer/PMO. Formulations for testing were added into the wells 20 min after combination. PEI 25k was used as control for delivery. Transfection efficiencies were determined quantitatively and relative efficiency was also recorded using Olympus IX71 inverted microscopy.

Transfection *in vivo*.

Three *mdx* mice aged 4 to 6 weeks were used for each experimental group. For each tibialis anterior (TA) muscle, 2 μg of PMO, PPMO with or without 5 μg polymer in 40 μL saline was used . The muscles were examined 14 days after injection by Olympus BX51 upright fluorescent microscope after P7 anti-dystrophin staining of 6 μm cryosectioned for dystrophin expression. The numbers of dystrophin expressing muscle fibers were counted from a minimum of 6 sections spanning at least half the length of the muscles. A maximum number of dystrophin positive fibers in one section for each TA muscle was used for comparison of transfection efficiency. Experimental protocols were approved by the Institutional Animal Care and Use Committee (IACUC), Carolinas Medical Center.

Synthesis and Characterization of PEAs.

One essential feature of new polymers required for effective gene delivery *in vivo* is the high cargo binding affinity and, moreover, ability to form stable complexes. This characteristic is strongly influenced by charge density and molecular weight. Furthermore, toxicity of polymers has to be minimized for *in vivo* applications. Cross-linking of the small polycation using degradable linkages can potentially meet these requirements, enhancing DNA or oligo binding capacity, polyplex stability, and high transfection efficiency with low toxicity. The ester bonds in these PEAs are susceptible to hydrolysis at physiological conditions to form the respective triol and corresponding acids, generating low-molecular-weight, low-toxicity byproducts.

In this study, biodegradable, hyperbranched poly(esteramine)s (PEAs) based on TAEI and LPEI, were prepared from nucleophilic addition of amines to acrylates under mild reaction conditions with low molecular weight PEI(Mw: 0.8, 1.2, and 2.0 kDa) as amine nucleophile and TAEI as a cross-linker at different feed ratios. Triacrylate linker reacts with PEI by Michael addition reaction to either primary or secondary amines, generating ester-based polymers. The compositions of synthesized PEAs were confirmed through1H NMR spectroscopy. The molecular weights of PEAs ranged from 4 to 10 kDa determined by viscosity at 25 °C. No significant difference in the Mw of PEAs was observed at variation in feed ratio of TAEI to LPEI for each series, although slightly higher-molecular weight PEAs were obtained using equal feed ratio of TAEI/PEI (1:1) than the ratio 1:2 or 1:4. The characteristics of synthesized PEAs at different TAEI/PEI feed ratios are summarized in Table 3.

CHAPTER 4: IDENTIFICATION OF GLYCOSYLATED α–DYSTROGLYCAN EPITOPES THROUGH PHAGE ARRAY METHODS

4.1 Abstract

Tissue and cell specific delivery has long been recognized to be of critical importance for gene and oligonucleotide therapy, as well as for delivery of drugs, imaging agents and proteins. Clearly, achieving such specificity will depend on the identification of ligands to specific receptors of interest on targeted cells and tissue. Identifying specific molecules, the receptor, on target cells is therefore the primary consideration. Ideal molecules should be abundantly expressed at the target cell surface and have sufficient properties to serve as a receptor for ligand binding and internalization. One such molecule for targeting muscle tissue is the protein alpha-dystroglycan (α-DG), expressed abundantly in muscle tissues, but at much lower levels in most other tissues. Dystroglycan (DG) is a highly glycosylated basement membrane receptor with a role in many physiological processes, such as in the development and maturation of the central nervous system. DG is critical for maintaining the integrity of skeletal muscle membrane, and functional central nervous system structure (Smalheiser and Schwartz 1987; Campbell and Kahl 1989; A. Varki et al. 2009; Oldstone and Campbell 2011) Dystroglycan is composed of two subunits, an α subunit (α-DG) and a transmembrane β subunit (β-DG). α-DG contains three domains with globular N-terminal and C-terminal domains flanking a central mucin domain, which undergoes extensive N-glycosylation,

mucin-type O-glycosylation and O-mannosylation. α-DG binds extracellular matrix (ECM) proteins such as laminin, agrin, and neurexin all of which bearing the laminin-G-domain.(Ibraghimov-Beskrovnaya, Ervasti et al. 1992) Alterations in glycosylation, specifically hypoglycosyaltion of α-DG are a common feature observed in the muscular dystrophies collectively termed dystroglycanopathies. These diseases are the result of mutations in confirmed or putative glycosyltransferase genes as discussed in the introduction section 1.7. (Kobayashi, Nakahori et al. 1998; Brockington, Blake et al. 2001; Yoshida, Kobayashi et al. 2001; Beltran-Valero de Bernabe, Currier et al. 2002)

However, the epitopes of functional importance for the binding of ECM ligands and maintenance of membrane integrity have not been well defined. Currently, the only methods to define the functionality of α-DG are the use of 2 monoclonal antibodies, IIH6 and VIA4 both recognizing sugar epitope(s) on α-DG, and laminin binding assay indicating the ability of the protein to bind ECM components as would normal α-DG. The exact epitopes of α-DG recognized by these antibodies remain unclear, but recent reports suggest that at least one repeat unit of biglycan, [–3-xylose– α1,3-glucuronic acid-b1–] extended from the phosphoryl mannose are one of such epitopes (Inamori et al., 2012). It is likely that other functional epitopes exist, and identifying them could greatly improve diagnosis, further clarify disease mechanisms and lead to the development of experimental therapies.

Relevant to muscle specific targeting, α-DG is most abundantly expressed in the periphery of the muscle fiber membrane and has been known to act as receptors for several Old World arenaviruses including Lymphocytic choriomenigitis virus (LCMV), Lassa fever virus (LFV), Oliveros, and Mobala viruses. The infection efficiency of this family of virus is closely related to the presence of α-DG. (Cao et al, SCIENCE VOL 282, 2709) These observations indicate that α-DG could be an effective receptor for ligand binding and internalization of muscle targeting drugs including AON.

The second necessary consideration for targeting delivery of genes, AON or other drugs is the chemical nature of the employed ligands. The importance of ligands has led to the exploitation of several classes of ligands, chiefly chemical compounds including polymers, peptides and more recently RNA/DNA Aptamers, all with the potential to be employed for delivery of oligonucleotides. The use of polymers has been discussed in chapter 1.5, with specific examples in chapter 2 and chapter 3.

Nucleotide aptamers are small single stranded DNA or RNA molecules with binding specificity not only to complementary DNA and RNA, but also to proteins and other cellular epitopes. Therefore it has the potential as carriers for oligonucleotide delivery as well as specific drugs targeting particular proteins and nucleic acid sequences. Aptamers that span 20–100 residues in length can generally be selected *in vitro* against target molecules with tissue and cell specificity. Most applications of aptamers however have been for binding target proteins in the circulatory system, where natural DNA/RNA aptamers are quickly degraded and cleared from circulation. A successful clinical application of aptamers is illustrated by the first aptamer-based drug, Macugen, approved by the U.S. Food and Drug Administration (FDA) in treatment of age-related macular degeneration (AMD) by OSI Pharmaceuticals. Macugen is an anti-vascular endothelial growth factor (VEGF) aptamers, which bind specifically to the 165 isoform of VEGF, as VEGF plays a critical role in angiogenesis. Macugen blocks VEGF binding of its receptor to achieve its therapeutic effect. Using aptamers of natural nucleic acids for drug delivery into cells is however difficult as they have short effective serum half-lives and are even more easily degraded within target cells. Despite significant efforts made to use chemically modified aptamers for serum/degradation resistance, the effectiveness of aptamers as vehicles for protein and oligonucleotide delivery into solid target tissues remain to be established.

Cell and tissue specific peptide ligands that can withstand physiological conditions can be selected by two main approaches, peptide library and phage-display. Small synthetic peptide libraries were initially used to study protein-protein interactions and for drug design. With advances in peptide synthesis, it has become possible to synthesize a library of hundreds of thousands of short peptides with random or selective sequences. This in combination with the development of methods for peptides to be synthesized on solid phase, such as resin has made it possible to select peptides with specific binding affinity to cell/tissue specific proteins. Theoretically, it is possible to use either a purified protein or cells expressing specific proteins at the cell surface to interact with an array of peptides on a chip. Bound cells or proteins can then be identified either through their markers such as GFP reporter expression or by secondary detection of the cells. Therefore, peptide arrays can identify peptide(s) directly with high potential of protein/cell specificity. However, currently, synthesis of large peptide library (for example with one million peptides) is quite costly and is not cost-effective for most studies. This method has therefore mainly been reserved for further optimization of existing or predicted peptide(s) with a library extended known sequences or motif. Another limitation in peptide arrays is that the method is not well suited for *in vivo* peptide selection. For all of these reasons, phage displayed peptides are the logical choice, as millions of peptides can be produced with limited cost and tested both *in vitro* and *in vivo*.

Gene and oligonucleotide therapies, the most promising and fundamental therapies for many human diseases from cancer to muscular dystrophy, face a common and significant barrier in specific delivery. The specific delivery of therapeutic agents, to target tissues and cells is the single greatest barrier for the successful translation of promising experimental therapies to effective clinical applications. Here I report a novel approach to identify tissue- and cell-targeting specific peptides by combining the powerful method of phage display with a uniquely available set of selection methods, combined with the most advanced nucleic acid next-generation sequencing technologies, to best study the selection of muscle targeted peptides. This unique combination overcomes the demonstrated limitations of traditional phage display for peptide selection by taking advantage of state-of-the-art next-generation sequencing power to distinguish millions of nucleic acid sequences under study. This application, along with careful and thorough selection design contributes a significant step forward and could provide truly applicable targeting peptides for-tissue/cell specific delivery of drugs as well as gene and oligonucleotides.

4.2 Introduction

Bacteriophage is a collective term used to describe virus which have co-evolved with defined bacterial hosts that support the bacteriophage infection and replication. Bacteriophage was investigated as a potential treatment for bacterial infection before being generally abandoned as a therapeutic when Alexander Fleming characterized a new compound produced by the *Penicillium* mold, which he termed “penicillin” a discovery which bore life-saving antibiotics and the pharmaceutical industry. However, bacteriophage research continued, resulting in the identification of various bacteriophage and their respective host bacteria, consequently producing many contributions to our current understanding of molecular biology. Examples include the first gene and RNA sequenced as early as 1972 (MS2) and the first full genome (Phage φX174) sequence published in 1977 (Min Jou, Haegeman et al. 1972, Fiers, Contreras et al. 1976, Sanger, Air et al. 1977)

The first application of bacteriophage expressing foreign DNA inserted into M13 phage gIII gene and displaying the corresponding peptide on the phage minor coat protein (pIII/g3p) was described in 1985 by George P. Smith.(Smith 1985) Since that time molecular modification and affinity screening of phage expressed peptides has enabled numerous investigators interested in determining or characterizing particular epitopes or interactions, to employ this technology. Selection of phage expressed peptides with an affinity to purified proteins and tissues of interest, along with basic research has provided new understanding of disease mechanisms while also presenting potential therapeutic options. In this capacity, phage array has been used to define protein: protein and peptide: DNA interactions, enzyme catalytic sites, and to identify short peptides with affinity to specific cell or tissue types.

To date, despite numerous reports of *in vitro* specificities, minimal success has been achieved in applying phage-derived peptides to target specific tissues *in vivo*. While *in vivo* applications of phage-selected peptides remain elusive, a notable exception is the vascular integrin $\alpha_v\beta_3$ targeting peptides selected *in vivo* by Arap et al. This particular success may be in part due to the high levels of ligand *in vivo*. Overall, success *in vivo* through the use of synthetic peptide or phage array has not met its full potential.

Recent attempts to identify muscle specific peptides have employed iterative *in vivo* selection methods, selecting for clones with greater affinity to muscle than liver, demonstrating some specificity of phage clones to C2C12 myoblasts by immunohistochemical methods and less convincingly using fluorescently labeled phage administered by systemic injection.(Seow, Yin et al. 2010)

Modification of attempts at similar or related studies with a more careful step-wise approach and controls, along with high-throughput methods could yield comparable if not more effective results.(Newton and Deutscher 2008) To date very few *in vivo* results of phage arrays have indicated much promise beyond published results *in vitro* and/or *ex vivo*.(Brown, Modzelewski et al. 2000, Brown 2000, Kelly, Clemons et al. 2006, Kelly, Waterman et al. 2006) The addition of high-throughput technologies not previously available as well as multiple disease model systems that are available in laboratories such as the McColl-Lockwood laboratory should yield a more specific and efficient methodology for selection of appropriate clones for further testing.(Brown, Modzelewski et al. 2000, Hruby 2002, Benedetti, Morelli et al. 2004, Kelly, Clemons et al. 2006, Kelly, Waterman et al. 2006, Krumpe and Mori 2006, Newton and Deutscher 2008, Yu, Yuan et al. 2009, Shi, Nguyen et al. 2010) Of particular note, is that although the reported panning experiments of the phage array have been tested and reported within a selection of tissues and origins, present and future studies must address the ability through phage display to also study disease models of particular variation from, and including the wild-type. (Kelly, Waterman et al. 2006, Newton and Deutscher 2008)

The general procedure of a phage array itself can be technically challenging, requiring vigilant and painstaking attention to detail, from selection design through execution. Many have reported of success *in vitro* in identifying peptide ligand candidates for a variety of target molecules, with >20,000 unique peptides identified through selection collected on databases such as MimoDB.(Huang, 2012) Increasingly investigators are realizing that screening to identify specific ligand to unique receptors, such as muscle surface protein αDG for use *in vivo* requires the selection in different systems, such as purified proteins, whole cell or *in vivo* tissue, in tandem in order to achieve significant and reproducible results. Previous studies have found the *in vitro* selection process to result in identification of multiple common peptide sequences or motifs relative to target molecules, but provide little support for the relationship of identified ligands beyond selection methods and demonstrated affinities,. The two greatest deficiencies in previous studies have been a lack of translation from *in vitro* results to *in vivo* application, and likely biased selection of peptides to targets in non-native states. One aim of the study reported in this chapter is focused on preliminary selection of phage clones which express peptides with a high affinity for both native and modified muscle targets.

The literature associated with muscle specific targeting through the use of phage array or synthetic peptide is limited to only a handful of reports, all of them presenting *in vitro* results without reproducible application *in vivo*. In this study, I propose to conduct the phage array with two systems in combination, a cell culture based selection and *ex vivo* tissue selection, with the aim to obtain a refined sub-library from which the majority of selected clones are of likely value. This hypothesis driven process is unique and afforded by the stringent experimental design leveraging the best knowledge and disease models available. The procedure is illustrated in Figure 27.

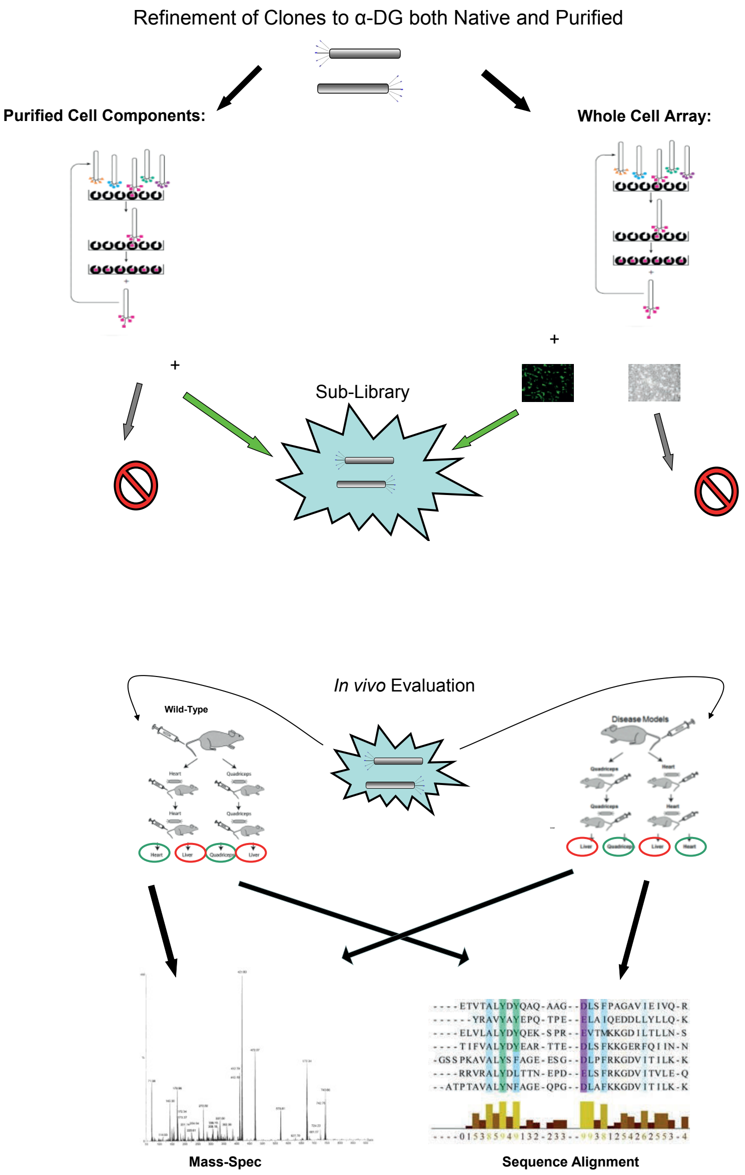
Refinement of Clones to α-DG both Native and Purified
Purified Cell Components:
Whole Cell Array:
+
+
Sub-Library
In vivo Evaluation
Wild-Type
Heart
Quadriceps
Heart
Quadriceps
Heart
Liver
Quadriceps
Liver
Disease Models
Quadriceps
Heart
Quadriceps
Heart
Liver
Quadriceps
Liver
Heart
----ETVTALYDYQAQ-AAG--DLSFPAGAVIEIVQ-R
------YRAVYAYEPQ-TPE--ELAIQEDDLLYLLQ-K
----ELVLALYDYQEK-SPR--EVTMKKGDILTLLN-S
----TIFVALYDYEAR-TTE--DLSFKKGERFQIIN-N
-GSSPKAVALYSFAGE-ESG--DLPFRKGDVITILK-K
----RRVRALYDLTTN-EPD--ELSFRKGDVITVLE-Q
--ATPTAVALYNFAGE-QPG--DLAFKKGDVITILK-K
----0153859491 32-233--9938125426 2553-4
Mass-Spec
Sequence Alignment

Figure 29: Schematic diagram of phage selection methods. A) Applying the naïve library, phage clones expressing peptides with binding affinity to targets on the cell surface, or purified target fixed to substrate, are retained after non-binding clones are removed by washing. Binding clones are then recovered through washes with weak detergents, or

collection of the target from the substrate entirely. Portions of the selected clones are stored while the remaining phage are amplified in host *E. coli*, with clones selected and PFU quantified on LB agar, and again recollected for further selection. B) Naïve or sub-library can be applied systemically *in vivo*, and target and control tissues collected for retrieval of remaining bound phage clones. Phage clones of interest at any point can be submitted for sequencing to determine the expressed peptide sequences, or mass-spec analysis/characterization of phage peptide or interaction.

For this study there were three separate but convergent aims.

1) To modify traditional selection methods to achieve higher throughput and more stringent criteria than had been used in previous studies.
2) To compare the selection techniques applied and the resulting candidate peptides with high affinity to the intended target.
3) To evaluate available sequencing technologies in regard to identification of candidate peptides produced through traditional selection. Specifically to evaluate the novel NGS methods for a much richer and valuable insight into target-specific selection.

4.3 Results

4.3.1 Phage selection using a-DG positive and negative CHO cells *in vitro*.

To determine the ability of phage-display techniques to identify muscle specific ligands with binding affinity to α-DG, I have applied the PhD-12 and PhD-7 M13 phage libraries from NEB. The random dodecapeptide or heptapeptide sequences expressed as a result of inserted sequences within the *gIII* gene, previously used to identify epitopes or characterize protein:protein interactions, were applied in a series of selective processes utilizing the muscle-membrane receptor a-DG. As demonstrated in figure 32 and schematic figure 43, the standard phage-display techniques were adapted to reduce the labor-intensive process of enrichment selections, clonal identification, isolation, and characterization, high-throughput applications were employed whenever possible. The greatest advantage to this adaptation was the ability to perform post-selective clonal isolation, resulting in collections of phage sub-libraries which could then be assessed in bulk instead of iterative assays, using 96-well 1mL plates for host-culture propagation and storage, and 96-well plates suitable for immunohistochemical methods and fluorescence detection using the Tecan500 microplate reader. As demonstrated in the figure, for initial selection methods the naïve library was exposed to live and fixed CHO cells expressing hyper-glycosylated a-DG as positive selection as well as glycosylation deficient CHO mutant (Pro5) cells. After each round of selection the resulting sub-library was plated for PFU quantification and isolation of viable clones. Once isolated, amplified where necessary and purified, each clone was exposed in matched 96-well plates across both of the aforementioned selective cell cultures, followed by detection of bound phage by anti-M13 major coat protein (g8p) followed by flurochrome labeled secondary antibodies. To determine the specificity of the assay, control cells were stained with IIH6 C4 antibody known to identify the target protein of glycosylated a-DG to ensure the assay reliability while also providing the data to assess the background and contrast ratio. Examples of these control cells stained for glycosylated a-DG are given in figure 31 of this chapter. As demonstrated, the relative fluorescence can be seen with the naked eye, but for the purpose of this assay values of 2.0 or higher signal to background and positive to negative controls were deemed differentially selected. The resulting relative fluorescence units (arbitrary) were then used to create plate-matched comparisons of each clone binding to each substrate. For the purposes of assay characterization of isolated clones, three possible outcomes from this assay were possible. The comparison outcomes were as follows: +/+ where RFU comparison indicated far higher phage binding to the intended target; +/- where the RFU values of clones were roughly equal, and -/- where individual phage clones were determined to have net negative values indicating specificity but not to the intended target. While great efforts were made to isolate single phage clones, it was expected that some of the evaluated clones were in fact mixed populations. Because of the included controls, significant variation between plates used in the assay or between net RFU values on repeated assays for an individual clone isolate could be identified and were noted, and samples with intra-experimental variance were reclassified to +/-. As an initial assessment of binding specificity this assay was quite efficient, easily completed by one person with as many as1000 isolated clones assessed at a time through pin replication, in 96-well format.

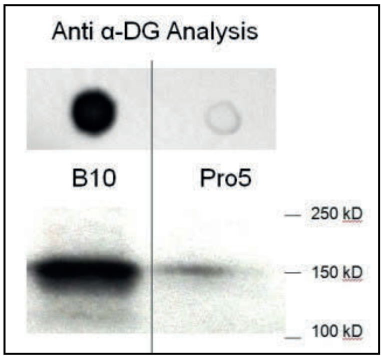

Figure 30: Immunodetection of a-DG in CHO used for phage selection. Through IIH6 detection of glycosylated a-DG, and HRP conjugated secondary antibody.

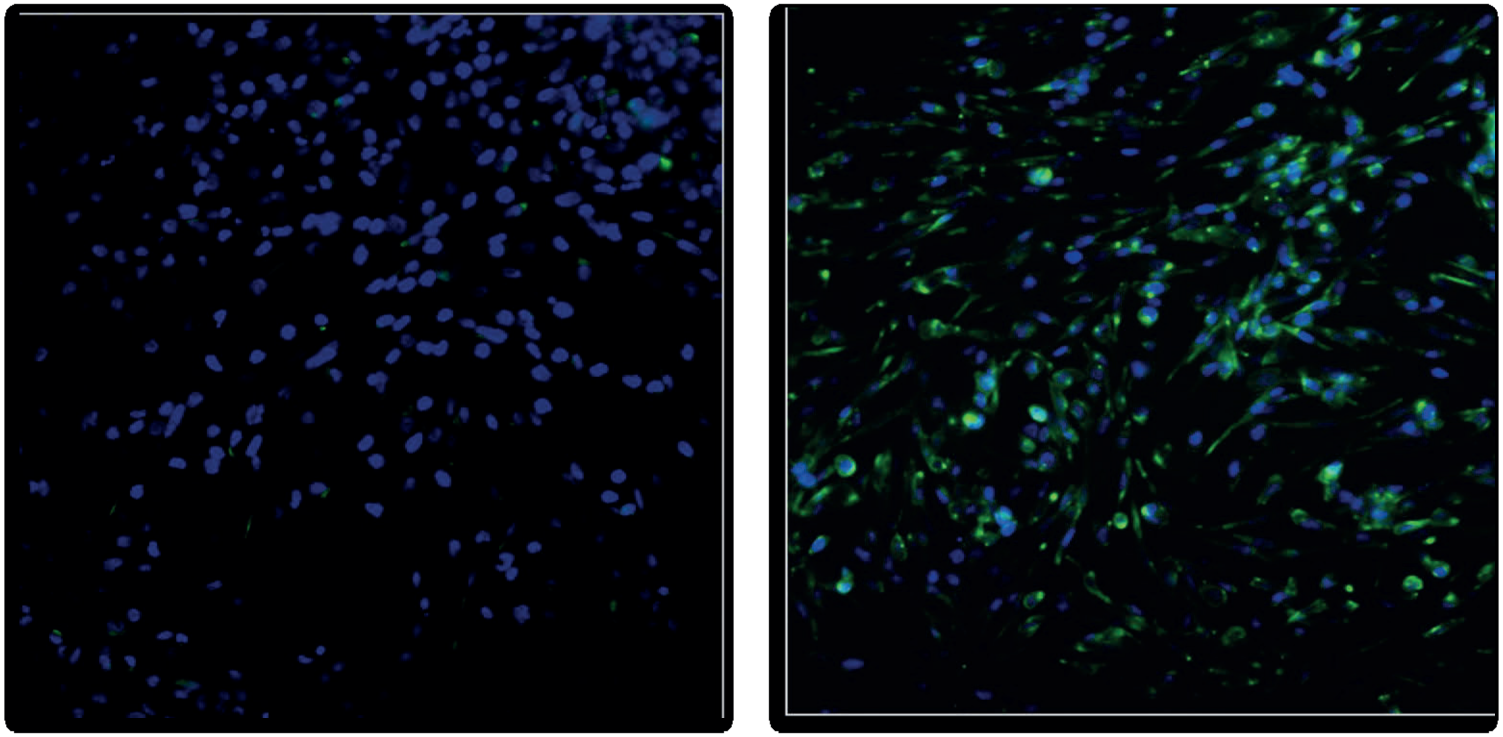

CHO Pro5

CHO Pro5 +LARGE

Fig 31: IHC of a-DG of CHO Pro5 and Pro5 +LARGE cells. Shown here, the cell lines used and IIH6 antibody recognition of epitopes of α-DG (green fluorescence) clearly demonstrates the contrasting levels of glycosylated α-DG between these two cell populations used for selection.

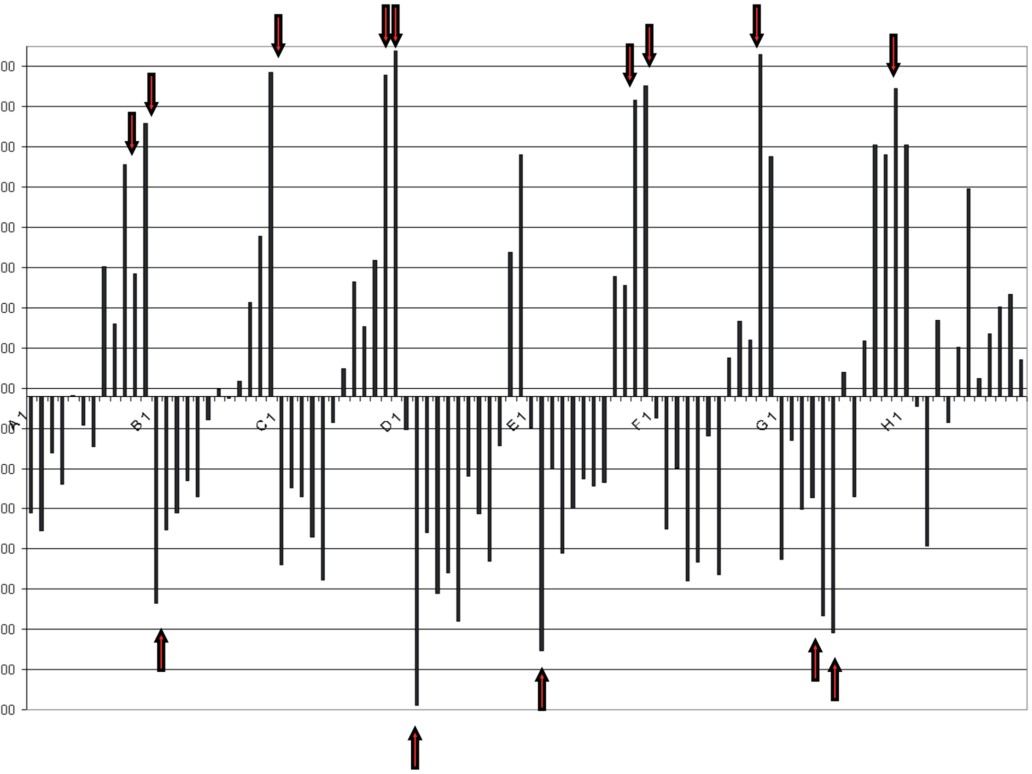

Greatest +/- away from the average RFU for fluorescent photomicrograp

Figure 32: HTS selection and validation of phage clones. Once selective panning has been completed and phage clones isolated, they can be evaluated for target binding by sandwich ELISA techniques, where relative fluorescence correlates to binding affinity when phage have been adjusted to similar PFU/volume. A typical example of assay results in two 96-well plates, phage are allowed to bind and those clones with the greatest difference between cell/protein populations, indicates a divergent selection, as indicated by the red arrows.

Once a subset of phage demonstrating binding affinity through selection and validated by HTS and scored, those selected clones were grouped as the most appropriate candidates they were pooled into a larger sub-library (<100) for additional characterization.

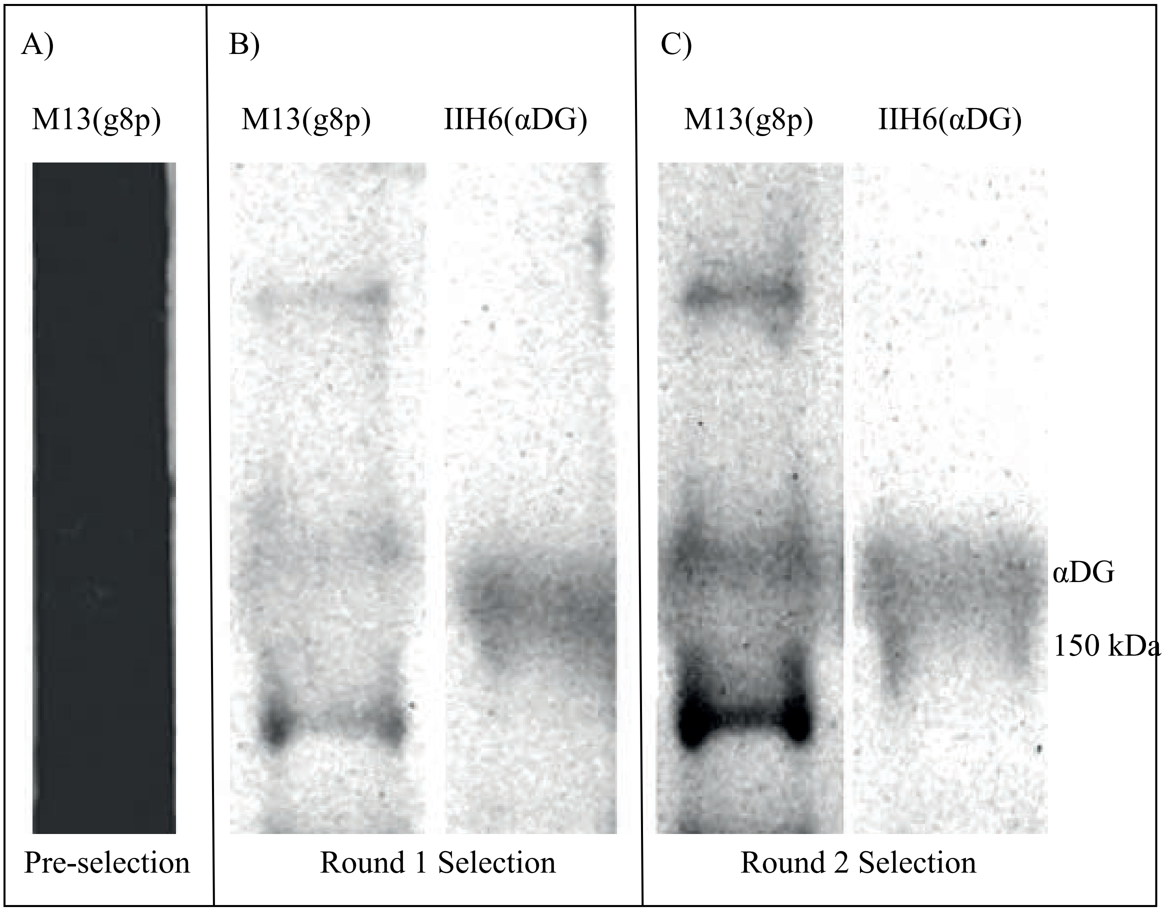
A)
M13(g8p)
Pre-selection
B)
M13(g8p)
IIH6(αDG)
Round 1 Selection
C)
M13(g8p)
IIH6(αDG)
αDG
150 kDa
Round 2 Selection

Figure 33: Phage detection of α-DG epitopes on western blot. Two selective rounds over B10 culture supernatant. A) first round of selection and detection of bound phage B)Second round selection sub-library detection of B10 culture supernatant α-DG C)Phage sub-library detection of epitopes after two rounds of selection with IIH6 anti-DG comparison.

4.3.2 Secondary phage selection using a-DG positive and negative muscle tissues *ex vivo*.

For the purpose of further evaluation of these top candidates, this subset was tested for appropriate location and signal to background using cryosectioned quadricep muscles from C57 wild type and the unique P448L Neo+ mouse model of LGMD generated by the McColl-Lockwood laboratory. These tissue samples represent both the normal and disease state, and like the CHO cell lines used for initial selection vary remarkably in glycosylation, as shown in the tissue samples within figure 34 as detected by IIH6 immunohistochemistry. Not surprisingly, a small proportion of the top selected clones bound some targets at the periphery of myofibers in both of the tissue types. However, the majority of these selected clones presented markedly different patterns between the C57 and P448L Neo-ex-vivo array. This is demonstrated in figure 35 where punctate patterns of “Clone X” on C57 tissues is distinguishable from “Clone A” or “Clone B” Furthermore, referencing the tissue array controls shown in figure 34, it is important to convey that the green fluorescence observed on the P448L Neo- section is in fact primarily background fluorescence created by high levels of immunoglobulins present from the presence of muscle damage and infiltration of leukocytes as the muscles of these dystrophic mice regularly cycle between muscle degeneration and regeneration. The final best set of clones expressing peptides with target specificity was ultimately narrowed to 54 clones, representing isolated phage from nearly all of the selection methods used. Interestingly, while the majority of the final phage are proportional to the number of post-selection isolations, One subset, where native and PFA fixed whole-cell selection was conducted only resulted in a single clone that met the final criteria for selection.

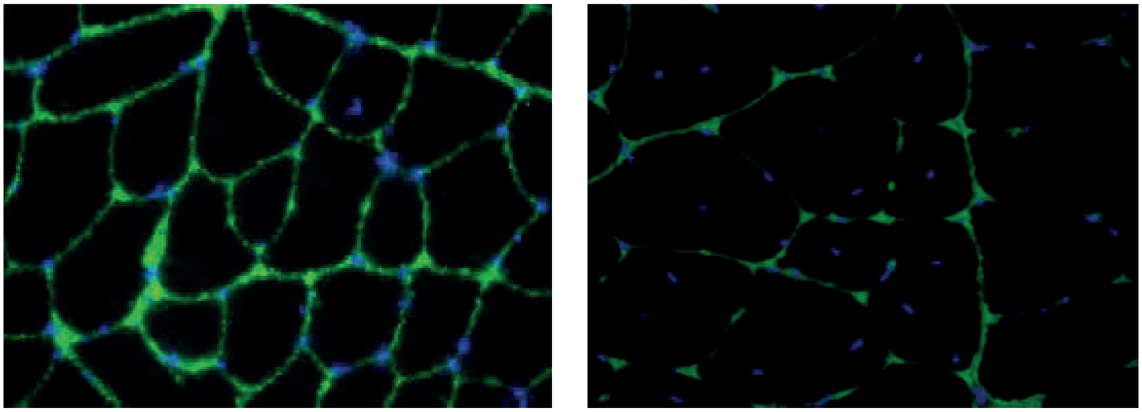

C57 wild type

P448L FKRP Mutant

Figure 34: C57 WT and FKRP P448L α-DG muscle IHC. This

This figure demonstrates the stark contrast between the wild type C57 muscle expression of glycosylated α-DG (Green) as compared to the FKRP mutant P448L mouse model of LGMD, where most of the fluorescent signal is the result of high levels of background immunoglobulins present from the disease state, and not IIH6 α-DG detection. Also demonstrated in this figure is the high number of centrally nucleated myofibers indicative of muscle degeneration and regeneration occurring in the phenotypically hypoglycosylated P448L mouse model of LGMD2I. These contrasting states of glycosylation give *ex vivo* screening and validation of selected phage clones additional power to identify those clones with true target-specificity.

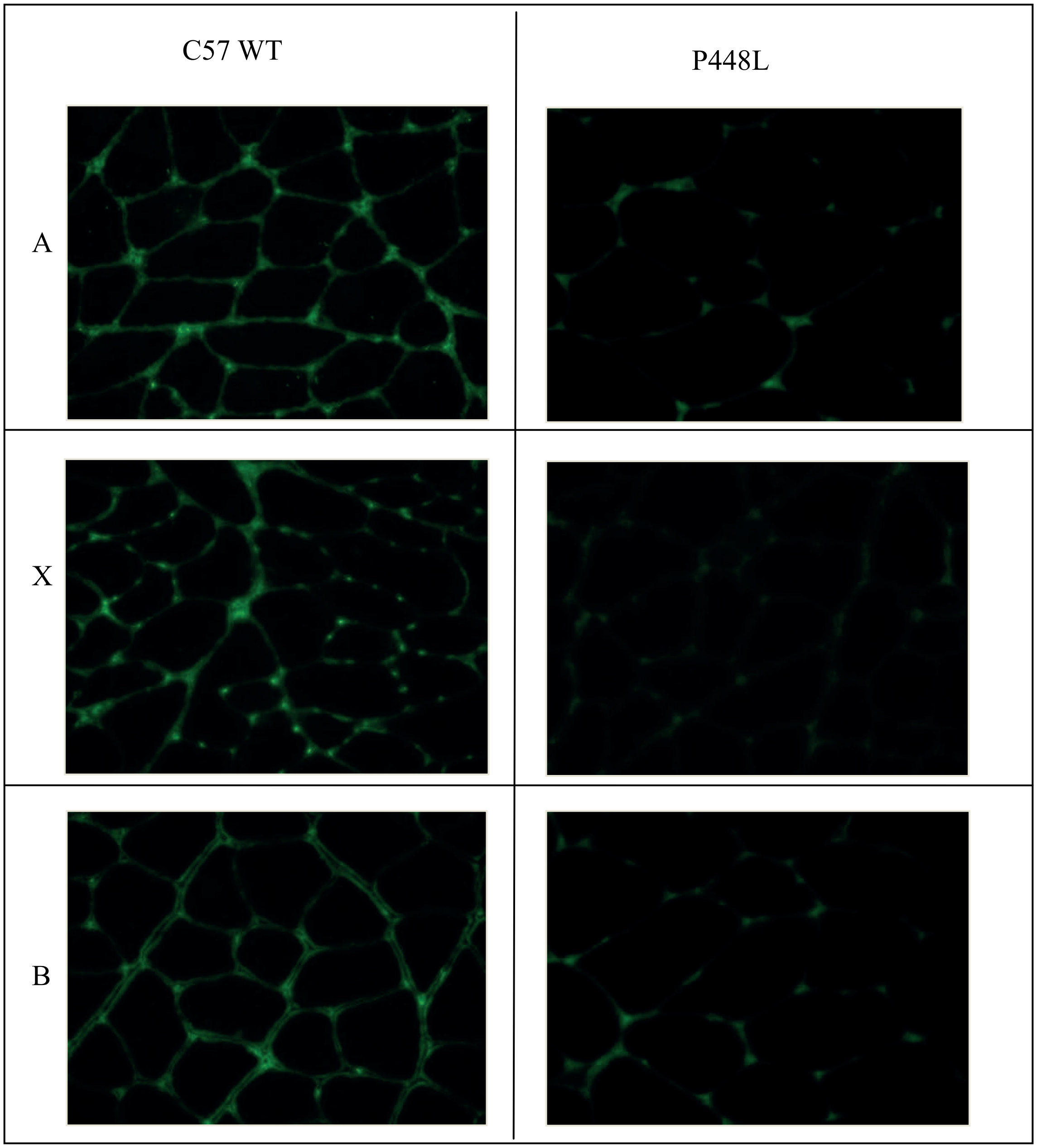

Figure 35: *Ex vivo* phage affinity to skeletal muscle. Phage affinity to wild type C57 (left column) and typically hypoglycosylated P448L quadricep was assessed *ex vivo*. Selected phage clones were incubated on tissue sections, and phage loci detected by anti-M13 major coat protein (M8P) and FITC tagged secondary. Phage clones demonstrating higher binding to wt myofiber periphery were retained for further evaluation. Clones binding

with punctate specificity (Clone X second row) and those similar to the IIH6 antibody commonly used to detect α-DG were of particular interest and also retained (Clone A, Clone B).

4.3.3 Conventional sequencing of the selected phage library.

With a comparably thorough characterization of the selection methods used and the demonstrated ability to select phage expressing peptides to varied presentation of targets of importance for the muscular dystrophies, genomic phage ssDNA was extracted from the final sub-library and was submitted for sequencing using the-28 and -96 primer set recommended by the library manufacturer.

As demonstrated in figure 36, submission of phage genomic DNA with the manufacturer recommended primers effectively returns a quality read on all the phage genome, other than the variable region. Across the genomic DNA samples submitted for sequencing, only partial reads were obtained and were insufficient to compare to achieve any meaningful data. In an attempt to reduce background noise from the genomic DNA, primers were designed to create cDNA amplicons with predicted product sizes of 240 and 266 bp. After an initial round of optimization using a PCR temperature gradient, the primer set "M13_66_F" and "M13_2-267.R" was chosen as it more reliably produced the intended PCR products from the genomic phage DNA template. As demonstrated in figure 38.

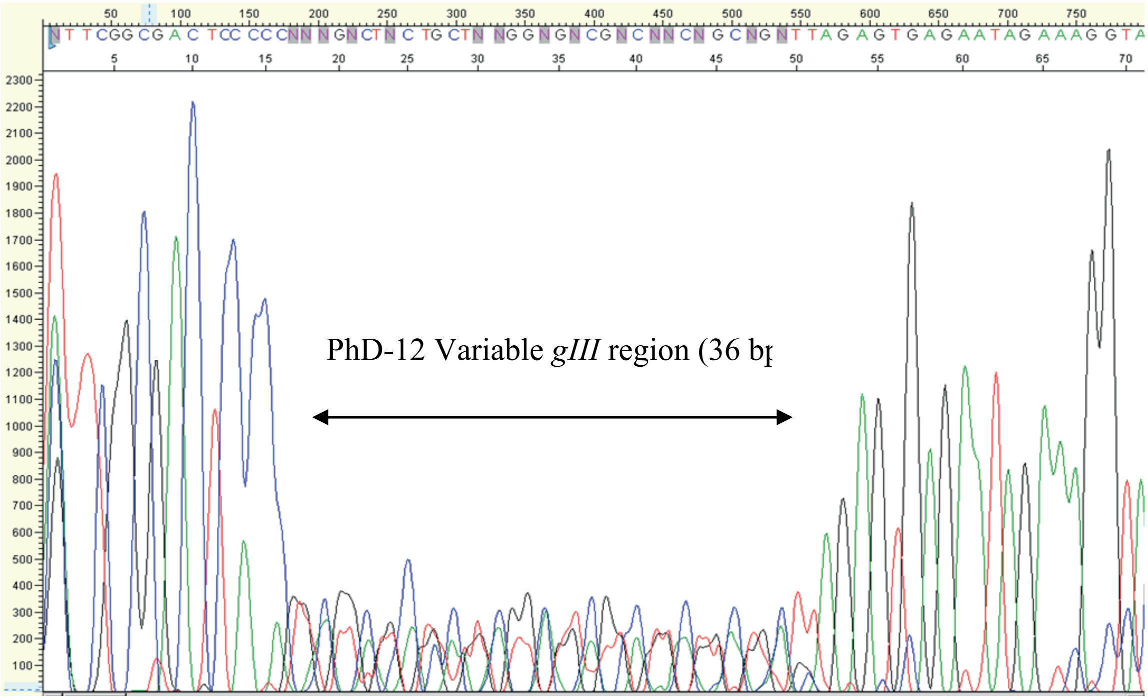

Figure 36: Representative histogram of phage *gIII* Sanger sequencing. Results show notably poor read quality corresponding to the phage variable region. This 36 bp (PhD-12) and 21 bp (PhD-7) variable sequence is complicated by clonal variation, and was not found to be resolved by adjusting sequencing primer positions, or PCR amplification of the ssDNA phage genome to cDNA. This figure highlights both the necessity for appropriate sequencing primers as well as likely PCR amplification or iterative re-isolation of selected phage to a monoclonal population. However, the actual data attained with Sanger sequencing represented in this figure does not indicate in any way which of these factors has attributed to poor read quality, reinforcing the need for additional sequencing technologies to best approach the fundamental aims of phage display programs.

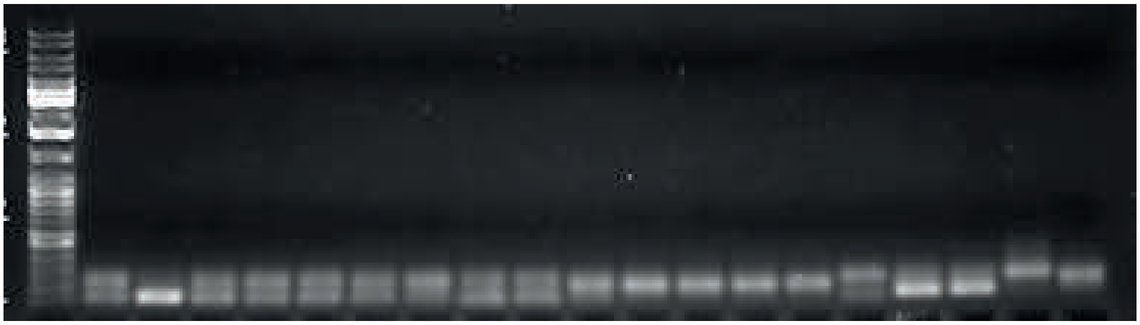

Figure 37: Initial PCR amplification of M13KE *gIII with 100mer flankers*. DNA from isolated phage was used for PCR amplification of the gIII DNA with variable sequence contained within ~100 mer flanking regions of conserved M13, with multiple bands indicating varied efficacy of PCR amplification due to intraclonal variation or polyclonal effects.

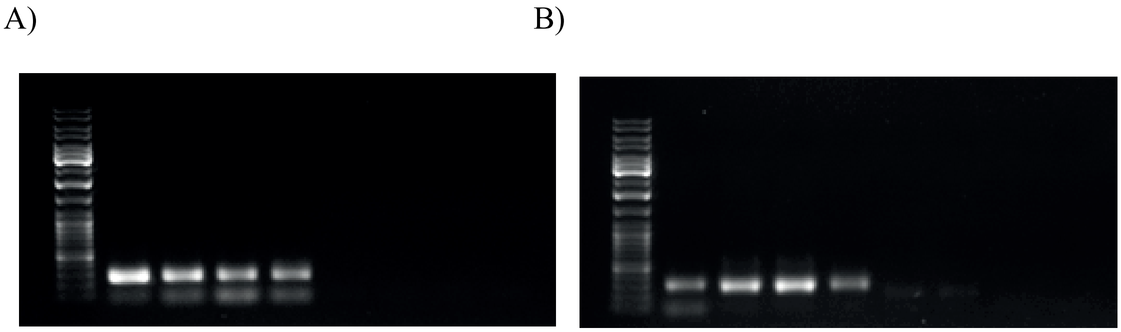

Figure 38: PCR optimization of 260 bp M13KE *gIII* amplifications.

specific primers from genomic phage ssDNA template. Within the same PCR conditions, A) The naïve library and B) The selected “Clone X” show slight signs that the primers designed to the variable-flanking regions from previous sequencing data and the reference sequence show improved performance in creating amplicons from selected phage than from the naïve library.

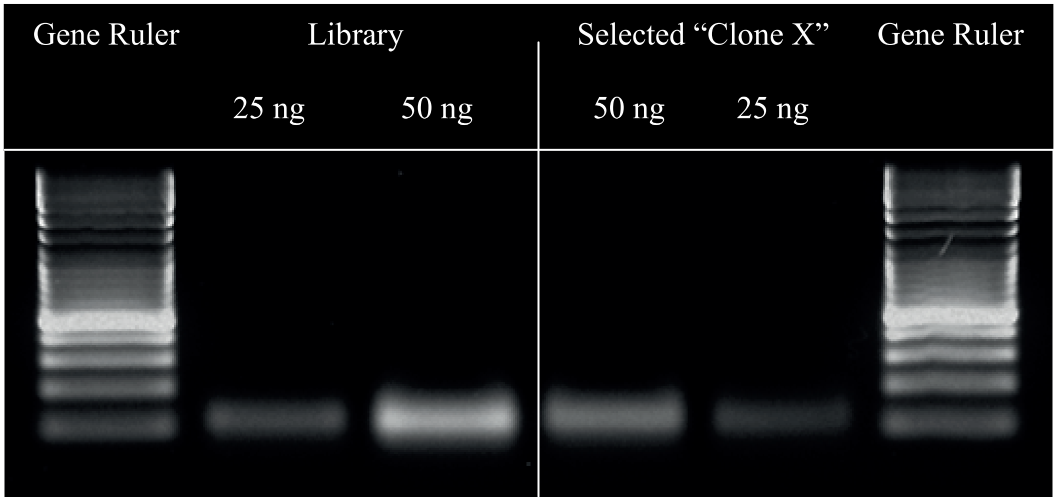

Figure 39: QC of 112 bp M13KE *gIII* amplifications. Product size and concentration in tandem to confirm UV-Spec DNA quantification. The ladder used was Gene Ruler (ThermoSMO241), of which the smallest band is roughly 100 bp, and ~40 ng as applied in this instance. DNA concentrations were obtained with at least two spectrophotometers in triplicate and 2% or 4% agarose gels were loaded with a concentration derived from prior quantification to verify using known band size and concentrations given by the Gene Ruler manufacturer.

4.3.4 NGS analyses of the original and selected phage library.

The difficulties encountered in sequencing all phage clones and the multiclonal nature of selected clones are difficult to resolve with the conventional chain-termination sequencing method. Subcloning of a few selected clones can eventually clarify the sequences, but is unlikely to provide any further insurance for cell/tissue specificity. I therefore decided to apply the powerful NGS method to determine the individual sequence of a selected phage sub-library as a whole.

To better understand the nature and the consequence of the selection procedure on the phage library composition, I also decided to sequence the original phage library for comparison

Almost all applications of NGS have been for genomic DNA sequencing and for RNA sequencing for quantitative analyses of gene expression profiling. The resulting sequences are read by the existing data analysis program relying on comparison with existing genome or RNA sequence libraries to establish the nature of testing sequences and the abundancy. Without such control libraries, our NGS service department and several service providers all initially refused to attempt the sequencing of the phage libraries. As they were not sure how the data could be processed and presented. I therefore designed a simple and practical method for NGS providers to undertake the challenge of data analyses. This only involved the analyses of the following factors: 1) the total number of the reads, 2) the total number of the reads of phage sequences, 3) the repeat number of each sequence and ranking them from higher frequency to lower frequency, 4) the comparison within the two libraries to identify the unique sequences form each other. I was able to successfully obtain clearly defined unique sequences of which there were more than 15 million.

The data obtained through NGS, both forward and reverse reads, were collected aligned with ClustalX, and assessed for conserved flanking regions of (NNK_{12}) as shown in figure 44 and once parsed, resulting variable region were translated into peptide sequences using the appropriate M13KE abbreviated codon usage, as given below in table 5. The resulting peptides from the data sets, were then subjected to further analyses consisting of peptide alignment with ClustalX, PSI-Blast (NCBI) for peptide sequence identity against available reference proteins, MimoDB search for previously identified peptide mimotopes, IceLogo analysis of variation from the M13 proteome and between libraries, and a comparison of observed amino acid distribution to manufacturer literature and summarized in Table 5.

The PSI-BLAST analysis of the select portion of the peptides from both the naïve library and selected clone resulting from NGS sequences is briefly summarized on the following page.There were 28 unique sequences identified from the naive phage library, while there were 73 unique sequences enriched in the selected library within the top 100 most frequently detected sequences across NGS sequencing runs. These sequences are therefore potential candidates for further validation of their muscle targeting specificity. However, there are sequences which were identified with high frequency in both libraries, but with significant variation in abundance. It is difficult to assess if these sequences with higher abundance in the selected library could also be the result of selective enrichment. A further validation experiment will be required.

To understand the significance of the sequence variation and abundance between the two libraries, the nature of the sequences were assessed using the programs and methods listed above. The prevalent sequence motif identified as part of the abundance analysis in both the selected and naïve library by PSI-BLAST is closely related to sequences of uncharacterized proteins. While I have not yet been able to define the precise significance of the observed phenomena of this prevalent sequence, I hypothesize that these sequences might have high binding affinity to many cell surface epitopes common in bacteria and in mammalian cells. Other factors for consideration include possible bias of PCR amplification, and/or of particular parameters used to align the NGS reads to an M13 reference sequence to determine relative abundance of variants within the two NGS data sets obtained, could also play a role for possible biases observed.

Another interesting feature of the most abundant peptide sequences through PSI-BLAST analysis is that they are most homologous to peptides of characterized domains of putative enzymes, conserved families of membrane transport receptors, such as acetyltransferase, and P2X receptor from bacterial, fungal, and animal (Trematode) pathogens and parasites. The most abundant hits of potential interest include the following:

Sel R1.10 – UDP-N-acetylmuramoylalanyl-D-glutamate ligase
Sel R1.53 – Glycosyltransferase (*Echinocola Sp*)
Sel R2.80 – Transmembrane fibronectin III Domain (*Legionella*)
Sel R2.39– peptide ABC transporter (*Mycoplasma)*
Sel R2.16, APC transporter (*Weissella*)
Sel R1.8, glycosyltransferase-like protein (*Streptosporangium*)
Sel R1.28- MFS transport proteins, (Multiple species)
Sel R2.98- Ig domain containing protein (*Paenibac*terium)
Sel R1.96- Suc-6-phosphate hydrolase (*Clostridium sp*)

The unique sequences of high frequency identified from the selected library include the peptides of IYTTISQAGTPI, LTRRSSDLWLL, and LYPNINNMYMWT. These sequences show great homology to kinase, phophohydrolase, alkaline phosphatase, methylpyrimidine kinase, and PSP-1/SACTE of *Streptomyces sp*.

Analyses of the peptides from both libraries by querying the MimoDB database, and to complement the PSI-BLAST, identified a previously selected and characterized peptide mimotope with the peptide NERALTL which has been reported as having specificity to epoxy substrate.(Swaminathan and Cui 2013). It is possible that phage peptides with specificity to some plastic ware can also be enriched.

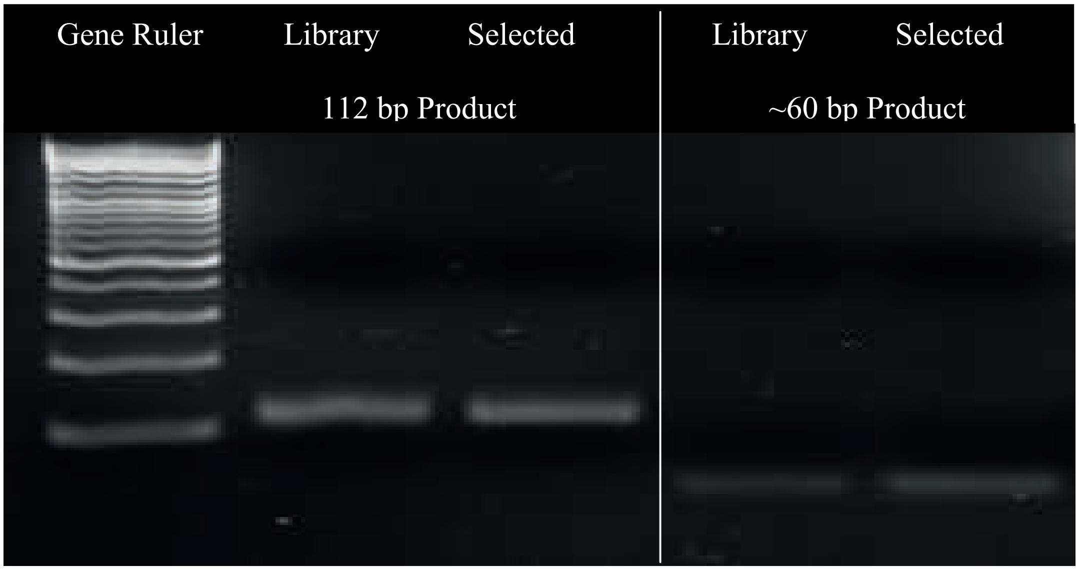

Figure 40: Separation of target/fragment PCR products for NGS. Intended 112 bp and fragment PCR products. Prior to sample submission for NGS, potentially confounding PCR products below the expected size were removed by excision of sample bands resolved by gel electrophoresis in a 2% agarose gel, purified, and validated by further electrophoresis in 4% agarose gel. The resulting product size was confirmed as shown, compared to the GeneRuler™ (Thermo) of which the lowest band is 100 bp. This amplicons clean-up is necessary as construction of the NGS library and quality of the resulting sequencing relies upon relatively homogenous samples of particular lengths.

Table 4: Comparison of NGS sequencing of PCR amplified phage variable region

ID	% Seq #1	% Seq #2
PhD-12 Naïve	17.91	.0174
PhD-12 Naïve	13.13	.0171
Selected Clone X	23.59	.0285
Selected Clone X	22.23	.0302

*Total NGS results consisted of 15,274,286 resulting sequences from the naïve PhD-12 library sample and 16,439,852 from the post-selection methods sample.

Target-Selected Phage Peptides

AHIPTSMPERHL
AHIPTSMPVGHL
AHIPTSMPVRHL
AHIPTSMPVRHL
APAHTVMRTNPD
APAHTVMRTNSD
APAHTVMRTNWD
APAHTVMRTNWD
DALLAKMRSNQL
DALLAKMRSNQL
DALLAKMRSNQL
DALLAKMRSNQL
DPPESRDGLLPR
DPPESRDGLMPR
DPPESRDGLMPR
DPPESRDGLMPR
DPPESRDGLMPR
DYHTKPDLILSY
DYHTKPDLILSY
DYTTKPDLIQSY
FWVSNTQGVHSL
GELSPQVSRSIA
GELSPQVTRSIA
HHSYLAKAGQSL
IPQGIVDQLHMY
IPQGIVDQLNMY
IYTTISQAGTPI
LRTRRSSDLWLL
LTVSNTQGVHSL
LYPNINNMYMWT
NEAKTENLNASG
NIFAEAQQMFQW
NYHTISQAGAPI
NYHTISQAGPPI
NYHTISQAGSPI
NYHTISQAGTGI
NYHTISQAGTPI
NYHTISQAGTPI
NYHTISQAGTPV
NYHTITQAGAPI
NYTTNRQAGTPI
PTRRSSDLCMG
PTRRSSDLW
TSQWSLPPAKPW
TTYLAKAGQSV
VLRHEFQEHNWY
VLRHEFQETNWY
VSTLLRGPGTDR
VSTLLTGPGTDR
VYHTKPDLILSY
WSQQTGMWLEVI
YELQTSNAMYPG
YFDRESOEHKVP
YFDRESPEHKVP
YFDRESPETKVP
YNVGVPHAFFLV
YNVREPHAFFLV
YNVRVPHAFFKV
YNVRVPHAFFLV
YVLQTSNAMYPG

Naïve PhD-12 Library Lot 10

FSGTFLSG
FTASNTQGVHSL
FTASNTQGVHSL
FTVSNTGVHSL
FTVSNTQGAHSL
FTVSNTQGVDSL
FTVSNTQGVHLL
FTVSNTQGVHQL
FTVSNTQGVHSL
FTVSNTQGVHSP
FTVSNTQGVSHL
FTVSNTQGVTSP
FTVSNTQGVYSL
HAMRAQP
IPQGIVDQLMY
IPQGIVDQLNMY
KSKRTLI
LPLSTQH
NERALTL
NIFAEAQQMLLW
NIFAEAQQMLQW
NIFAEAQQMLRW
NYHTISQAGTP
NYHTISQAGTPI
NYHTISQAGTPI
TAMGAQP
TPTTVSY
TSQWSLPPAKPW
WSTTNVP

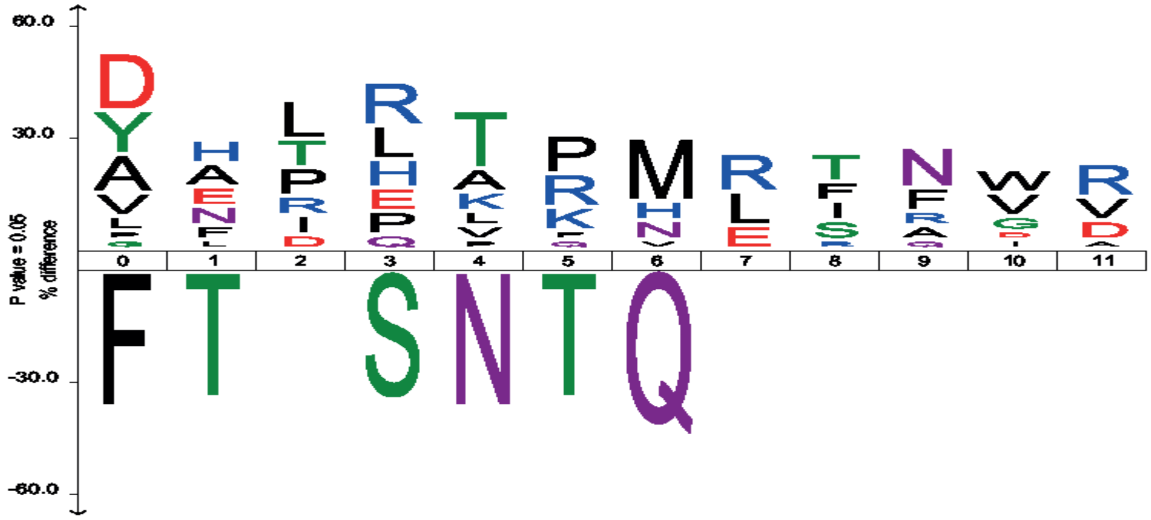

Figure 41: Comparison of the most prevalent naïve and selected peptides from NGS sequencing (P<.05). While this figure underscores the prevalence of the peptide sequence FT_SNTQ, it demonstrates the positional and amino acid diversity within the selected phage sample compared to the naïve library. By positional comparison, the % difference between the two data sets is represented here by the size of the single-letter amino acid abbreviation, confined to P<.05. Comparable comparison within the selected library (data not shown) highlights positional importance or motifs within the data set, if not discernible by eye in data sets like that given immediately preceding this figure.

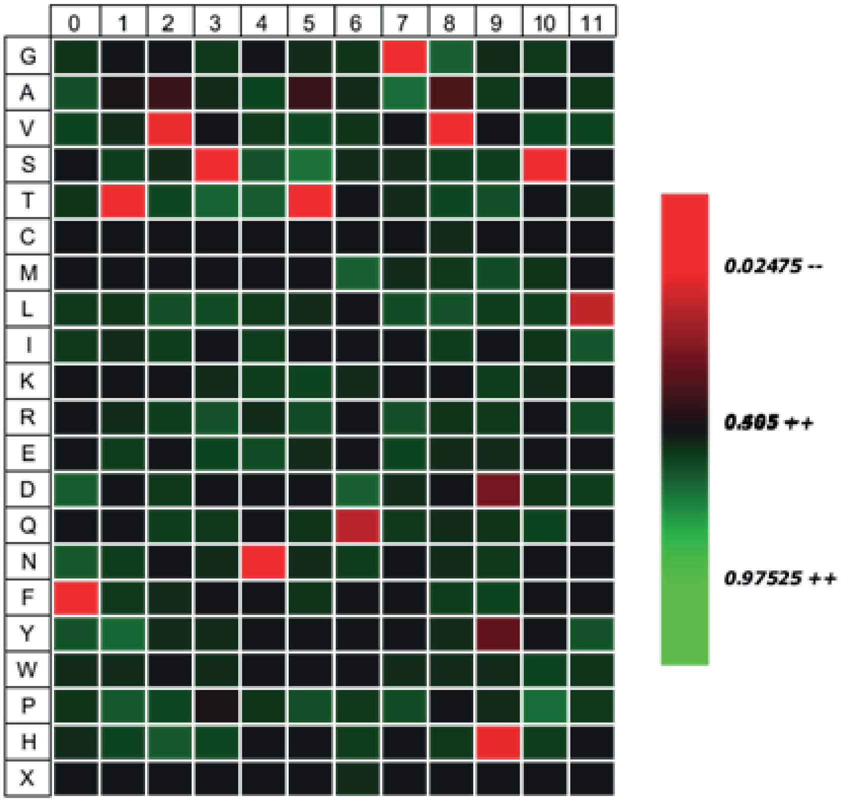

Figure 42: Heat-Map of identified peptides compared to M13 proteome. Comparison of selected peptides and M13 reference proteome. Comparison of selected peptides using M13 phage reference proteome highlights pairwise position based analysis of each peptide in the identified sequences to the known M13 phage proteome. Areas in Red indicate unique peptides by position, while areas in green indicate expected positions based upon the reference sequence, (generated using IceLogo). This comparison indicates the unlikely possibility of this peptide to be expressed by the M13 bacteriophage. This and further analyses are critical for determining the manipulation or biases introduced experimentally or those pre-existing upon library construction.

Table 5: Phage Library Amino Acid Expected and Observed Frequencies

Codon		Amino Acid	Phd-12 Lot 11	PhD-7 Lot 7	PhD-12 Lot-208	NGS Lib	NGS Sel
CGK, AGG	R	Arginine	3.72	3.4	5.7	1.5	5.9
CTK, TTG	L	Leucine	8.1	9.6	8.9	8.5	8.3
TCK, AGT	S	Serine	9.8	10.8	11.2	10.8	7.9
GCK	A	Alanine	6.2	8.6	7.4	6.9	7.1
GGK	G	Glycine	4.1	4.5	5.8	7.7	4.9
CCK	P	Proline	7.4	6.9	8.1	5.0	9.3
ACK	T	Threonine	10.3	10	7.8	15.8	8.2
CAG, TAG	Q	Glutamine	4.4	4.7	3.9	11.2	4.9
GTK	V	Valine	5.2	4.4	6.1	7.3	5.4
AAT	N	Asparagine	5.9	5.1	4.5	8.1	5.1
GAT	D	Aspartic Acid	4.1	4.4	4.6	1.2	4.9
TGT	C	Cysteine	0.5	0.29	1.5	0.0	0.1
GAG	E	Glutamic Acid	3.5	4.1	3.1	1.5	3.4
CAT	H	Histidine	4.8	4.8	4.6	4.6	5.2
ATT	I	Isoleucine	4.1	3.8	3.4	3.5	4.2
AAG	K	Lysine	3.4	4.1	2.3	1.2	2.3
ATG	M	Methionine	4.4	2	3.1	1.5	3.5
TTT	F	Phenylalanine	3.1	3.1	2.7	6.6	2.3
TGG	W	Tryptophan	1.7	1	2.3	2.7	1.8
TAT	Y	Tyrosine	5.4	4.5	3.6	1.9	5.2

It is clear that data from the NGS allowed me to understand the phage array technique with a fundamentally different perspective from my original thoughts, and those generally held among the researchers. So far, I have not been able to validate any of the identified peptides for muscle specific targeting efficacy and specificity, as I believe a portion of those identified could likely be non-specifically selected under the existing procedure. However, the initial data are able to answer many questions related to the applications of the phage array system for ligand peptide selection. More importantly, the data provide highly valuable information for a rational design of a better phage array system, so that tissue specific peptides can be more effectively selected with each step of the procedure verifiable and optimized. I will describe the significance of my finding in the following discussion.

4.4 Discussion

Phage libraries containing millions and billions of peptide sequences hold great potential for selection of targeting peptides and have been initially considered to be the replacement for antibody creation. Yet, despite the fact that phage array for peptide selection has been practiced for more than 3 decades with many different protocols and applied to both *in vitro* and *in vivo* systems, the potential has been rarely realized. Although it has generally been acknowledged that the procedure of array systems is not satisfactory, the precise reasons behind such contrast between the technique's potential and difficulty to achieve specific goals practically have not been well explained. As a result, nearly all reported applications up to the present have effectively relied on chance odds to identify clones with specificity to the proposed targets after several rounds of selection.

One critical piece of information missing from the phage array procedure is our collective lack of understanding of the phage composition of a specific library. While we do know the total number of phage clones, the diversity of even an initial library is only roughly estimated through limited sequencing of selected clones. It is impossible to assess the changes in phage composition after every step of the cycles of selection and re-amplification, due to the lack of methods capable to determine the majority if not all of phage ligands within a library. As a result, little significant improvement has been made to the phage array technique and to the outcome. My initial results from this exploitation allow us the ability to dissect the procedure, to find the hidden barriers and more importantly to devise new or improved procedures to achieve effective selection of peptide ligands specific to targets. Specifically, my results from the use of NGS for phage library identification provide several key factors for consideration.

First, phage libraries are generally created by degenerative RT-PCR with great diversity and possibly containing all possible peptide sequence combinations. The initial sequences are then cloned into phage vectors and propagated as the original library. The phage library producers will most likely perform at least one amplification cycle to produce enough quantity for customer end use. It is now clear from our NGS data of the original library that a big proportion of any phage library purchased already likely contains a biased population, likely through the preferential infection and/or host-replication-introduced selection bias as early as amplification as part of the library manufacture. This phenomenon has also been described by a very recent (late last year) publication describing those preferentially amplified phage as parasitic phage bias, which I prefer to call prevalent pre-existing artifacts. It is therefore critical for any phage array study to have the original library sequenced and the abundance of the clones determined.

Secondly, data from this study also showed that many of the abundant sequences persist after cells or tissue panning. It is difficult to determine if this is the result of target selection or again the selective amplification in the host bacteria. With the use of NGS, it is now possible to directly sequence the selected clones before amplification in the host bacteria. In fact, in an ideal circumstance, I would suggest this direct sequencing immediately after the selection should become the most critical step to identify ligand peptide specific to intended targets.

Thirdly, the classic methodology of phage array to identify specific peptides relies on the collection of viable phage with mild detergent to retrieve any bound phage from target cells/tissue or target molecules. The collected phage is then amplified in the bacterial host for further identification or further panning experiments. Therefore, only those phage stuck on to the target without losing the ability to host-infect could be collected, whereas those having already entered target cells could not be retrieved. The later population is potentially more relevant with higher affinity to target epitopes. This is especially important for targeting delivery of therapeutic cargo such as oligonucleotide. The ability of certain phage to enter the target cells could be more important than the ability of phage to bind target cells. This is particularly relevant to phage array *in vivo*. More phage are likely bind to natural barriers in the extracellular matrix, and selection of infectious phage could only recover those non specific to target cells if I intend to identify peptides targeting muscle fiber for oligo delivery. With the NGS platforms, it now becomes possible to collect and identify those phage already entering the target cells regardless of reduced host- infectivity. This is especially important for *in vivo* phage selection through the systemic route. Collecting phage already entering the target cells would indicate the ability of the peptides to effectively bypass the entrapment of serum and extracellular matrix components and the ability to maintain circulation in the vasculature, a critical feature required of potential delivery vehicles.

Currently, although the selection of phage can be conducted with both positive and negative selection, often, the positive and negative selections have been used to enrich and eliminate phage sequentially for more specific enrichment. One cannot realistically use the negative target cells or molecules as controls to verify the positively selected phage. However, with the use of NGS, it is now possible to directly compare the phage sequences selected from the control and the targeted cells or molecules, so the specificity of the selected phage from the targeted experiments can be verified, both quantitatively and qualitatively.

The limitation of conventional panning cycles of phage array also include the potential of enrichment and selection of phage with binding capacity to materials used in the experiments. One noticeably sensitive response by phage libraries is indicated by our finding using the MIMo database, where phage with binding specificity to epoxies were identified. Such phenomenon has also been described by Swaminathan et.al. Therefore avoiding repeated use of plastic ware would also reduce the background phage selected.

Considering all of the factors described above, I now propose a novel and simplified strategy of phage array for cell specific peptide identification as my next working model.

1. Amplify sufficient phage library once to produce sufficient amount (at least enough for more than 10 rounds of panning and selection). The original library and the replicate samples are then sequenced to verify the diversity.

2. Apply sufficient amounts of phage library to the target cells and relevant control target cells. For targeting muscle cells with functionally glycosylated α-DG as the target, the control cells of the same cell type, but lacking expression of functionally glycosylated a-DG. After appropriate incubation and washes to remove non binding phage, the bound phage will be collected and divided into two portions, one for further amplification in

host cells (utilizing the power of host bacteria for amplification, but under close monitoring of the sequence before and after the procedure) and the remaining portion for limited PCR amplification directly to NGS in tandem with the original library. The phage DNA should also collected from cells after the bound phage and amplified directly by PCR for NGS.

3. Compare the NGS data of the phage collected from the targeted tissue with that from control sample and identify those unique phage with affinity to the targeted tissue. Also compare the NGS data of phage DNA directly extracted from the targeted and control samples. This allows identification of the phage uniquely present in targeted samples.
4. The unique phage identified from targeted samples (both cell surface-bound and within target cells) can then be processed for the following two purposes: 1) for sequence analysis to identify the most frequent peptide sequences and the common motifs within those phage sequences with low frequency. 2) For new construction of a small phage library for further cycle of panning as described in step 2 to 3.
5. Repeated or duplicated rounds of steps 2 and 3 is needed to verify if the consistency of the results.
6. Synthesis of a small peptide library with markers for further screening. This can be done after the data from the second cycle of library panning is completed or independent from the first cycle of panning.

The same procedure can be applied for phage array both *in vitro* and *in vivo* locally as well as systemically as required. This method is expected to be especially useful for systemic evaluation as the phage enters the target tissue and cells can now be reliably retrieved and the sequence identified. However, a proper time frame of collection of infectious phage and phage DNA needs to be established and is among the experiments on my agenda for future experiments. My longer term goal is to establish a practical and effective standard operating procedure (SOP) for phage array.

In summary, my study of phage array for identifying targeting peptides to functionally glycosylated a-DG has identified major barriers which help to explain the major reasons behind the largely failed attempts historically with this technique. More importantly, my study indicates that most of these barriers can be overcome through the application of powerful NGS, thus turning an empirical approach into a much more controlled process by which each step can be effectively monitored for its efficacy. This together with a well designed positive and negative control target cell/tissue, prompted me to design a unique procedure which I expect will greatly improve the probability of using this technique to identify cell specific ligands *in vivo*. With the advance of the techniques of both sequencing and peptide synthesis, the cost for doing both NGS and small peptide library synthesis proposed in my SOP is now becoming affordable for most laboratories.

4.5 Methods

Phage Library Amplification and Maintenance:

Generally, the phage library was maintained per the manufacturer's recommendation for storage and culture as noted in the product instructions provided, and available on the NEB website under products E8110 and E8100S (PhD-12 and PhD-7 libraries respectively.)The manufacturer recommends avoiding host-replicating the library in order to maintain stocks of the library, as competitive inhibition of some phage clones can/will occur. Therefore, upon receipt of the library kit, aliquots of the library sufficient to contain at least 10 to 100 copies of each of the 10^9 variations of phage expressed peptides. As the initial volume of the library is quite small (100 µl of 10^{13} PFU/ml) this was diluted as necessary in TBS, or in the appropriate storage buffer (TBS w/ 50% Glycerol) Whole and fractionated whole cell lysates, CHO derived purified α-Dystroglycan was used as target molecules in multi-well format for high throughput screening of phage binding. Stable CHO cell lines with reduced LARGE and α-Dystroglycan expression will be used in selection as negative controls, as shown in the project schematic [Figure 43]. Often omitted from final publications, refinement of the sub-library is an important step before further selection or experimental evaluation. While the goal of this project overall was to achieve a small number of specific muscle-binding bacteriophage clones, it is important that any one phase of selection not eliminate a viable and unique clone. Given the sheer number of clones from the initial library, upwards of $1x10^{15}$ variations of phage-expressed dodecapeptide sequences, binding clones with less than maximum affinity in the array may be discarded as non-binding false negatives. Maximizing the number of binding clones with a variety of affinities increases the overall chance of success in further testing or application. While the target selection affinity may be effective *in vitro* and *ex vivo*, conditions *in vivo* may limit the availability, conformation, or modification of ligands and/or receptors. Because of this often overlooked nuance in environmental variation, collection of a sub-library with target affinity across multiple selective methods provides the best odds of obtaining viable candidate peptide on *in vivo* evaluation.

Per the manufacturer, the Ph.D-12(NEB E8110 (Lot11)) and Ph.D-7(NEB 8100S (Lot7)) libraries containing upwards of $4.1x10^{15}$ (PhD-12) variants were supplied at a concentration of ~$1x10^{13}$ PFU/mL were supplied. While generally avoiding unnecessary host replication, some initial amplification of library stock was performed in host strain E. coli ER2738 F+ to validate culture and detection methods to be used in later experiments. The selected clones resulting from the phage display experiments were amplified, where necessary for successive selections, in the host *E. coli* strain and isolated by performing a plaque assay on Luria-Bertani agar by standard techniques. Each individual clone isolated through the selection processes and plaque assays was be placed into individual sections of a 1ml deep 96-well plate containing a host broth for culture amplification, infectivity assessment, and long term storage(-80^0 C with addition of 50% glycerol). Infectivity was assessed by comparison of A600 values vs. positive and negative controls. Reduction or increase in absorbance from controls would indicate an equal, improved, or attenuated viral infectivity of host bacteria, and was noted in the sample log. This was performed repeatedly after clonal separation and host propagation, using a Tecan500 plate reader with fixed wavelength of 600 nm before storage of the cataloged plate at -20 or -80°C.

Each plate of collected phage clones or sub-library was numbered and dated, and an excel spreadsheet maintained to catalog stored clones in the format: “plate number-location on plate-selection-date” *Example*: 01-A1-Pos-01012011 and placed at -80° C. Periodically, or as needed for experiments, plates were duplicated by pin inoculation to fresh host culture and incubated at 37° C overnight before phage recollection by 2.5 M NaCl/PEG precipitation.

Prior to beginning any experiments pilot assays were performed to assess the detection and quantification of phage clones using the anti-M13-antibody, β-gal activity and detection on infected host culture for plaque assay, and 2uL pin replicated dot-blot with anti-M13 antibody were performed post-phage precipitation. Once optimal conditions had been established or confirmed, this reduced the likelihood of false positive and false negative results as experimental procedures continued.

Cell culture:

CHO cell lines Pro5 ATCC CRL-1781(Stanley)(Stanley, Caillibot et al. 1975) and LARGE transfected Pro5 (kindly provided by Dr. Xiaohua Wu) were recovered from frozen stocks and seeded onto plastic in F12 media supplemented with 10% FBS and L-glutamine. Cultures were routinely assessed for their expression of glycosylated α-DG by IIH6 immunohistochemical methods, including cell surface staining, supernatant detection, and western blot. As noted in the ATCC documentation and the original publication, Pro5 CHO cells are proline auxotroph and the cell population is subject to reversion to glycosylated form at a rate of 1 in 250. The level of revertant cells, as determined by IIH6 cell staining was noted for each application of this cell line, and when necessary the culture was replaced by freshly recovered stocks generated as subcultures from the original stock.

Immunohistochemical detection methods:

α-DG detection by IIH6 C4 monoclonal mouse-anti-α-DG primary antibody and fluorescent or HRP conjugated fluorophore-tagged goat anti-mouse IgG (A1101/488)(A11032/594) (Life technologies)) /HRP-conjugated goat-anti-mouse (BioRad 170616) M13 phage major coat protein (g8p)immunodetection was performed using monoclonal Mouse anti-M13 g8p (RL-ph1) (Santa Cruz sc-53004) or polyclonal Rabbit anti-M13/Fd phage coat protein followed by goat anti-rabbit (A11012/594)(A11008/488)(Life technologies). Alexafluor-tagged goat anti-mouse IgG (A1101/488) (A21042/488) (Life technologies)/HRP-conjugated goat-anti-rabbit(BioRad 1706515) Unless applied concurrently, blocking was performed using TBS with 10% BSA and 10% NGS, primary antibodies were diluted in TBS with 10% BSA,10% NGS and 0.1% Tween20, all of which were followed by at least 3 washes with PBS. Whole cell staining immunodetection of α-DG, cells were fixed with 2% PFA for 10 minutes followed by 3 PBS washes of 5 minutes each with gentle shaking.

Selection Methods:

Due to high numbers of clones from the initial phage library selections for binding phage, serial dilution arrays were performed to determine the number of clones by PFU/β-gal. This process after selection rounds afforded a more manageable subset of clones from the input naïve or sub-library.

Whole Cell and Purified α-DG Selection Methods:

The first selection method used was in an array using CHO Pro5 cells expressing sufficient LARGE and α–Dystroglycan on their surface to bind passing phage. The cells were then washed with PBS and bound phage was collected through a mild wash with SDS as per manufacturer’s instructions. Subsequent clones were aseptically isolated by plaque assay and the array repeated as necessary a maximum of three times. Collected phage were isolated and quantified by PFU counts over bacterial host culture and cataloged.

The previously isolated phage selected from the initial array using whole-cell LARGE transfected CHO Pro5 cells, were then subjected to further selection, (along with the naïve library) using wheat germ agglutinin (WGA Vector Labs) purified glycosylated α-Dystroglycan collected from culture supernatant. Briefly, collected supernatant from LARGE transfected CHO cells was cleared by centrifugation to remove cell and debris (1200g 5 minutes 4C) and the residual supernatant was allowed to bind with WGA-agarose at a ratio of 10:1 at 4C with constant shaking for 24 hours, before being loaded to a disposable column, equilibrated with three washes with PBS and the captured α-DG was stripped by the addition of 1ml of 0.5 M N-acetylglucosamine in 0.1% TX-100 buffer, incubated 6 hours and the eluate fraction collected, validated by IIH6 anti-α-DG staining after the eluate protein concentration was assessed by Bradford assay. Purified α-DG from the LARGE CHO transfected culture was applied in excess to coat the bottom of 96-well plates, pre-treated with 0.2% gelatin in PBS to promote protein adherence. Phage clones were allowed to bind the purified protein fixed to the well floor, and after three PBS washes were detected by anti-M13 primary and FITC tagged secondary antibodies. Fluorescent intensity was assessed using aTecan500 plate reader, with plastic and primary/secondary controls. Concurrently the non-binding phage collected from the initial wash of the CHO whole-cell experiments were be subjected to the same array over the purified cellular components. This was done to ensure that weak binding phage clones were not discarded as non-binding when suitable to bind molecules modified through the WGA-Lectin purification process. This fluorescence intensity assay using 96-well plate format was later used to evaluate whole-cell binding in the same manner as an efficient manner of identifying phage clones with greatest affinity to the target protein.

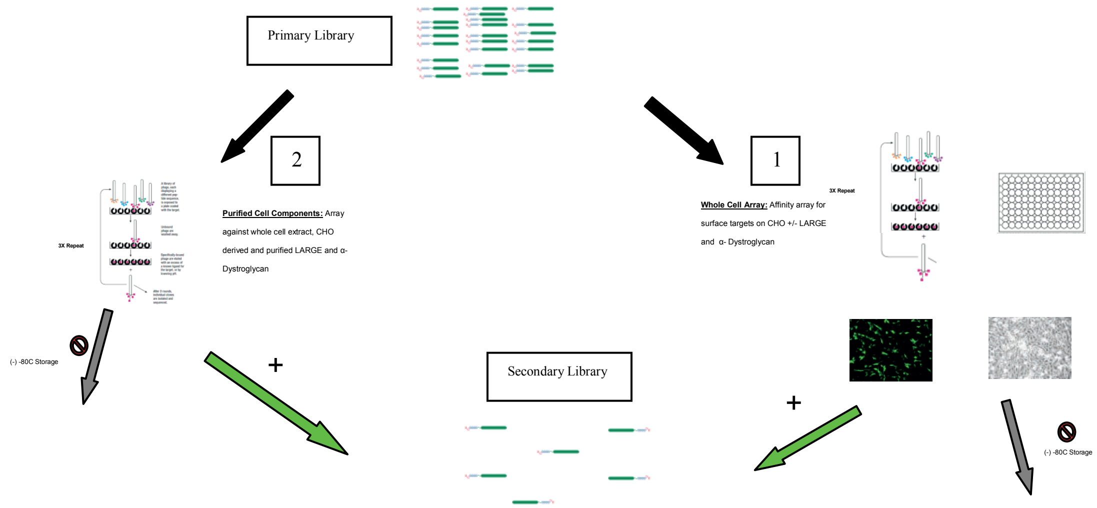
Primary Library
2
1
Purified Cell Components: Array against whole cell extract, CHO derived and purified LARGE and α-Dystroglycan
Whole Cell Array: Affinity array for surface targets on CHO +/- LARGE and α- Dystroglycan
3X Repeat
A library of phage, each displaying a different peptide sequence, is exposed to a plate coated with the target.
Unbound phage are washed away.
Specifically-bound phage are eluted with an excess of a known ligand for the target, or by lowering pH.
After 3 rounds, individual clones are isolated and sequenced.
3X Repeat
(-) -80C Storage
+
Secondary Library
+
(-) -80C Storage

Figure 43: General schematic of phage display methods employed

Beginning with the primary naïve library, one or more selection methods as indicated (1) for HTS screening to more rapidly reduce the library to target and (2) by selection to a purified target. In either or both cases the resulting sub library can then be subjected to refinement with further selection or with new NGS methods, can be prepared for sequence analysis.

Clonal Validation:

Ex-vivo experiments were conducted using excised skeletal muscle tissue collected from euthanized C57 wild type and P448L mice under an IACUC approved protocol, snap frozen in 2-methylbutane and cut to 6um sections and affixed to prepared glass slides. These slides were then used to test the binding affinity of the previously selected phage clones. Anti-M13 antibody was again used to visualize tissue-binding phage. Where successful this assay resulted in further selection of best possible clones for *in vivo* affinity testing, but also the best candidates for further validation and/or selection methods.

One of the most commonly used antibodies for the detection of α–DG, likely recognizing glycosylated epitopes of this protein is the monoclonal IIH6 C4. To determine the potential application of selected phage-expressed peptides, similarly to the *ex vivo* binding of particular muscle tissue samples at expected positions, naïve phage library was supplemented with promising peptide candidates and selected in two rounds over purified α-DG western blots. Blots were sectioned by lane and in the same manner as antibody mediated detection of epitopes of a certain size, blocked nitrocellulose membranes were used for selection. The first round of selection proved to demonstrate that phage at high concentration in primary selection rounds are non-specific and result in the saturated membrane when probed with anti-M13 g8p primary and HRP-conjugated secondary. After two round of selection however, with additional off-target binding, this sub library mimicked the pattern observed when using the IIH6 antibody with yet poorly uncharacterized epitopes.

All clones identified in one or more of the binding assays were additionally purified after scaled up culture. For each of these selected best candidates, a 5ml aliquot of F+ *E.coli* ER2738 under tetracycline, in LB broth was spiked with $1x10^3$ PFU and cultured overnight. Host bacteria were removed by centrifugation and the resulting supernatant was supplemented to 2.5M NaCl with 20% PEG 4000 and stored overnight at 4^oC. After sufficient time for the PEG to bind and precipitate phage such that they could be collected by centrifugation, samples were subjected to 5000 g for 20 minutes at $4\ ^oC$ and the resulting precipitate was resuspended in TBS with a portion placed in storage after sterile glycerol was added to a final concentration of 50%. Phage clones selected for sequencing were again precipitated with 2.5M NaCl with 20% PEG 4000 and stored overnight at 4^{o}C, recollected by centrifugation at 5000 g for 20 minutes at 4 ^{o}C. The cleared supernatant was discarded and to the resulting pellet was added 100ul Iodide buffer and mixed gently. This was followed by addition of 250ul ethanol and allowed to rest10- 20 minutes at room temperature before precipitation of phage genomic DNA by centrifugation at14,000 g for 10 minutes at 4 ^{o}C. The supernatant was discarded and the pellet briefly allowed to dry before being resuspended in 30 µl of TE buffer. Successful phage gDNA extractions were confirmed by gel electrophoresis and identification /quantification of a 7kb band. Poor extractions were identified by weak bands, or large amounts of the gDNA retained in the well bound to residual phage protein from the DNA extraction, and were further purified. From these purified samples, quantified by UV-spec and NanoDrop UV, a specified quantity of DNA from each selected clone was submitted for Sanger sequencing with the forward and reverse sequencing primers recommended by the manufacturer, and are as follows

“-28 Sequencing Primer” 5’-^{HO}GTATGGGATTTTGCTAAACAA-3’and

”-96 Sequencing Primer”5’-^{HO}CCCTCATAGTTAGCGTAACG-3’.

PCR amplification of M13 phage *gIII* variable regions:

To achieve more consistent data from samples submitted for sequencing, PCR of the purified phage gDNA was performed with USB Taq Master mix using the following primers: ‘M13-66.F’ 5’-GTAATGAATTTTCTGTATGGGA-3’

’M13.4-245 ’5’-ATTGCGCCTTCGACGTTGT-3’,

‘M13.2-247’ 5’-TGGGCGATGGTTGTTGTCAT-3’and

'M13.2-267' 5'-TCGGCGCAACTATCGGTATC-3'

After a gradient PCR reaction was conducted, it was determined that using 'M13-66.F' and 'M13.2-267' with conditions of 95 ^{o}C for 5 min, 95^{o}C for 30 sec, 51.6 ^{o}C for 30 seconds, 72 ^{o}C for 30 seconds, with 20 repetitions from the denaturing phase, followed by 72 ^{o}C for 10 minutes, produced a reliable 270 bp cDNA product. Optimal conditions for NGS RNA-Seq on the Illumina platform required additional amplification to ~500 ng of amplicons, with an optimal size of near 100 bp. For production of these amplicons, the following primers were used:

'M13.V-50' 5'-CTGTATGGGATTTTGCTAAAC-3'
'M13.V+10' 5'-CTTTAGTGGTACCTTTCTAT-3' and
'M13.V+5.R' 5'-GTGGTACCTTTCTATTCTC-3'

Optimal PCR conditions were determined experimentally and consisted of a denaturing stage of 95 ^{o}C for 5 minutes, 95 ^{o}C for 30 seconds, 40.6 ^{o}C annealing for 30 seconds, 72 ^{o}C elongation cycles for 30 seconds, with 25 repetitions from the second denaturing stage. Of the two reverse primers tested, M13.V+5 most reliably produced a 110 bp product under the conditions listed.

Extrapolation and Analyses of Phage-expressed Peptides:

From data obtained through NGS RNA-Seq, both forward and reverse reads were collected, aligned, assessed for conserved flanking regions of (NNK_{12}) as shown in figure 44 below and once parsed, resulting peptide sequences were translated using the appropriate M13KE abbreviated codon usage, as given below in table 6.

Table 6: M13KE Amino Acid Codon Table

Codon	Amino Acid		
CGK, AGG	R	Arginine	Arg
CTK, TTG	L	Leucine	Leu
TCK, AGT	S	Serine	Ser
GCK	A	Alanine	Ala
GGK	G	Glycine	Gly
CCK	P	Proline	Pro
ACK	T	Threonine	Thr
CAG, TAG	Q	Glutamine	Gln
GTK	V	Valine	Val
AAT	N	Asparagine	Asn
GAT	D	Aspartic Acid	Asp
TGT	C	Cysteine	Cys
GAG	E	Glutamic Acid	Glu
CAT	H	Histidine	His
ATT	I	Isoleucine	Ile
AAG	K	Lysine	Lys
ATG	M	Methionine	Met
TTT	F	Phenylalanine	Phe
TGG	W	Tryptophan	Trp
TAT	Y	Tyrosine	Tyr

NGS Forward Read Output:
GTGGTACCTTTCTATTCTCACTCTAATTATCATACGATTTCGCAGGCGGGGAC
TCCGATTGGTGGAGGTTCGGCCGAAACTGTTGAAAGTTGTTTAGCAA

Parsed:
GTGGTACCTTTCTATTCTCACTCT/AATTATCATACGATTTCGCAGGCGGGGAC
TCCGATTGGTGGAGGTTCGGCCGAAACTGTTGAAAGTTGTTTAGCAA

Translated Insert:

AAT TAT CAT ACG ATT TCG CAG GCG GGG ACT CCG ATT
N Y H T I S Q A G T P I

NGS Reverse Read Output:
CTGTATGGGATTTTGCTAAACAACTTTCAACAGTTTCGGCCGAACCTCCACCA
ATCGGAGTCCCCGCCTGCGAAATCGTGTAATAATTAGAGTGAGAATA

Parsed:
GTGGTACCTTTCTATTCTCACTCGGCCGAAACTGTTGAAAGTTGTTTAGCAAA
ATCC CATACAGAGATCGGAAGAGCACACGTC
TGAACTCCAGTCACCCATACAG

Translated and Reframed Insert:

AAT CGG AGT CCC CGC CTG CGA AAT CGT GTA ATA ATT
I P T G A Q S I T H Y N
N Y H T I S Q A G T P I

Figure 44: Extrapolation and analyses of phage-expressed peptides. In order to determine peptide sequences from the data generated through NGS RNA-Seq, both forward and reverse reads were collected, aligned, assessed for conserved flanking regions of (NNK_{12}) as shown above, and once parsed, resulting peptide sequences could be translated using the appropriate M13KE abbreviated codon usage, as given in table 6.

CHAPTER 5: DISCUSSION AND FUTURE DIRECTIONS

5.1 Summary

One of the most promising experimental therapies for Duchenne muscular dystrophy is antisense oligonucleotide (AON) therapy. AON therapy works to restore dystrophin expression by modulation of pre-mRNA splicing such that mutation bearing exons are removed from the mRNA resulting in maintenance of the translational reading frame producing a modified but functional dystrophin isoform. This therapy has been thoroughly evaluated *in vitro*, in animal models of DMD and most recently in clinical trials. The leading AON chemistry phosphorodiamidate morpholino has been demonstrated to be the most effective at dystrophin restoration due to its stability and low toxicity profile. However, the net-neutral charge of PMO which makes such a suitable chemistry for the intended exon-skipping effect, relies on passive uptake mechanisms to transfect cells *in vitro*, and more importantly to transfect muscle tissue *in vivo*. Direct modifications to PMO such as octa-guanidine and poly-arginine components increase transfection, however the nature of these cationic modifications increase toxicity, thus excluding them as viable candidates for clinical applications such as AON therapy for DMD. Moreover, there are no viable (muscle) tissue-specific ligands identified to date that can be used to increase PMO delivery efficiency. With the barriers to effective PMO delivery and transfection identified as being the low efficiency and non-specificity, I pursued the three aims in an effort to approach these issues. I addressed the first issue, the low efficiency of PMO delivery in two aims using PEA polymers as delivery vehicles and as direct PMO modifications, to study their effect on transfection efficiency while also studying the role of polymer construction components in designing optimal delivery vehicles. In aim #1 I studied Tris[2-(acryloyloxy)ethyl]isocyanurate Cross-linked Polyethylenimine (poly ester amine PEA) polymers as vehicles for effective trans gene and PMO delivery. In aim #2 I evaluated this promising new class of poly(ester-amine) (PEAs) as directly conjugated modifications to phosphorodiamidate (PMO) AON through experiments performed *in vitro* and *in vivo*, to determine their efficiencies in transfection, exon skipping and restoration of dystrophin.

I chose to address the second of these barriers, the non-specific nature of PMO delivery by attempting to identify peptide ligands to the glycosylated protein α-dystroglycan. This target was selected as ideal due to higher levels of expression in muscle than in other tissues and the availability of appropriate selection systems, namely the elevated glycosylation of CHO cells transfected with like-glycosyltransferase (LARGE) and the FKRP mutant mouse (P448L) unique to the McColl-Lockwood Laboratory. While there are a number of methods to attempt identification of muscle-specific peptides for aim #3, I chose to design experiments using phage display methods to identify ligands expressed on the surface of engineered bacteriophage selecting for those phage with specificity to the glycosylated muscle membrane protein α-Dystroglycan.

I have attempted to demonstrate in this text that synthetic polymers designed for gene and oligo delivery, specifically PEA, are effective and safe means to increase transfection efficiencies. The biodegradable Tris[2-(acryloyloxy)ethyl]isocyanurate

Cross-linked Polyethylenimine effectively condense oligonucleotide and trans gene cargo to nano-sized particles that retain sufficient charge to promote interaction with cellular membranes while having less toxicity than other available transfection reagents. This more efficient cargo delivery without increased toxicity has allowed the extension of in vitro experiments to in vivo applications demonstrating great potential for increasing delivery efficiency of PMO AON and dystrophin restoration in the *mdx* mouse.

Toward optimal delivery, I have described how polymers from the PEA series (A12, B12, and C12) are also amenable to direct conjugation as PMO modifications. With the biodegradable PEA polymers imparting charge to the bound PMO, increases in transfection efficiency and exon-skipping was observed in myoblast cell culture as well as increasing dystrophin restoration in treated muscles of *mdx* mice.

Designing and executing a series of phage display experiments, I have succeeded in identifying peptides resulting from selection of clones with affinity to glycosylated α-DG on the cell surface, as well as WGA purified and membrane transferred α-DG. This was performed with my high throughput modifications to the laborious traditional methods to perform secondary screening and subsequent validation of isolated phage. Phage selected for binding affinity to α-DG in varied and multiple assays were evaluated for binding affinity to wild type glycosylated C57 muscle *ex vivo*, resulting in a final sub-library of 54 phage isolates. In attempting to determine the peptides expressed by these selected phage through chain-termination DNA sequencing methods, I found a serious hurdle in the current phage display methods commonly practiced. To bypass the difficulty in chain-terminating sequence methods to determine the phage DNA sequence and thereby the peptide sequence, I turned to Next Generation Sequencing (NGS) technologies. Using NGS methods, I was able to identify peptide sequences unique to the selection process with relative abundancy as compared to the naïve phage library, providing possible muscle-specific peptides for further study. Through NGS I have also identified in my samples evidence of inherent flaws in long-held phage display methodologies, likely contributing to numerous reports of target-specific peptides identified through phage array that lack efficacy on further evaluation. This observation from my data, prompted me to propose a revision to phage display methods using increasingly affordable NGS methods that I feel will rejuvenate the maligned but capable phage display platform, which I have detailed in figure 45.

Collectively, in approaching these three aims I have demonstrated methods to overcome the current barriers to AON therapy with PMO, demonstrating improvement in both the delivery efficiency through polymer vehicles and polymer-conjugated PMO while identifying peptides which with further evaluation could be used to deliver PMO with muscle-targeted specificity. (depicted in Figure 46)

While the current outlook for AON therapy for DMD in clinical trials seems disappointing, with failure to meet significant functional gains and delayed regulatory processes, I believe that the spirit of those involved remains bright, and that the future holds great promise in treating this devastating disease.

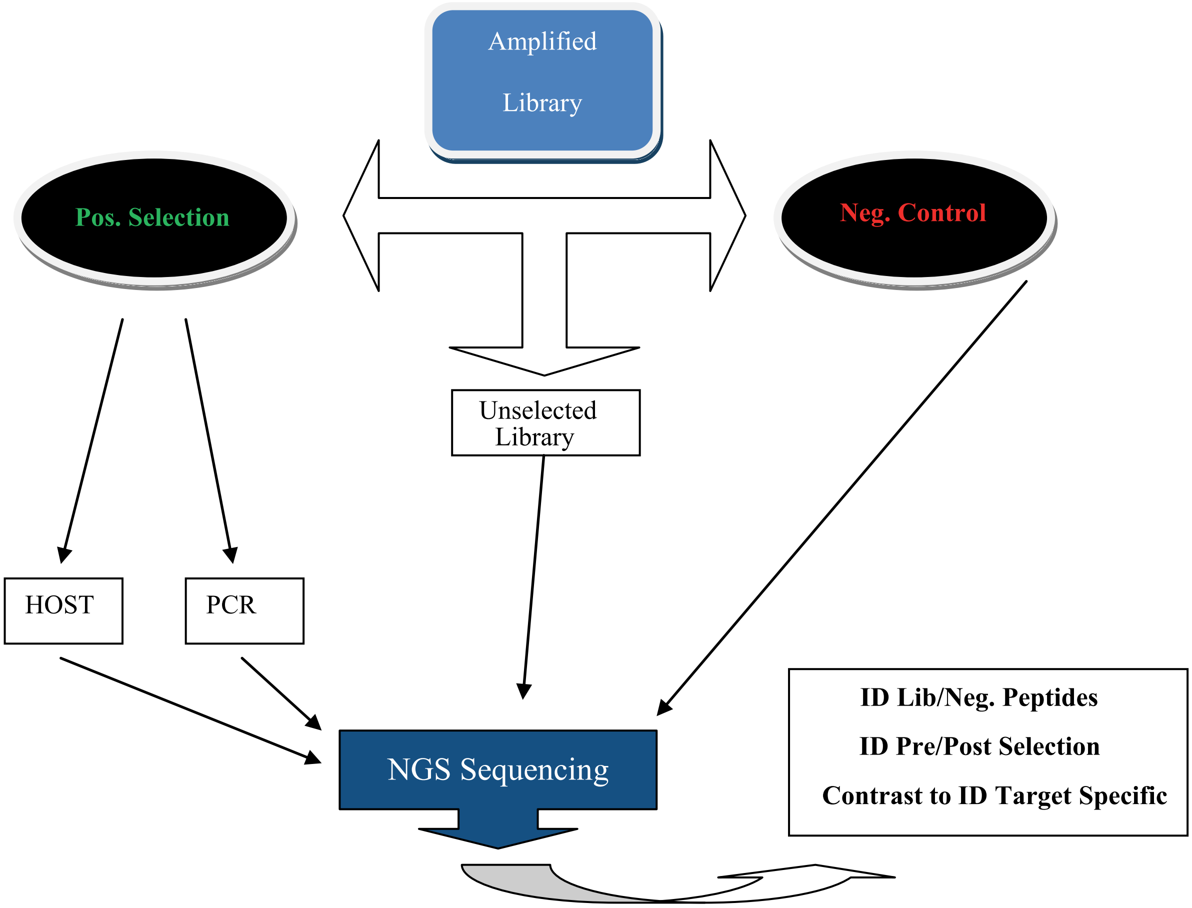

Figure 45: Proposed phage array NGS method diagram. Through experience gained in my study, I propose a novel and simplified strategy of phage array for cell specific peptide identification as detailed in this figure.1.) Sufficient phage library amplified once to produce sufficient amount for planned rounds of panning and selection. The original library and the replicate samples are then sequenced to verify the diversity. 2) Array sufficient phage library to the target cells and relevant control target cells. Wash to remove non binding phage, collecting bound phage to be divided into two portions, one for further amplification in host cells, and the remaining portion for limited PCR amplification directly to NGS in tandem with the original library. Phage DNA collected from homogenized target cells after bound phage removal should be amplified directly by PCR for NGS. 3.) Compare the NGS data of the phage collected from the targeted tissue and control sample identifying unique sequence with affinity to the targeted tissue. Also compare the NGS data of phage DNA directly extracted from the targeted and control samples. This allows identification of the phage uniquely present in targeted samples.4.) The unique phage identified from targeted samples can then be processed for sequence analysis to identify the most frequent peptide sequences and the common motifs of phage sequences with low frequency. 6.) Synthesis of a small peptide library with markers for further screening. The same procedure can be applied for phage array both *in vitro* and *in vivo* as required, and is expected to be especially useful for systemic evaluation as the

phage enters target tissue and cells can be retrieved and the sequence identified, decreasing necessary resource and time requirements.

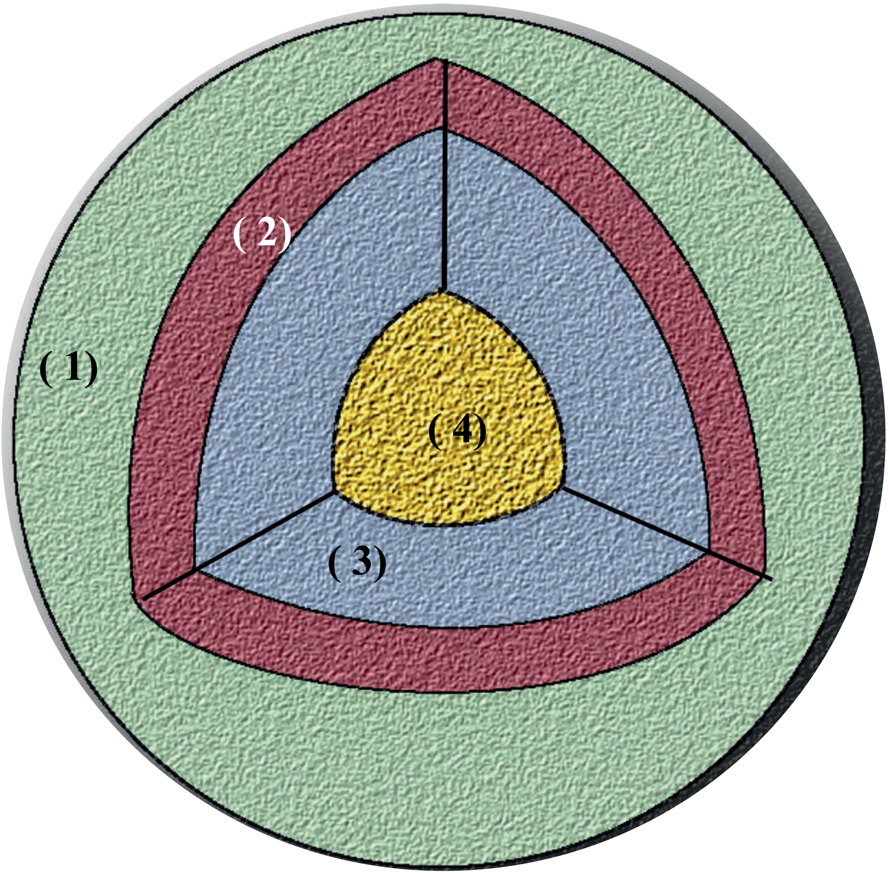

Figure 46: Future vehicle design model. As the field of gene therapy continues to advance basic research from the bench to translational applications, effective delivery mechanisms will become increasingly important. This figure demonstrates what I have identified as the ideal delivery vehicle concept, composed of multifunctional units to meet the demands of systemic delivery yet no more complex than is necessary. (1) Components such as PEG have been shown to increase circulation time and thereby increase distribution while not permanently blocking the actions of other functional components.2) With increased time in circulation, inclusion of effective target tissue-specific ligands would allow increased interaction and delivery of vehicles to intended target tissues. 3) Polymers, particularly biodegradable compounds like the PEA polymer series could likely be used to condense the gene or oligo cargo and allow stable interaction between the cargo and functional components toward the vehicle exterior 4) Cargo must be condensed and protected such that the maximal delivery and transfection afforded by the vehicle itself allow effective release of the cargo for its intended function with minimal interference.

5.2 Publications and Presentations

Wang, M., P. Lu, B. Wu, **J. D. Tucker**, C. Cloer and Q. Lu (2012). "High efficiency and low toxicity of polyethyleneimine modified Pluronics (PEI-Pluronic) as gene delivery carriers in cell culture and dystrophic mdx mice." Journal of Materials Chemistry 22(13): 6038-6046.

Wang, M., **J. D. Tucker**, P. Lu, B. Wu, C. Cloer and Q. Lu (2012). "Tris[2-(acryloyloxy)ethyl]isocyanurate cross-linked low-molecular-weight polyethylenimine as gene delivery carriers in cell culture and dystrophic mdx mice." Bioconjug Chem 23(4): 837-845.

Wang, M., B. Wu, P. Lu, C. Cloer, **J. D. Tucker** and Q. Lu (2013). "Polyethylenimine-modified pluronics (PCMs) improve morpholino oligomer delivery in cell culture and dystrophic mdx mice." Mol Ther 21(1): 210-216.

Wang, M., B. Wu, P. Lu, **J. D. Tucker**, S. Milazi, S. N. Shah and Q. L. Lu (2013). "Pluronic-PEI copolymers enhance exon-skipping of 2'-O-methyl phosphorothioate oligonucleotide in cell culture and dystrophic mdx mice." Gene Ther.

Wang, M., B.Wu, **J. D. Tucker**, P. Lu, C. Cloer, Q. L. Lu (2014). "Evaluation of Tris[2-(acryloyloxy)ethyl]isocyanurate Cross-linked Polyethylenimine as Antisense Morpholino Oligomer Delivery Vehicle in Cell Culture and Dystrophic mdx Mice." Hum Gene Ther.

J. D. Tucker, M. Wang, B. Wu, P. Lu, Q. L. Lu (2014-2015). "Tris[2-(acryloyloxy)ethyl]isocyanurate Cross-linked Polyethylenimine Conjugated Morpholino Oligomer Improves Delivery and Dystrophin Restoration in the *mdx* Mouse." *manuscript prepared for submission.*

J. D. Tucker, B.Wu, P. Lu, X.Wu, Q. L. Lu (2014-2015). "Muscle Targeted Peptides Identified Using Next Generation Sequencing for the Next Generation of Phage Display." *manuscript prepared for submission.*

Wang M, Lu PJ, Wu B, **Tucker JD**, Cloer C, Lu QL. High efficiency and low toxicity of polyethyleneimine modified Pluronics (PEI–Pluronic) as gene delivery carriers. 239th ACS National Meeting and Symposia, March 24, 2010

Jason D. Tucker Identification and Characterization of Muscle Specific Peptides Through Phage Array.UNC at Charlotte, Department of Biological Sciences, Departmental Seminar December 2, 2011

Jason D. Tucker, Mingxing Wang, Bo Wu , Peijuan Lu, Qilong Lu
Polymer-mediated Delivery of Genes / Oligonucleotides for Muscular Dystrophy.
Charlotte Life Sciences Conference, Charlotte Research Institute October 25, 2012

Jason D. Tucker Targeting the Glycosylated Epitopes of α-Dystroglycan for Oligonucleotide Therapies. Department of Biological Sciences, Departmental Seminar April 27, 2012

Jason D. Tucker, Mingxing Wang, Bo Wu , Peijuan Lu, Qilong Lu Poly-esteramine Polymer-mediated Delivery of Oligonucleotides for Muscular Dystrophy Therapies University of North Carolina at Charlotte, Graduate Research Symposia March 23, 2013

Professional Society Memberships:

American Society for Microbiology (ASM)

American Society of Gene and Cell Therapy (ASGCT)

American Association for the Advancement of Science (AAAS)

American Society of Clinical Pathology (ASCP)

REFERENCES

107th Congress, n. S., 2002 (2002). "Rare Diseases Act of 2002." **116 Stat. 1988**: 1988 - 1991.

Aartsma-Rus, A., W. E. Kaman, R. Weij, J. T. den Dunnen, G. J. van Ommen and J. C. van Deutekom (2006). "Exploring the frontiers of therapeutic exon skipping for Duchenne muscular dystrophy by double targeting within one or multiple exons." Mol Ther **14**(3): 401-407.

Abes, R., A. Arzumanov, H. Moulton, S. Abes, G. Ivanova, M. J. Gait, P. Iversen and B. Lebleu (2008). "Arginine-rich cell penetrating peptides: design, structure-activity, and applications to alter pre-mRNA splicing by steric-block oligonucleotides." J Pept Sci **14**(4): 455-460.

Abes, R., A. A. Arzumanov, H. M. Moulton, S. Abes, G. D. Ivanova, P. L. Iversen, M. J. Gait and B. Lebleu (2007). "Cell-penetrating-peptide-based delivery of oligonucleotides: an overview." Biochem Soc Trans **35**(Pt 4): 775-779.

Alonso, M., D. A. Stein, E. Thomann, H. M. Moulton, J. C. Leong, P. Iversen and D. V. Mourich (2005). "Inhibition of infectious haematopoietic necrosis virus in cell cultures with peptide-conjugated morpholino oligomers." J Fish Dis **28**(7): 399-410.

Alter, J., F. Lou, A. Rabinowitz, H. Yin, J. Rosenfeld, S. D. Wilton, T. A. Partridge and Q. L. Lu (2006). "Systemic delivery of morpholino oligonucleotide restores dystrophin expression bodywide and improves dystrophic pathology." Nat Med **12**(2): 175-177.

Arechavala-Gomeza, V., I. R. Graham, L. J. Popplewell, A. M. Adams, A. Aartsma-Rus, M. Kinali, J. E. Morgan, J. C. van Deutekom, S. D. Wilton, G. Dickson and F. Muntoni (2007). "Comparative analysis of antisense oligonucleotide sequences for targeted skipping of exon 51 during dystrophin pre-mRNA splicing in human muscle." Hum Gene Ther **18**(9): 798-810.

Bates, F. S., M. A. Hillmyer, T. P. Lodge, C. M. Bates, K. T. Delaney and G. H. Fredrickson (2012). "Multiblock polymers: panacea or Pandora's box?" Science **336**(6080): 434-440

Baudy, A.R., E. K. Reeves, J. M. Damsker, C. Heier, L. M. Garvin, B. C. Dillingham, J. McCall, S. Rayavarapu, Z. Wang, J. H. Vandermeulen, A. Sali, V. Jahnke, S.Duguez, D. DuBois, M. C. Rose, K. Nagaraju and E. P. Hoffman (2012). "Delta-9,11 modification of glucocorticoids dissociates nuclear factor-kappaB inhibitory efficacy from glucocorticoid response element-associated side effects." J Pharmacol Exp Ther **343**(1): 225-232.

Benedetti, E., G. Morelli, A. Accardo, R. Mansi, D. Tesauro and L. Aloj (2004). "Criteria for the design and biological characterization of radiolabeled peptide-based pharmaceuticals." BioDrugs **18**(5): 279-295.

Bhagat, L., M. R. Putta, D. Wang, D. Yu, T. Lan, W. Jiang, Z. Sun, H. Wang, J. X. Tang, N. La Monica, E. R. Kandimalla and S. Agrawal (2011). "Novel oligonucleotides containing two 3'-ends complementary to target mRNA show optimal gene-silencing activity." J Med Chem **54**(8): 3027-3036.

Brown, C. K., R. A. Modzelewski, C. S. Johnson and M. K. Wong (2000). "A novel approach for the identification of unique tumor vasculature binding peptides using an E. coli peptide display library." Ann Surg Oncol **7**(10): 743-749.

Brown, K. C. (2000). "New approaches for cell-specific targeting: identification of cell-selective peptides from combinatorial libraries." Curr Opin Chem Biol **4**(1): 16-21.

Bushby, K., F. Muntoni and J. P. Bourke (2003). "107th ENMC international workshop: the management of cardiac involvement in muscular dystrophy and myotonic dystrophy. 7th-9th June 2002, Naarden, the Netherlands." Neuromuscul Disord **13**(2): 166-172.

Cao, W., M. D. Henry, P. Borrow, H. Yamada, J. H. Elder, E. V. Ravkov, S. T. Nichol, R. W. Compans, K. P. Campbell and M. B. Oldstone (1998). "Identification of alpha-dystroglycan as a receptor for lymphocytic choriomeningitis virus and Lassa fever virus." Science **282**(5396): 2079-2081.

Cardamone, M., B. T. Darras and M. M. Ryan (2008). "Inherited myopathies and muscular dystrophies." Semin Neurol **28**(2): 250-259.

Caruso, F., T. Hyeon and V. M. Rotello (2012). "Nanomedicine." Chem Soc Rev **41**(7): 2537-2538.

Chen, C. C., C. Zhu, E. R. White, C. Y. Chiu, M. C. Scott, B. C. Regan, L. D. Marks, Y. Huang and J. Miao (2013). "Three-dimensional imaging of dislocations in a nanoparticle at atomic resolution." Nature **496**(7443): 74-77.

Chen, X. A., L. J. Zhang, Z. J. He, W. W. Wang, B. Xu, Q. Zhong, X. T. Shuai, L. Q. Yang and Y. B. Deng (2011). "Plasmid-encapsulated polyethylene glycol-grafted polyethylenimine nanoparticles for gene delivery into rat mesenchymal stem cells." Int J Nanomedicine **6**: 843-853.

Cho, K., S. Choi and T. Park (2006). "Low molecular weight PEI conjugated pluronic copolymer: Useful additive for enhancing gene transfection efficiency." Macromolecular Research **14**(3): 348-353.

Cirak, S., V. Arechavala-Gomeza, M. Guglieri, L. Feng, S. Torelli, K. Anthony, S. Abbs, M. E. Garralda, J. Bourke, D. J. Wells, G. Dickson, M. J. Wood, S. D. Wilton, V. Straub, R. Kole, S. B. Shrewsbury, C. Sewry, J. E. Morgan, K. Bushby and F. Muntoni (2011). "Exon skipping and dystrophin restoration in patients with Duchenne muscular dystrophy after systemic phosphorodiamidate morpholino oligomer treatment: an open-label, phase 2, dose-escalation study." Lancet **378**(9791): 595-605.

D'Herelle, F. (1929). "Studies Upon Asiatic Cholera." Yale J Biol Med **1**(4): 195-219.

David, S., C. Passirani, N. Carmoy, M. Morille, M. Mevel, B. Chatin, J. P. Benoit, T. Montier and B. Pitard (2013). "DNA nanocarriers for systemic administration: characterization and in vivo bioimaging in healthy mice." Mol Ther Nucleic Acids **2**: e64.

De Clercq, E., E. Eckstein and T. C. Merigan (1969). "[Interferon induction increased through chemical modification of a synthetic polyribonucleotide]." Science **165**(3898): 1137-1139.

Dubowitz, V. and L. Crome (1969). "The central nervous system in Duchenne muscular dystrophy." Brain **92**(4): 805-808.

Dunckley, M. G., M. Manoharan, P. Villiet, I. C. Eperon and G. Dickson (1998). "Modification of splicing in the dystrophin gene in cultured Mdx muscle cells by antisense oligoribonucleotides." Hum Mol Genet **7**(7): 1083-1090.

Emery, A. E. (1991). "Population frequencies of inherited neuromuscular diseases--a world survey." Neuromuscul Disord **1**(1): 19-29.

Ervasti, J. M. and K. P. Campbell (1991). "Membrane organization of the dystrophin-glycoprotein complex." Cell **66**(6): 1121-1131.

Fiers, W., R. Contreras, F. Duerinck, G. Haegeman, D. Iserentant, J. Merregaert, W. Min Jou, F. Molemans, A. Raeymaekers, A. Van den Berghe, G. Volckaert and M. Ysebaert (1976). "Complete nucleotide sequence of bacteriophage MS2 RNA: primary and secondary structure of the replicase gene." Nature **260**(5551): 500-507.

Furst, D., R. Nave, M. Osborn, K. Weber, A. Bardosi, N. Archidiacono, M. Ferro, V. Romano and G. Romeo (1987). "Nebulin and titin expression in Duchenne muscular dystrophy appears normal." FEBS Lett **224**(1): 49-53.

Goemans, N. M., M. Tulinius, J. T. van den Akker, B. E. Burm, P. F. Ekhart, N. Heuvelmans, T. Holling, A. A. Janson, G. J. Platenburg, J. A. Sipkens, J. M. Sitsen, A. Aartsma-Rus, G. J. van Ommen, G. Buyse, N. Darin, J. J. Verschuuren, G. V. Campion, S. J. de Kimpe and J. C. van Deutekom (2011). "Systemic administration of PRO051 in Duchenne's muscular dystrophy." N Engl J Med **364**(16): 1513-1522.

Goldstein, J. A. and E. M. McNally (2010). "Mechanisms of muscle weakness in muscular dystrophy." J Gen Physiol **136**(1): 29-34.

Hao, J., X. Sha, Y. Tang, Y. Jiang, Z. Zhang, W. Zhang, Y. Li and X. Fang (2009). "Enhanced transfection of polyplexes based on pluronic-polypropylenimine dendrimer for gene transfer." Arch Pharm Res **32**(7): 1045-1054.

Heemskerk, H. A., C. L. de Winter, S. J. de Kimpe, P. van Kuik-Romeijn, N. Heuvelmans, G. J. Platenburg, G. J. van Ommen, J. C. van Deutekom and A. Aartsma-Rus (2009). "In vivo comparison of 2'-O-methyl phosphorothioate and morpholino antisense oligonucleotides for Duchenne muscular dystrophy exon skipping." J Gene Med **11**(3): 257-266.

Hoffman, E. P., R. H. Brown, Jr. and L. M. Kunkel (1987). "Dystrophin: the protein product of the Duchenne muscular dystrophy locus." Cell **51**(6): 919-928.

Hoffman, E. P., C. M. Knudson, K. P. Campbell and L. M. Kunkel (1987). "Subcellular fractionation of dystrophin to the triads of skeletal muscle." Nature **330**(6150): 754-758.

Hruby, V. J. (2002). "Designing peptide receptor agonists and antagonists." Nat Rev Drug Discov **1**(11): 847-858.

Hu, Y., Z. F. Li, X. Wu and Q. Lu (2011). "Large induces functional glycans in an O-mannosylation dependent manner and targets GlcNAc terminals on alpha-dystroglycan." PLoS One **6**(2): e16866.

Hubbell, J. A. and A. Chilkoti (2012). "Chemistry. Nanomaterials for drug delivery." Science **337**(6092): 303-305.

Imbert, N., C. Vandebrouck, B. Constantin, G. Duport, C. Guillou, C. Cognard and G. Raymond (1996). "Hypoosmotic shocks induce elevation of resting calcium level in Duchenne muscular dystrophy myotubes contracting in vitro." Neuromuscul Disord **6**(5): 351-360.

Inamori, K., Y. Hara, T. Willer, M. E. Anderson, Z. Zhu, T. Yoshida-Moriguchi and K. P. Campbell (2013). "Xylosyl- and glucuronyltransferase functions of LARGE in alpha-dystroglycan modification are conserved in LARGE2." Glycobiology **23**(3): 295-302.

Inamori, K., T. Yoshida-Moriguchi, Y. Hara, M. E. Anderson, L. Yu and K. P. Campbell (2012). "Dystroglycan function requires xylosyl- and glucuronyltransferase activities of LARGE." Science **335**(6064): 93-96.

Jager, M., S. Schubert, S. Ochrimenko, D. Fischer and U. S. Schubert (2012). "Branched and linear poly(ethylene imine)-based conjugates: synthetic modification, characterization, and application." Chem Soc Rev **41**(13): 4755-4767.

Jearawiriyapaisarn, N., H. M. Moulton, P. Sazani, R. Kole and M. S. Willis (2010). "Long-term improvement in mdx cardiomyopathy after therapy with peptide-conjugated morpholino oligomers." Cardiovasc Res **85**(3): 444-453.

Kang, J. K., A. Malerba, L. Popplewell, K. Foster and G. Dickson (2011). "Antisense-induced myostatin exon skipping leads to muscle hypertrophy in mice following octa-guanidine morpholino oligomer treatment." Mol Ther **19**(1): 159-164.

Kaspar, R. W., H. D. Allen and F. Montanaro (2009). "Current understanding and management of dilated cardiomyopathy in Duchenne and Becker muscular dystrophy." J Am Acad Nurse Pract **21**(5): 241-249.

Kelly, K. A., P. A. Clemons, A. M. Yu and R. Weissleder (2006). "High-throughput identification of phage-derived imaging agents." Mol Imaging **5**(1): 24-30.

Kelly, K. A., P. Waterman and R. Weissleder (2006). "In vivo imaging of molecularly targeted phage." Neoplasia **8**(12): 1011-1018.

Kendall, G. C., E. I. Mokhonova, M. Moran, N. E. Sejbuk, D. W. Wang, O. Silva, R. T. Wang, L. Martinez, Q. L. Lu, R. Damoiseaux, M. J. Spencer, S. F. Nelson and M. C. Miceli (2012). "Dantrolene enhances antisense-mediated exon skipping in human and mouse models of Duchenne muscular dystrophy." Sci Transl Med **4**(164): 164ra160.

Keren, H., G. Lev-Maor and G. Ast (2010). "Alternative splicing and evolution: diversification, exon definition and function." Nat Rev Genet **11**(5): 345-355.

Kinali, M., V. Arechavala-Gomeza, L. Feng, S. Cirak, D. Hunt, C. Adkin, M. Guglieri, E. Ashton, S. Abbs, P. Nihoyannopoulos, M. E. Garralda, M. Rutherford, C. McCulley, L. Popplewell, I. R. Graham, G. Dickson, M. J. Wood, D. J. Wells, S. D. Wilton, R. Kole, V. Straub, K. Bushby, C. Sewry, J. E. Morgan and F. Muntoni (2009). "Local restoration of dystrophin expression with the morpholino oligomer AVI-4658 in Duchenne muscular dystrophy: a single-blind, placebo-controlled, dose-escalation, proof-of-concept study." Lancet Neurol **8**(10): 918-928.

Kole, R., A. R. Krainer and S. Altman (2012). "RNA therapeutics: beyond RNA interference and antisense oligonucleotides." Nat Rev Drug Discov **11**(2): 125-140.

Krumpe, L. R. and T. Mori (2006). "The Use of Phage-Displayed Peptide Libraries to Develop Tumor-Targeting Drugs." Int J Pept Res Ther **12**(1): 79-91.

Lebleu, B., H. M. Moulton, R. Abes, G. D. Ivanova, S. Abes, D. A. Stein, P. L. Iversen, A. A. Arzumanov and M. J. Gait (2008). "Cell penetrating peptide conjugates of steric block oligonucleotides." Adv Drug Deliv Rev **60**(4-5): 517-529.

Lu, Q. L., S. Cirak and T. Partridge (2014). "What Can We Learn From Clinical Trials of Exon Skipping for DMD?" Mol Ther Nucleic Acids **3**: e152.

Lu, Q. L., C. J. Mann, F. Lou, G. Bou-Gharios, G. E. Morris, S. A. Xue, S. Fletcher, T. A. Partridge and S. D. Wilton (2003). "Functional amounts of dystrophin produced by skipping the mutated exon in the mdx dystrophic mouse." Nat Med **9**(8): 1009-1014.

Lu, Q. L., A. Rabinowitz, Y. C. Chen, T. Yokota, H. Yin, J. Alter, A. Jadoon, G. Bou-Gharios and T. Partridge (2005). "Systemic delivery of antisense oligoribonucleotide restores dystrophin expression in body-wide skeletal muscles." Proc Natl Acad Sci U S A 102(1): 198-203.

Lu, Q. L., T. Yokota, S. Takeda, L. Garcia, F. Muntoni and T. Partridge (2011). "The status of exon skipping as a therapeutic approach to duchenne muscular dystrophy." Mol Ther **19**(1): 9-15.

Mady, M. M. (2011). "Interaction of DNA and polyethylenimine: Fourier-transform infrared (FTIR) and differential scanning calorimetry (DSC) studies." International Journal of the Physical Sciences **6**(32): 7328-7334.

Magee, K. R. and G. M. Shy (1956). "A new congenital non-progressive myopathy." Brain **79**(4): 610-621.

Manzur, A. Y., T. Kuntzer, M. Pike and A. Swan (2008). "Glucocorticoid corticosteroids for Duchenne muscular dystrophy." Cochrane Database Syst Rev(1): CD003725.

Matsuo, M., T. Masumura, H. Nishio, T. Nakajima, Y. Kitoh, T. Takumi, J. Koga and H. Nakamura (1991). "Exon skipping during splicing of dystrophin mRNA precursor due to an intraexon deletion in the dystrophin gene of Duchenne muscular dystrophy kobe." J Clin Invest **87**(6): 2127-2131.

Mendell, J. R., L. R. Rodino-Klapac, Z. Sahenk, K. Roush, L. Bird, L. P. Lowes, L. Alfano, A. M. Gomez, S. Lewis, J. Kota, V. Malik, K. Shontz, C. M. Walker, K. M. Flanigan, M. Corridore, J. R. Kean, H. D. Allen, C. Shilling, K. R. Melia, P. Sazani, J. B. Saoud, E. M. Kaye and G. Eteplirsen Study (2013). "Eteplirsen for the treatment of Duchenne muscular dystrophy." Ann Neurol **74**(5): 637-647.

Min Jou, W., G. Haegeman, M. Ysebaert and W. Fiers (1972). "Nucleotide sequence of the gene coding for the bacteriophage MS2 coat protein." Nature **237**(5350): 82-88.

Ming, X., K. Carver, M. Fisher, R. Noel, J. C. Cintrat, D. Gillet, J. Barbier, C. Cao, J. Bauman and R. L. Juliano (2013). "The small molecule Retro-1 enhances the pharmacological actions of antisense and splice switching oligonucleotides." Nucleic Acids Res **41**(6): 3673-3687.

Mo, R., Q. Sun, N. Li and C. Zhang (2013). "Intracellular delivery and antitumor effects of pH-sensitive liposomes based on zwitterionic oligopeptide lipids." Biomaterials **34**(11): 2773-2786.

Moulton, H. M., S. Fletcher, B. W. Neuman, G. McClorey, D. A. Stein, S. Abes, S. D. Wilton, M. J. Buchmeier, B. Lebleu and P. L. Iversen (2007). "Cell-penetrating peptide-morpholino conjugates alter pre-mRNA splicing of DMD (Duchenne muscular dystrophy) and inhibit murine coronavirus replication in vivo." Biochem Soc Trans **35**(Pt 4): 826-828.

Moulton, J. D. and S. Jiang (2009). "Gene knockdowns in adult animals: PPMOs and vivo-morpholinos." Molecules **14**(3): 1304-1323.

Neuman, B. W., L. H. Bederka, D. A. Stein, J. P. Ting, H. M. Moulton and M. J. Buchmeier (2011). "Development of peptide-conjugated morpholino oligomers as pan-arenavirus inhibitors." Antimicrob Agents Chemother **55**(10): 4631-4638.

Newton, J. and S. L. Deutscher (2008). "Phage peptide display." Handb Exp Pharmacol(185 Pt 2): 145-163.

Nigro, G., S. Di Somma, L. I. Comi, L. Politano, S. Papparella, B. Restucci, V. R. Petretta, M. A. Giugliano, A. Carotenuto, F. M. Limongelli and et al. (1995). "Structural basis of cardiomyopathy in Duchenne/Becker carriers. Endomyocardial biopsy evaluation." Ann N Y Acad Sci **752**: 108-110.

Nilsen, T. W. and B. R. Graveley (2010). "Expansion of the eukaryotic proteome by alternative splicing." Nature **463**(7280): 457-463.

Oerlemans, C., W. Bult, M. Bos, G. Storm, J. F. Nijsen and W. E. Hennink (2010). "Polymeric micelles in anticancer therapy: targeting, imaging and triggered release." Pharm Res **27**(12): 2569-2589.

Oudet, C., A. Hanauer, P. Clemens, T. Caskey and J. L. Mandel (1992). "Two hot spots of recombination in the DMD gene correlate with the deletion prone regions." Hum Mol Genet **1**(8): 599-603.

Paul G. Higgs, T. K. A. (2005). "Boiinformatics and Molecular Evolution."

Popplewell, L. J., A. Abu-Dayya, T. Khana, M. Flinterman, N. Abdul Khalique, L. Raju, C. L. Opstad, H. R. Sliwka, V. Partali, G. Dickson and M. D. Pungente (2012). "Novel cationic carotenoid lipids as delivery vectors of antisense oligonucleotides for exon skipping in Duchenne muscular dystrophy." Molecules **17**(2): 1138-1148.

Prior, T. W. and S. J. Bridgeman (2005). "Experience and strategy for the molecular testing of Duchenne muscular dystrophy." J Mol Diagn **7**(3): 317-326.

Ruska, E. (1987). "Nobel lecture. The development of the electron microscope and of electron microscopy." Biosci Rep **7**(8): 607-629.

Sanger, F., G. M. Air, B. G. Barrell, N. L. Brown, A. R. Coulson, C. A. Fiddes, C. A. Hutchison, P. M. Slocombe and M. Smith (1977). "Nucleotide sequence of bacteriophage phi X174 DNA." Nature **265**(5596): 687-695.

Seow, Y., H. Yin and M. J. Wood (2010). "Identification of a novel muscle targeting peptide in mdx mice." Peptides **31**(10): 1873-1877.

Shi, Q., A. T. Nguyen, Y. Angell, D. Deng, C. R. Na, K. Burgess, D. D. Roberts, F. C. Brunicardi and N. S. Templeton (2010). "A combinatorial approach for targeted delivery using small molecules and reversible masking to bypass nonspecific uptake in vivo." Gene Ther **17**(9): 1085-1097.

Shoji-Kawata, S., R. Sumpter, M. Leveno, G. R. Campbell, Z. Zou, L. Kinch, A. D. Wilkins, Q. Sun, K. Pallauf, D. MacDuff, C. Huerta, H. W. Virgin, J. B. Helms, R. Eerland, S. A. Tooze, R. Xavier, D. J. Lenschow, A. Yamamoto, D. King, O. Lichtarge, N. V. Grishin, S. A. Spector, D. V. Kaloyanova and B. Levine (2013). "Identification of a candidate therapeutic autophagy-inducing peptide." Nature **494**(7436): 201-206.

Smith, G. P. (1985). "Filamentous fusion phage: novel expression vectors that display cloned antigens on the virion surface." Science **228**(4705): 1315-1317.

Sparks, S., S. Quijano-Roy, A. Harper, A. Rutkowski, E. Gordon, E. P. Hoffman and E. Pegoraro (1993). Congenital Muscular Dystrophy Overview. GeneReviews(R). R. A. Pagon, M. P. Adam, T. D. Bird et al. Seattle (WA).

Stanley, P., V. Caillibot and L. Siminovitch (1975). "Selection and characterization of eight phenotypically distinct lines of lectin-resistant chinese hamster ovary cells." Cell **6**(2): 121-128.

Stein, D. A. (2008). "Inhibition of RNA virus infections with peptide-conjugated morpholino oligomers." Curr Pharm Des **14**(25): 2619-2634.

Stephenson, M. L. and P. C. Zamecnik (1978). "Inhibition of Rous sarcoma viral RNA translation by a specific oligodeoxyribonucleotide." Proc Natl Acad Sci U S A **75**(1): 285-288.

Summerton, J. E. (2007). "Morpholino, siRNA, and S-DNA compared: impact of structure and mechanism of action on off-target effects and sequence specificity." Curr Top Med Chem **7**(7): 651-660.

Swaminathan, S. and Y. Cui (2013). "Recognition of epoxy with phage displayed peptides." Mater Sci Eng C Mater Biol Appl **33**(5): 3082-3084.

van Deutekom, J. C., A. A. Janson, I. B. Ginjaar, W. S. Frankhuizen, A. Aartsma-Rus, M. Bremmer-Bout, J. T. den Dunnen, K. Koop, A. J. van der Kooi, N. M. Goemans, S. J. de Kimpe, P. F. Ekhart, E. H. Venneker, G. J. Platenburg, J. J. Verschuuren and G. J. van Ommen (2007). "Local dystrophin restoration with antisense oligonucleotide PRO051." N Engl J Med **357**(26): 2677-2686.

Wang, M., P. Lu, B. Wu, **J. D. Tucker**, C. Cloer and Q. Lu (2012). "High efficiency and low toxicity of polyethyleneimine modified Pluronics (PEI-Pluronic) as gene delivery carriers in cell culture and dystrophic mdx mice." Journal of Materials Chemistry **22**(13): 6038-6046.

Wang, M., Q. Lu, B. Wu and P. LU (2013). Amphiphilic cationic polymers for the delivery of therapeutic agents, Google Patents.

Wang, M., **J. D. Tucker**, P. Lu, B. Wu, C. Cloer and Q. Lu (2012). "Tris[2-(acryloyloxy)ethyl]isocyanurate cross-linked low-molecular-weight polyethylenimine as gene delivery carriers in cell culture and dystrophic mdx mice." Bioconjug Chem **23**(4): 837-845.

Wang, M., B. Wu, P. Lu, C. Cloer, **J. D. Tucker** and Q. Lu (2013). "Polyethylenimine-modified pluronics (PCMs) improve morpholino oligomer delivery in cell culture and dystrophic mdx mice." Mol Ther **21**(1): 210-216.

Wang, M., B.Wu, **J. D. Tucker,** P. Lu, C. Cloer, Q. L. Lu (2014). "Evaluation of Tris[2-(acryloyloxy)ethyl]isocyanurate Cross-linked Polyethylenimine as Antisense Morpholino Oligomer Delivery Vehicle in Cell Culture and Dystrophic mdx Mice." Hum Gene Ther.

Watts, J. K. and D. R. Corey (2012). "Silencing disease genes in the laboratory and the clinic." J Pathol **226**(2): 365-379.

Wehrens, X. H., S. E. Lehnart, S. Reiken, J. A. Vest, A. Wronska and A. R. Marks (2006). "Ryanodine receptor/calcium release channel PKA phosphorylation: a critical mediator of heart failure progression." Proc Natl Acad Sci U S A **103**(3): 511-518.

Wellman-Labadie, O. and Y. Zhou (2010). "The US Orphan Drug Act: rare disease research stimulator or commercial opportunity?" Health Policy **95**(2-3): 216-228.

Wells, L. (2013). "The o-mannosylation pathway: glycosyltransferases and proteins implicated in congenital muscular dystrophy." J Biol Chem **288**(10): 6930-6935.

Wood, D. S., M. Zeviani, A. Prelle, E. Bonilla, G. Salviati, A. F. Miranda, S. DiMauro and L. P. Rowland (1987). "Is nebulin the defective gene product in Duchenne muscular dystrophy?" N Engl J Med **316**(2): 107-108.

Wu, B., Y. Li, P. A. Morcos, T. J. Doran, P. Lu and Q. L. Lu (2009). "Octa-guanidine morpholino restores dystrophin expression in cardiac and skeletal muscles and ameliorates pathology in dystrophic mdx mice." Mol Ther **17**(5): 864-871.

Wu, B., P. Lu, C. Cloer, M. Shaban, S. Grewal, S. Milazi, S. N. Shah, H. M. Moulton and Q. L. Lu (2012). "Long-Term Rescue of Dystrophin Expression and Improvement in Muscle Pathology and Function in Dystrophic mdx Mice by Peptide-Conjugated Morpholino." Am J Pathol **181**(2): 392-400.

Wu, B., H. M. Moulton, P. L. Iversen, J. Jiang, J. Li, J. Li, C. F. Spurney, A. Sali, A. D. Guerron, K. Nagaraju, T. Doran, P. Lu, X. Xiao and Q. L. Lu (2008). "Effective rescue of dystrophin improves cardiac function in dystrophin-deficient mice by a modified morpholino oligomer." Proc Natl Acad Sci U S A **105**(39): 14814-14819.

Yin, H., H. M. Moulton, C. Betts, T. Merritt, Y. Seow, S. Ashraf, Q. Wang, J. Boutilier and M. J. Wood (2010). "Functional rescue of dystrophin-deficient mdx mice by a chimeric peptide-PMO." Mol Ther **18**(10): 1822-1829.

Yokota, T., Q. L. Lu, T. Partridge, M. Kobayashi, A. Nakamura, S. Takeda and E. Hoffman (2009). "Efficacy of systemic morpholino exon-skipping in Duchenne dystrophy dogs." Ann Neurol **65**(6): 667-676.

Yu, C. Y., Z. Yuan, Z. Cao, B. Wang, C. Qiao, J. Li and X. Xiao (2009). "A muscle-targeting peptide displayed on AAV2 improves muscle tropism on systemic delivery." Gene Ther **16**(8): 953-962.

Yuan, J., D. A. Stein, T. Lim, D. Qiu, S. Coughlin, Z. Liu, Y. Wang, R. Blouch, H. M. Moulton, P. L. Iversen and D. Yang (2006). "Inhibition of coxsackievirus B3 in cell cultures and in mice by peptide-conjugated morpholino oligomers targeting the internal ribosome entry site." J Virol **80**(23): 11510-11519.

Zamecnik, P. C. and M. L. Stephenson (1978). "Inhibition of Rous sarcoma virus replication and cell transformation by a specific oligodeoxynucleotide." Proc Natl Acad Sci U S A **75**(1): 280-284.

Zhang, Y. M., C. H. Tung, J. He, N. Liu, I. Yanachkov, G. Liu, M. Rusckowski and J. L. Vanderheyden (2006). "Construction of a novel chimera consisting of a chelator-containing Tat peptide conjugated to a morpholino antisense oligomer for technetium-99m labeling and accelerating cellular kinetics." Nucl Med Biol **33**(2): 263-269.